

*Digital Comprehensive Summaries of Uppsala Dissertations
from the Faculty of Science and Technology 2375*

Searching for Dyson spheres in the Milky Way

MATÍAS SUAZO



ACTA UNIVERSITATIS
UPSALIENSIS
2024

ISSN 1651-6214
ISBN 978-91-513-2066-3
urn:nbn:se:uu:diva-524893



UPPSALA
UNIVERSITET

Dissertation presented at Uppsala University to be publicly examined in 101195, Ångströmlaboratoriet, Lägerhyddsvägen 1, Uppsala, Friday, 3 May 2024 at 13:15 for the degree of Doctor of Philosophy. The examination will be conducted in English. Faculty examiner: Hector Socas-Navarro (Universidad de La Laguna, Facultad de Físicas, Departamento de Astrofísica).

Abstract

Suazo, M. 2024. Searching for Dyson spheres in the Milky Way. *Digital Comprehensive Summaries of Uppsala Dissertations from the Faculty of Science and Technology* 2375. 101 pp. Uppsala: Acta Universitatis Upsaliensis. ISBN 978-91-513-2066-3.

The quest to find intelligent extraterrestrial life has captivated humanity for a long time, motivating the development of various strategies to search for signs of advanced civilizations. These strategies comprise multiple techniques and span different regions of the electromagnetic spectrum. One approach considers the existence of Dyson spheres, one specific type of megastructure theorized by Freeman Dyson over sixty years ago. Dyson hypothesized that advanced civilizations would eventually outgrow their planetary resources and aim to collect the energy of their central star by building colossal structures to harness the star's energy. The potential existence of these structures represents a potential technosignature that might be hiding in large astronomical surveys, and this thesis revolves around exploring such a premise. First, we devote our search to assessing upper limits on the prevalence of Dyson spheres in the Milky Way by analyzing combined optical and mid-infrared photometric data. These upper limits are presented on the fraction of stars that may potentially host Dyson spheres and are model-dependent. We find robust limits of 1 over 100,000 stars for 300 K Dyson spheres at a 90% completion level within 100 pc. After that, we develop a pipeline especially tailored to identify potential Dyson sphere candidates in a sample of five million objects with available optical, near, and mid-infrared photometric data. This pipeline yields seven M dwarfs exhibiting anomalous infrared excess that deserve further analysis. Finally, we present an analysis of photometric and, in some cases, spectroscopic data on these seven objects, plus three additional sources sharing similar properties. The stellar parameters, derived from calibrated empirical relationships for M dwarfs, reveal no irregularities compared to the typical M dwarf population. While the infrared properties of our targets resemble, in some cases, those of young stars, spectroscopic data show no signs of youth usually observed for such objects. We still lack a clear explanation for the infrared excess of these stars, but we acknowledge that future follow-up observations could probe scenarios in which the infrared excess is due to circumstellar dust emission.

Keywords: Extraterrestrial intelligence, infrared:stars

Matías Suazo, Department of Physics and Astronomy, Observational Astronomy, 516, Uppsala University, SE-751 20 Uppsala, Sweden.

© Matías Suazo 2024

ISSN 1651-6214

ISBN 978-91-513-2066-3

URN urn:nbn:se:uu:diva-524893 (<http://urn.kb.se/resolve?urn=urn:nbn:se:uu:diva-524893>)

Dedicated to those who made this possible

List of papers

This thesis is based on the following papers, which are referred to in the text by their Roman numerals.

- I **Suazo, M.**, Zackrisson, E., Wright J.T., Korn A.J., Huston, M., (2022)
Project Hephaistos – I. Upper limits on partial Dyson spheres in the Milky Way
Monthly Notices of the Royal Astronomical Society, Volume 512, Issue 2, p.2988-3000.
- II **Suazo, M.**, Zackrisson, E., Mahto P.K., Lundell F., Nettelblad. C., Korn A.J., Wright J.T., Majumdar S., (2024)
Project Hephaistos – II. Dyson sphere candidates from Gaia DR3, 2MASS, and WISE
Monthly Notices of the Royal Astronomical Society, submitted.
- III **Suazo, M.**, Zackrisson, E., Cortés-Zuleta P., Rains A.D., Korn A.J., Nabizadeh A. (2024)
Project Hephaistos – III. Characterizing anomalous infrared sources identified as Dyson Sphere candidates
In preparation.

Reprints were made with permission from the publishers.

Contents

Part I: The Search for Extraterrestrial Technology	9
1 History and concepts	11
1.1 Early SETI	11
1.2 Key concepts	14
1.2.1 The Kardashev Scale	14
1.2.2 The Drake and The Seager Equations	16
1.2.3 Fermi-Hart paradox	18
1.2.4 Nine axes of merit	20
2 Radio and Optical/Laser SETI	23
2.1 Radio Overview	23
2.2 Laser/Optical Overview	24
2.3 Historical searches	25
2.3.1 Narrowband searches	26
2.3.2 Pulses	27
2.3.3 Large projects	27
2.4 The nine axes of merit for optical/radio searches	28
3 Artificial megastructures	30
3.1 Stellar engines	30
3.2 Dyson spheres	31
3.2.1 The thermodynamics of Dyson spheres	32
3.2.2 Simple Dyson sphere models	42
3.2.3 Dyson sphere searches	45
3.2.4 Alternative power sources for Dyson spheres.	48
3.3 The nine axes of merit for waste heat searches	48
Part II: Infrared excess stars	51
4 Infrared excess stars	53
4.1 Extrinsic	53
4.1.1 Dusty regions	53
4.1.2 Chance alignments	54
4.2 Intrinsic	57
4.2.1 Evolved stars	57
4.2.2 Binaries	58

4.2.3	Young stars	59
Part III: Summary of papers		65
5	Paper I	67
6	Paper II	70
7	Paper III	72
8	Popular Science Summary	74
9	Populärvetenskaplig sammanfattning	77
10	Acknowledgements	80
Bibliography		82

Part I: The Search for Extraterrestrial Technology

Are we alone in the Universe? With hundreds of billions of stars in our Galaxy alone, with potentially billions of habitable planets orbiting them, it seems unlikely that the answer is a definitive “no.” Further afield, the number of stars – and hence planets – grows radically as we contemplate the vast amount of galaxies beyond our own. However, despite decades of stringent searches, unambiguous evidence of extraterrestrial life remains frustratingly elusive. This chapter embarks on a journey through some part of the Search for Extra-Terrestrial Intelligence (SETI).

1. History and concepts

1.1 Early SETI

For centuries, humankind has pondered the question of whether we are the only inhabitants of the Galaxy. For many years, the hypothesis of other species living on other planets and possessing technology surpassing ours stayed in the realm of science fiction. It was not until 1959 that the first scientific paper proposing a concrete method for searching for extraterrestrial signals was published. In this innovative work, Cocconi and Morrison (1959) explored the optimal region of the electromagnetic spectrum for potential interstellar communication, assuming that other intelligent civilizations exist in systems hosted by stars similar to our Sun and might be attempting to contact us. Specifically, they suggested directing efforts to detect signals of extraterrestrial intelligence emanating from the stars τ Ceti and ϵ Eridani. The publication of this seminal paper marked the dawn of what we now recognize as modern SETI.

Within the subsequent two years, three new articles emerged, each offering novel strategies for pursuing signatures of extraterrestrial intelligence. Bracewell (1960) postulated that long-range communication signals seem improbable when considering a small number of advanced civilizations within the vast number of stars in the Galaxy. Instead, Bracewell advocated exploring our Solar System for potential probes of extraterrestrial origin, serving as beacons for intergalactic communication channels.

In the second paper, Dyson (1960) introduced a pioneering approach by proposing the detection of infrared signatures originating from stars. This infrared light might come from the waste heat emitted by megastructures built by highly advanced civilizations to exploit the energy of their host stars. Dyson's hypothesis relied on the premise that as civilizations progress, they would inevitably seek to harness the energy resources of their host stars, which would potentially culminate in the construction of such colossal megastructures.

Finally, Schwartz and Townes (1961) introduced a proposal to search for interstellar communication signals within the optical spectrum, motivated by the recent invention of lasers during that period.

Numerous pivotal moments in SETI history took place after the publication of these seminar papers. Table 1.1 provides an overview of some of these milestones up to the year 2000. One particularly noteworthy



Figure 1.1. The 26-m Howard E. Tatel Radio Telescope at NRAO used in Project Ozma. CC BY-SA 4.0

milestone is the execution of the first SETI radio search, famously known as “Project Ozma.” This project targeted the nearby stars τ Ceti and ϵ Eridani (Drake, 1961) and focused on detecting emission in the 21-cm line, which corresponds to the energy of a photon emitted from a hydrogen atom during an electronic ground-state spin-flip transition. Figure 1.1 depicts the 28-meter Howard E. Tatel Radio Telescope utilized for this project, situated at the National Radio Astronomy Observatory in Green Bank, West Virginia. This facility played a pivotal role in the early endeavors of SETI research, symbolizing one of humanity’s first quests to explore the cosmos for signs of extraterrestrial intelligence.

Another milestone corresponds to the creation of the renowned Kardashev scale to classify civilizations according to their energy consumption, which was introduced in Kardashev (1964). This conceptual framework has since become an influential tool in the field of SETI, aiding in the categorization of potential extraterrestrial civilizations.

A decade later, Crick and Orgel (1973) delved into the intriguing possibility of life being deliberately seeded on Earth by an advanced extraterrestrial civilization. This hypothesis sparked considerable debate and speculation within the scientific community, underscoring the interdisciplinary nature of SETI research.

In 1975, Michael H. Hart thoroughly examined the arguments surrounding the absence of extraterrestrials on Earth, concluding that the

likely explanation for the lack of colonization by aliens is the non-existence of other civilizations in the Milky Way (Hart, 1975). This provocative assertion prompted further reflection and discussion within the SETI community, highlighting the ongoing quest for understanding humanity’s place in the Universe.

Table 1.1: *Timeline of some of the milestones in SETI history until 2000*

Year	Milestone
1959	The first modern SETI article is published (Cocconi and Morrison, 1959)
1960	Frank Drake conducts the first SETI search, <i>Project OZMA</i> . The results are published the following year (Drake, 1961)
1960	Searching for interstellar probes is proposed as an alternative SETI strategy (Bracewell, 1960)
1960	The possibility of searching for megastructures based on their infrared waste heat signature is presented (Dyson, 1960)
1961	The search for continuous optical laser beacons is proposed (Schwartz and Townes, 1961)
1961	The first SETI Conference, <i>Order of the Dolphin</i> , takes place. Frank Drake introduces his famous equation
1964	The Kardashev scale is introduced (Kardashev, 1964)
1972 - 1973	The Pioneer Plaques, containing a message about our planet are placed on board of the <i>Pioneer 10</i> and <i>Pioneer 11</i> space probes
1973	Francis Crick and Leslie Orgel evaluate the possibility of life on Earth originating elsewhere in the Universe (Crick and Orgel (1973))
1975	Michael H. Hart publishes a detailed examination of the Fermi paradox, and argues for the non-existence of other civilizations (Hart, 1975)
1977	The Ohio State Big Ear telescope detects the famous “Wow!” signal from the constellation Sagittarius
1977	<i>Voyager 1</i> and <i>Voyager 2</i> space probes launched carrying gold records containing images and sounds of Earth
1979	The Planetary Society is founded by Carl Sagan, Bruce Murray, and Louis Friedman
1981	The Proxmire Amendment kills congressional

Table 1.1 continued from previous page

	support of NASA SETI
1981	The Planetary Society begins advocacy for NASA to conduct searches for extraterrestrial signals. Dr. Sagan, then-president of the Society, persuades senator Proxmire to stop opposition
1983	The International Astronomical Union establishes Commission 51, dedicated to astrobiology and the search for extraterrestrial life
1984	The SETI Institute is founded as a home for research, investigating all aspects of life in the Universe. Initially, its activities were supported by NASA
1989	The Planetary Society takes over the publishing of “Bioastronomy News” as one of its special-interest newsletters
1992	NASA’s High-Resolution Microwave Survey (HRMS) observations begin to operate at the Goldstone Observatory and at the Arecibo radio telescope
1993	Funding for NASA’s HRMS searches is eliminated by the US Congress
1994	The SETI League was founded, which became the world’s major privatized SETI observational program
1995	The SETI league has since grown to 1100 members in 56 countries
1995	51 Pegasi B is detected – the first confirmed planet around a nearby Sun-like star (Mayor and Queloz, 1995)
1998	The SETI Institute and The Planetary Society now support searching for optical laser signals

1.2 Key concepts

1.2.1 The Kardashev Scale

Similarly to Cocconi and Morrison (1959), Kardashev (1964) also conducted an analysis to determine the most efficient region for the transmission of electromagnetic signals, with the aim of evaluating the transmission rate of information. In his study, Kardashev explored the optimal frequency range for signal transmission within the frequencies considered by Cocconi and Morrison (1959), ultimately arriving at conclusions aligned with the advantages of utilizing radio signals. Additionally, Kardashev identified a critical factor influencing the assessment

of information transmission: the noise temperature T_N . He observed that a significant source of uncertainty in this assessment stems from the estimation of the power emitted by the civilization in question. To address this, Kardashev proposed a classification system categorizing civilizations based on their energy consumption. This categorization scheme, known as the Kardashev scale, is presented below.

- Type I: Civilization possessing technology enabling energy consumption at a level comparable to that of Earth in the 1960s (approximately 4×10^{12} watts).
- Type II: Civilization capable of harnessing the energy of its host star. The energy consumption is comparable to the luminosity of the Sun (approximately 4×10^{26} watts).
- Type III: Civilization capable of harvesting the energy of its host galaxy. The energy consumption is comparable to the luminosity of the Milky Way (approximately 4×10^{37} watts).

Several modifications have been proposed after the original formulation of the Kardashev scale. Sagan (1973) advocated using Arabic numerals instead of Roman numerals to allow for intermediate values. Additionally, Sagan proposed significant changes to the energy consumption criteria for a Type I civilization, arguing that Kardashev (1964)'s initial estimation was outdated. Building on Sagan's ideas, Gray (2020) further suggested using Arabic numerals and intervals of 10^{10} to accommodate decimal fractions, thereby providing finer resolution in the scale. Within the frameworks proposed by Sagan (1973) and Gray (2020), the Kardashev scale can be represented as:

$$K = \frac{\log_{10}(P) - 6}{10}, \quad (1.1)$$

where K is the Kardashev scale value, and P is the power emitted by the civilization in Watts.

Gray (2020) also introduced the concept of civilizations Type 0.0 and Type 4.0 by extrapolating the energy consumption required by Equation 1.1 to derive these K values. A Type 0.0 civilization would exhibit a power level comparable to the metabolic power of the largest terrestrial animals and groups of animals on Earth. Conversely, a Type 4.0 civilization would wield power approaching the current estimates for the luminosity of the observable universe (e.g., Wijers, 2005).

The original Type I civilization proposed by Kardashev (1964) would correspond to $K = 0.67$ according to Equation 1.1. In contrast, our current civilization would correspond to $K = 0.73$ if we consider the world energy consumption during 2022, as provided by Ritchie et al. (2023).

The Anti-Kardashev scale

The Kardashev scale traditionally revolves around the manipulation of large-scale structures, with the numerical values representing the size of these structures. However, an intriguing departure from this perspective is presented by Barrow (1999) in the form of the “anti-Kardashev scale.” In this concept, Barrow highlights humanity’s tendency to prioritize the enhancement of our ability to manipulate our environment on increasingly smaller scales, rather than exclusively focusing on larger ones. Consequently, he proposes a reverse classification system, spanning from Type I-minus to Type Ω -minus:

- Type I-minus: Civilization capable of manipulating objects on the scale of itself: building structures, mining, etc.
- Type II-minus: Civilization capable of manipulating genes and alter the development of living things.
- Type III-minus: Civilization adept at manipulating molecules and molecular bonds, thereby being able to create new materials.
- Type IV-minus: Civilization capable of manipulating individual atoms and create complex artificial life forms.
- Type V-minus: Civilization capable of manipulating atomic nuclei and engineering its components.
- Type VI-minus: Civilization that manipulates most elementary particles of matter, capable of creating organized and complex populations of elementary particles.
- Type Ω -minus: Civilization that exploits the fundamental structure of space and time.

Notice that the traditional Kardashev scale and the Anti-Kardashev are simultaneously compatible.

1.2.2 The Drake and The Seager Equations

One of the most significant inquiries in the field of SETI revolves around the estimation of the number of civilizations within our Galaxy with which communication could potentially occur. This idea holds utter importance as it aids in approximating the frequency at which we might encounter signals indicative of extraterrestrial communication. In 1961, Frank Drake devised an equation to address this question. Drake formulated this equation while preparing for a SETI (*Order of the Dolphin*) conference focused on the detection of radio signals. Although there is no direct reference to this equation, one version of it can be found in Papagiannis (1980), where the Drake equation is articulated as follows:

$$N = R_{\star} \cdot f_p \cdot n_e \cdot f_i \cdot f_c \cdot L, \quad (1.2)$$

where N is the number of civilizations in our galaxy with which communication might be possible, R_\star is the average rate of star formation (expressed in numbers of stars formed per unit time) in our Galaxy, f_p the fraction of stars that host planets, n_e the average number of stars hosting planets that can potentially support life, f_l the fraction of such planets that actually develops life at some point, f_i the fraction of planets with life where intelligent civilizations emerge, f_c the fraction of civilizations that develop a technology that releases detectable signs of their existence into space, and L the length of time for which such civilizations release detectable signals into space.

In Equation 1.2, the parameter $N \ll 1$ suggests that the probability of us being alone in the Galaxy is high, indicating that we would need to survey numerous galaxies to locate our closest radio-communicating neighbors. Conversely, $N \gg 1$ implies the existence of numerous civilizations with which we could potentially establish contact. However, it is essential to note that depending on the assumptions made, the value of N can vary significantly (e.g., Wilson, 2001).

Various modifications and refinements have been applied to the original form of the Drake Equation to better guide searches for technosignatures. For instance, Frank and Sullivan (2016) constrained the Drake Equation by incorporating observable quantities. Additionally, other studies have utilized statistical methods to constrain the equation (e.g., Maccone, 2010; Glade et al., 2012; Lares et al., 2020; Smith, 2021).

In contrast, Haqq-Misra and Kopparapu (2017) explored the influence of the Drake Equation parameters on the spectral type of the host star and the age of the Galaxy. Their analysis led them to conclude that F and G spectral types represent optimal targets for contemporary technosignature searches.

During an interview in 2013¹, Sara Seager introduced a different equation, similar in concept to the Drake equation, but different in term of the input factors. This equation, now known as the Seager Equation, aims to estimate the number of exoplanets with detectable signs of life. The Seager Equation is formulated as follows:

$$N = N_\star \cdot f_Q \cdot f_{\text{HZ}} \cdot f_O \cdot f_L \cdot f_S, \quad (1.3)$$

where N represents the number of planets with detectable signs of life, N_\star denotes the number of stars observed, f_Q stands for the fraction of quiet stars (whose flare activity and other disruptions do not mask data), f_{HZ} represents the fraction of stars with rocky planets in the habitable zone, f_O signifies the fraction of stars with observable planets, f_L denotes the fraction of planets hosting life, and f_S indicates the fraction of life

¹<https://www.centauri-dreams.org/2013/09/11/astrobiology-enter-the-seager-equation/>

forms that produce planetary atmospheres with one or more detectable signature gases. As noted by Maccone (2015), mathematically speaking, the Drake and the Seager Equations are equivalent, but with a different scientific meaning.

1.2.3 Fermi-Hart paradox

Our Milky Way Galaxy harbors approximately $\sim 10^{11}$ stars. If we posit that a fraction of these stars accommodates the conditions conducive to the emergence of life, it becomes reasonable to believe that we are not the sole planet to foster life. This probability escalates further when we contemplate the potential for life in other galaxies. Indeed, Zackrisson et al. (2016) suggests that there could be as many as $\sim 10^{18}$ habitable planets orbiting Solar-type stars within the observable Universe.

However, despite these vast numbers, the absence of contact with other civilizations prompts Enrico Fermi's famous question, "Where is everyone?" (Jones, 1985). This apparent disparity between the abundance of stars in our Galaxy and the absence of extraterrestrial evidence is commonly known as "The Fermi Paradox," named after Fermi's question.

This paradox has generated discussion throughout the history of SETI and about the purpose of the research itself. Hart (1975) restated the Fermi paradox, claiming that the colonization of the Galaxy by intelligent species should be fast compared to the age of the Galaxy. Hart (1975) concluded that we are the first species in the Galaxy, hence justifying the difficulties in detecting signs of extraterrestrial intelligence. Because of this work, the Fermi paradox is often referred to as the Fermi-Hart paradox.

Numerous authors have endeavored to elucidate this paradox by presenting arguments for why we have yet to encounter or be contacted by any extraterrestrial intelligence (ETI). Hart (1975) categorized these arguments into four distinct categories:

- Physical: The distances are so vast in the Galaxy that extraterrestrial civilizations have not been able to reach us;
- Sociological: This point considers arguments that state that either ETIs are not interested in us, that they have already self-destructed, or that they keep us isolated as a sort of natural reserve;
- Temporal: They have not had time to reach us;
- They visited in the past, but we have not found any evidence for this visit.

Physical Arguments

Hart argued that interstellar probes seemed plausible in terms of technical feasibility at the time of his article. He foresaw that our technological advancement will put further strength behind this argument. He concluded that the vast distances in the galaxy cannot correspond to one of the reasons we have not encountered or been contacted by extraterrestrial civilizations.

Sociological arguments

Sociological explanations often postulate typical behavior patterns of alien species. These behaviors may include a lack of interest in travel or communication, a desire not to interfere with our ecosystem, self-destruction, a reluctance to admit immature species into their ranks, achievement of a transcendent state, or transfer of consciousness into computers.

Hart acknowledged that while some of these points may apply to individual civilizations, it is inappropriate to assume they universally apply to every alien species in the Galaxy. Moreover, he recognized that civilizations evolve, suggesting that their perspectives on interstellar communication may change over time.

Temporal Arguments

Assuming the age of the Galaxy to be 10^{10} years, Hart argued that alien civilizations would have had ample time to emerge and colonize other planetary systems.

They have come, but we have not noticed them

Hart also stated that it is improbable for aliens to have visited the Solar System without leaving discernible traces of their presence. He invoked the monocultural fallacy to argue that if numerous extraterrestrial intelligences (ETIs) had traversed near the Solar System, it would be erroneous to assume that none desired colonizing our planetary system. Additionally, he contended that, given the timelines for the emergence of civilizations and Galactic colonization, we should have been visited multiple times throughout the history of the Solar System.

Rebuttals to Hart's arguments

Several authors have demonstrated potential flaws in the arguments used by Hart to argue for the non-existence of extraterrestrial civilizations. For example, Webb (2015) provides an overview of no less than seventy-five potential proposed solutions to the Fermi-Hart paradox.

Additionally, Wright et al. (2014b) thoroughly re-studied Hart's arguments, agreeing with some perspectives while finding caveats to others.

To begin with, Wright et al. (2014b) re-estimated some of the timescales involved. They concluded that galactic colonization timescales are at least one order of magnitude shorter than the ages of galaxies. Additionally, they found that rotational shear and thermal motions would disperse colonies if the latter were clustered. They found the maximum timescale for Galactic colonization to be on the order of a Galactic rotation (10^8 yr). They showed that this fact would generate a smooth distribution of alien civilizations across the Galaxy, and their technosignatures would distribute in the same way.

Wright et al. (2014b) were also very critical of Hart’s argument on the possibility of ETI passing through the Solar System and not leaving any evidence of their existence. Hart assumed that at least one visitor to the Solar System would have stayed, arguing that if the Galaxy is filled with ETIs, then they would have colonized us. Wright et al. (2014b) claimed that it is much less fallacious to argue that none of the ETIs *that has happened to visit the Solar System* has decided to colonize it. Hart’s argument fails under the assumption that every ETI would have effectuated interstellar travel and that they would have passed by our Solar System if so.

1.2.4 Nine axes of merit

Formulating an efficient search strategy for technosignatures presents a significant challenge, requiring careful consideration to ensure effectiveness and balance. To address this challenge, NASA Technosignatures Workshop Participants (2018) introduced a framework that was subsequently enhanced in Sheikh (2020) to aid in planning technosignature detection strategies. This framework introduces the concept of the “nine axes of merit,” providing a structured approach to evaluating a given search strategy’s relative strengths and weaknesses.

The nine axes of merit are visually shown in Figure 1.2, and are described as follows:

- Observing capability: This axis evaluates whether existing technological resources, such as telescopes, detectors, or databases, suffice for the proposed technosignature search, or if new technologies are necessary.
- Cost: This factor encompasses financial expenses as well as considerations like telescope time and computing resources required for the search.
- Ancillary benefits: This aspect considers whether the proposed search offers valuable scientific outcomes even in the case where no evidence of extraterrestrial intelligence is detected.

- **Detectability:** This criterion assesses how easily the technosignature can be detected given current observational methods and instruments.
- **Duration:** Referring to the timescale over which a technosignature would remain detectable, this axis evaluates the longevity of the signal.
- **Ambiguity:** This point reflects the potential for confusion, indicating how easily the observed signal could be mistaken for natural phenomena rather than evidence of extraterrestrial technology.
- **Extrapolation:** This axis gauges the confidence in the existence of a specific technology based on its resemblance to technologies already understood and utilized on Earth, thus assessing how advanced it is beyond current human capabilities.
- **Inevitability:** This factor estimates the likelihood that a particular type of extraterrestrial technology produces detectable technosignatures, based on the assumed distribution of such technology in the universe.
- **Information:** This axis measures the scientific insight gained from detecting a technosignature, considering the depth of knowledge it provides about potential extraterrestrial civilizations.

2. Radio and Optical/Laser SETI

In the hypothetical scenario of reaching out to our neighbors from a distant stellar system, transmitting electromagnetic signals into space for communication purposes requires careful planning. We must also consider the intended objective of the communication: are we simply signaling our existence, or do we aim to convey a specific message encrypted within the electromagnetic waves? Each approach requires thoughtful consideration of the communication process and how we wish to convey it.

A fundamental parameter in telecommunications planning is the free-space loss, which denotes the attenuation of energy between the feed points of two antennas. This loss is contingent upon factors such as the antenna's capture area and the path traversed by the wavelength. In free space, the free-space loss (*FSL*) is mathematically expressed as:

$$FSL \propto \frac{d^2}{\lambda}, \quad (2.1)$$

where d represents the distance between the emitting antenna and the receiver, and λ signifies the wavelength of the emitted photons.

The free-space loss increases with the square of the distance (d) due to the power density of electromagnetic waves diminishing in accordance with the inverse square law. Conversely, it decreases with shorter wavelengths (λ) since more electromagnetic waves of shorter length can be accommodated by a receiver antenna.

Radio and optical wavelengths offer distinct advantages depending on the intended purpose of our communication endeavors, and the free-space loss offers a metric that helps us ponder which wavelength is optimal if information content is relevant to a communication task. If we consider the scenario where our neighbors initiate communication, radio and optical/laser SETI emerge as natural fields aimed at capturing their attempts to contact us. In the following sections, we delve deeper into each approach, exploring their respective advantages and disadvantages while also providing historical insight to enrich our understanding of these fields.

2.1 Radio Overview

Section 1.1 already mentioned the foundational work of Cocconi and Morrison (1959) in the field of SETI. Their pioneering paper argued

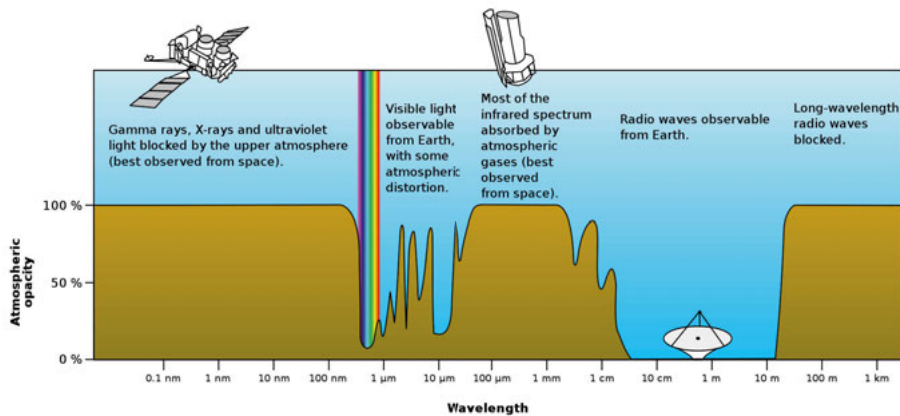


Figure 2.1. Earth’s atmospheric opacity to various wavelengths of the electromagnetic spectrum. Image credit: NASA

that the ideal channel for extraterrestrial communication should minimize interference from stellar and Galactic backgrounds, leading them to advocate for the radio wave part of the electromagnetic spectrum. Specifically, they proposed the 1.42 GHz line (21-cm) of neutral hydrogen, reasoning that it would be universally recognized by technologically advanced civilizations. Moreover, the transparency of Earth’s atmosphere to radio waves (as depicted in Figure 2.1) further solidified radio SETI as a prominent avenue of inquiry.

Radio searches are particularly well-suited for scenarios where tight directivity is not required. This is because the number of photons reaching the receiver is maximized for low-energy photons in terms of power, detector efficiency, and extinction. Therefore, isotropic sources are most plausible in the radio regime, as each photon is relatively inexpensive, and large apertures can be constructed at low cost, although with low information content. This has positioned the radio region as the most widely explored electromagnetic spectrum for the search for interstellar communication signals up to date.

2.2 Laser/Optical Overview

After the publication of the foundational SETI article (Cocconi and Morrison, 1959), the discovery of Light Amplification by Stimulated Emission of Radiation (LASER; Maiman, 1960) and the proposal of interstellar optical communication by Schwartz and Townes (1961) introduced another dimension to SETI. Although laser and optical SETI are often used interchangeably, these approaches encompass wavelengths ranging from ultraviolet to near-infrared.

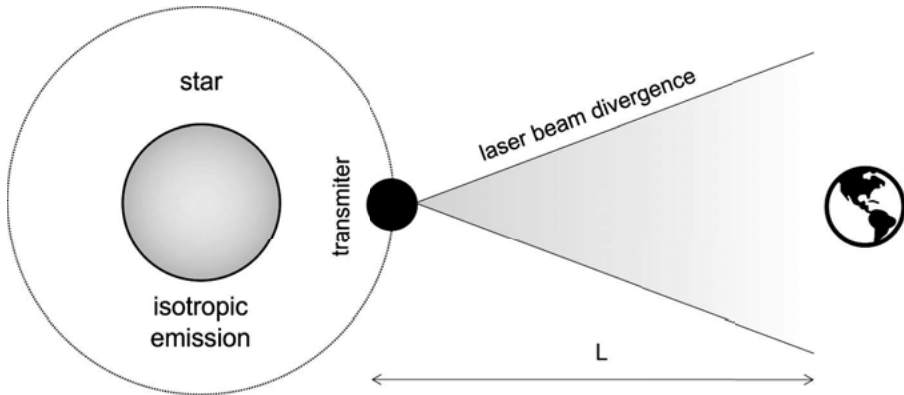


Figure 2.2. Illustration exemplifying how laser communication works. L is the distance between the Earth and the civilization willing to contact us. Image credit: Rafael Vieira.

Communication in the optical regime seems to be a better choice (e.g., Zuckerman, 1985) when civilizations desire to transmit only as a highly directional beam. Even though laser beams usually imply small apertures, huge interstellar distances compensate for it since the area covered follows $A = 4\pi r^2\theta$, where A is the area covered, r the distance between the transmitter and the receiver, and θ the beam aperture. Additionally, if communication prioritizes the maximization of the amount of data delivered, then shorter wavelengths are preferred (Hippke and Forgan, 2017) because of their reduced free-space loss (Equation 2.1). Figure 2.2 shows a simple illustration exemplifying how laser SETI would work.

Furthermore, other authors (e.g., Kingsley, 1993) advocate for optical SETI based on the premise that advanced civilizations would prioritize optimizing power over empty space, utilizing sophisticated signaling techniques. Moreover, the feasibility of optical SETI is supported by the notion that existing lasers and telescopes possess the capability to transmit signals across vast distances (Howard et al., 2004).

2.3 Historical searches

Drake (1961) performed the first modern attempt to detect interstellar radio transmissions. This project named “Project Ozma” searched for 21-cm transmissions of artificial origin from τ ceti and ϵ Eridani. After this pioneering experiment, other searches for signals from the directions of other stars began. We categorized these searches into two categories: Pulses and narrowband emission lines. From the history of searches in the radio vs. optical domain, one can tell the difference in the amount of work devoted to the first type.

2.3.1 Narrowband searches

After *Project Ozma*, numerous researchers continued scanning for transmissions near the 21-cm line (e.g., Verschuur, 1973; Horowitz et al., 1986). However, besides the **21-cm** line, several other **special frequencies** drew the attention of SETI enthusiasts. Oliver (1973, 1979) acknowledged the **18-cm** (1.66 GHz) line, generated by the hydroxyl radical (OH) and corresponds to one of the endpoints of an especially radio-quiet band along with the 21-cm line produced by neutral hydrogen (H). This band is often referred to as the cosmic *waterhole* due to the fact that H and OH are the components of the water molecule. Tarter et al. (1980) conducted a search targeting this OH line around nearby stars.

Additionally, Kardashev (1979) recognized the potential of searches around 1.5-mm, in addition to the 18-cm and 21-cm lines. At 1.47 mm lies the spectral line of the hyperfine ground-state transition of positronium: an artificially created atom consistent of a proton and a positron. Steffes and Deboer (1994) conducted a search for narrow-bandwidth signals near this line around solar-type stars. Similarly, Mauersberger et al. (1996) conducted a similar search among a few stars exhibiting excess infrared radiation.

Technological advancements have significantly propelled the capabilities of modern telescopes, enabling them to cover broad frequency bands across much wider areas of the sky. This progress, as elaborated by Enriquez et al. (2017) among others, has shifted the focus away from narrow emission lines, marking a pivotal evolution in the methodologies employed in the search for extraterrestrial intelligence.

In the branch of searches for monochromatic emission lines in the optical, Reines and Marcy (2002) and Tellis and Marcy (2017) analyzed high-resolution spectra of over 5000 stars of spectral type F, G, K, and M in the wavelength region from 3600 to 9500 Å, while Marcy (2021) searched for laser lines of artificial origin from Proxima Centauri, the closest star from Earth.

Regarding the optimal region to seek optical lines, Narusawa et al. (2018) proposes, from an engineering perspective, that most effective transmitters should emit at wavelengths of 393.8 nm, 656.5 nm (H α), 589.1 nm (NaD₂), 1064 nm (Nd:YAG), and 532.1 nm (Nd:YAG second harmonic). On the other hand, Hippke (2018) thoroughly investigated the extinction in space, atmospheric transparency, scintillation, and noise conditions for these laser lines. Hippke (2018) advises filtering towards these wavelengths using very narrow filters, and moreover to focus on optical wavelengths for stars out to a distance of 1 kpc only, whereas infrared wavelengths would be more appropriate for more dis-

tant stars. He further discouraged using the 393.8 nm line due to the close proximity of the CaK Fraunhofer line at 393.368 nm.

2.3.2 Pulses

The foundation of modern American SETI owes much to the pioneering work of Cocconi and Morrison (1959) and Drake (1961). Nonetheless, the Soviet Union quickly embarked on its own exploratory journey, motivated by the influential study of Kardashev (1964). This led to a succession of investigative efforts within the Soviet domain. Diverging from their American peers, Soviet scientists embraced an innovative method, focusing on the detection of variability and pulses to discern an artificial origin, a technique highlighted in the works of Sholomitsky (1965), Troitskii et al. (1973), and Troitskii et al. (1979).

Despite the subsequent discovery of radio variability in quasars diminishing the appeal of radio variability for SETI pursuits, these Soviet-led inquiries significantly advanced the comprehension of such celestial bodies.

On the side of optical pulses, Howard et al. (2004), Hanna et al. (2009), and Abeysekara et al. (2016) delved into the examination of optical signals from diverse stellar sources, on the lookout for artificially induced pulses. Although these rigorous searches did not unveil any extraterrestrial signals, the observations made, especially those by Howard et al. (2004) regarding pulse-emitting sources devoid of any repetitive patterns, are noteworthy. These occurrences were ascribed to the random fluctuations inherent in background processes.

2.3.3 Large projects

In the initial years, SETI was characterized by limited-scale investigations and intermittent financial support. Yet, as SETI gained global recognition, it paved the way for the development of ambitious projects with the goal of discovering signs of extraterrestrial life. In the following list, we briefly summarize some of these projects.

- **SERENDIP**: Search for Extraterrestrial Radio Emissions from Nearby Developed Intelligent Populations (SERENDIP) was a project launched in 1979 by the Berkeley SETI Research center (Bowyer et al., 1983). It focused on detecting stable narrowband spectral signals in the radio frequency spectrum that could be attributed to an alien civilization. Six versions of this project have taken place, each one being an upgrade of the previous version. The latest version, SERENDIP VI (Archer et al., 2016), has been installed in various telescopes worldwide, and its real-time multi-beam SETI spectrometer has provided

a data stream that keeps being utilized until recent days (e.g. Zhang et al., 2020; Wang et al., 2023).

- **The Phoenix Project:** Originally conceived as the NASA High-Resolution Microwave Survey (HRMS: Tarter and Gulkis, 1993), this initiative faced early termination after one year of its start (see Table 1.1). Nevertheless, it was revitalized through private contributions. The Phoenix Project covered around two billion channels for narrowband emissions within the 1.2 to 3.0 GHz frequency range, targeting approximately 800 stars within a 60 parsec radius. Despite the broad scope of this search, no signals of interest for further investigation were detected (Backus and Project Phoenix Team, 2002, 2004).
- **Breakthrough listen:** Breakthrough Listen¹ is the most comprehensive search for alien communications to date. It conducts searches across both radio and optical regimes. The project commenced in January 2016, with plans to span a decade. A notable milestone in 2016 was including the Five-hundred-meter Aperture Spherical Telescope (FAST) into the Breakthrough Listen framework. Situated in China, FAST is the world's largest single-dish radio telescope that became fully operational by 2020. One example of the SERENDIP VI real-time multi-beam SETI spectrometer is installed in this telescope.

2.4 The nine axes of merit for optical/radio searches

Both radio and optical approaches share the same philosophy: searching for artificially generated electromagnetic signals, whether they are anomalous pulses or exotic emission lines. Therefore, they have the same ranking in the nine-axes-of-merit framework that evaluates how favorable a method is based on the axes described in Section 1.2.4. Figure 2.3 illustrates how Radio/Optical searches fare within this framework.

- **Observing Capability and Cost:** Positively rated because these searches leverage existing astronomical instruments.
- **Ancillary Benefits:** Rated negatively, as these methods focus on parts of the parameter space that do not coincide with phenomena known in astrophysics.
- **Detectability:** The likelihood of detecting these signals is highly dependent on the distance from their source.
- **Duration:** Viewed negatively due to the continuous energy source requirement for signal transmission, which inherently restricts their potential duration.

¹<https://breakthroughinitiatives.org/>

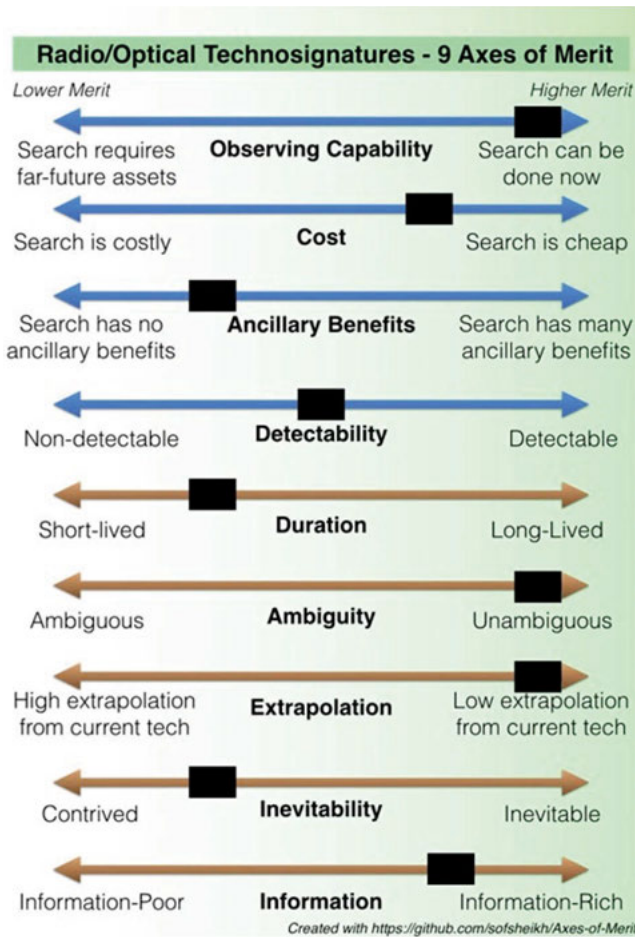


Figure 2.3. The nine axes of merit for radio/optical technosignatures (Sheikh, 2020). Image credit: Sofia Sheikh <https://github.com/sofsheikh/Axes-of-Merit>

- Ambiguity: Rated positively. Signals meant for communication are expected to be clearly distinguishable from natural cosmic sources, reducing confusion.
- Extrapolation: Positively assessed, as prior investigations into nearby targets have set upper bounds on the power of potential transmitters. These limits are comparable to the output of Earth’s most potent radio transmitters.
- Inevitability: Rated negatively because the act of sending intentional signals presupposes a certain level of sociological intent or behavior.
- Information: Viewed positively, under the assumption of intentionality behind the signals, suggesting they would contain some form of decodable information.

3. Artificial megastructures

In the early 1960s, Dyson (1960) introduced a novel concept for detecting extraterrestrial civilizations. He postulated that technologically advanced societies would eventually outgrow their planetary energy resources and begin harnessing the energy of their host star. Given that technological evolution progresses much faster than the lifespan of stars, Dyson reasoned that such civilizations might construct massive infrastructures later coined as “Dyson spheres” to capture stellar energy. These megastructures would emit infrared radiation, commonly referred to as “waste heat,” making them detectable from Earth.

The idea of Dyson spheres sparked further speculation and research into possible megastructures created by civilizations of Kardashev Types II and III, indicating an advanced level of technological capability to manipulate energy on a stellar or even galactic scale, but also regarding the purposes of building specific structures. For example, if we consider that the Universe is full of hazards that threaten life everywhere, such as the radiation emitted by supernovae or encounters with diffuse matter clouds, any civilization would be in potential danger. Because of this, “stellar engines” (Shkadov, 1988; Badescu and Cathcart, 2000), megastructures whose purpose is to alter the star’s movement in the Galaxy, have been proposed as a possibility to escape from these hazards (Kingsley, 1993).

3.1 Stellar engines

One of the pioneering concepts of a stellar engine was introduced by Shkadov (1988). Shkadov envisioned a parabolic mirror that would capture and reflect sunlight back toward the Sun. This reflection would create an asymmetric distribution of solar radiation pressure, exerting a net force on the Sun towards the direction of the mirror. Importantly, this system is designed to maintain its position relative to the Sun, as the forces of gravity and radiation pressure counterbalance each other.

At the beginning of the millennium, Badescu and Cathcart (2000) built upon the idea of a Dyson sphere, expanding its utility from an energy-capturing structure to a stellar engine capable of propelling a star. This concept took advantage of the idea developed by Shkadov (1988), and involves strategically placing a large mirror on a portion of

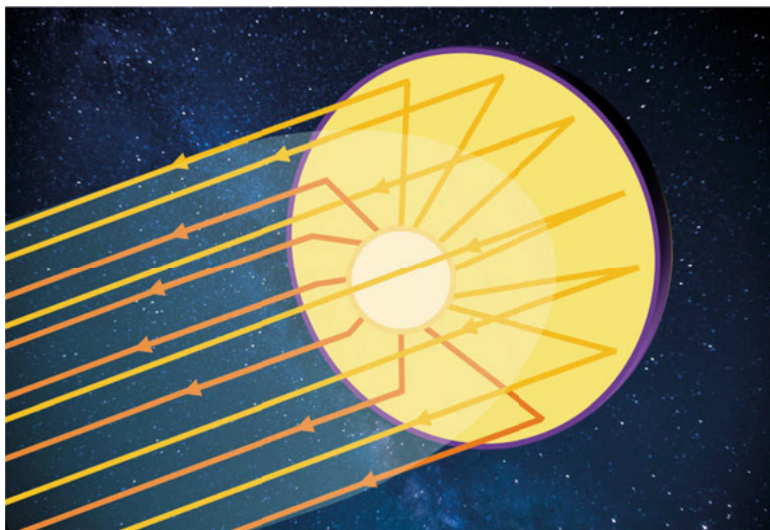


Figure 3.1. Artistic representation of a Shkadov thruster. Image credit: Rafael Vieira.

the Dyson sphere's surface. The key to this design is the creation of non-uniform reflections of stellar radiation by the mirror, which in turn generates thrust. This thrust is directed in such a manner as to move the central star, effectively turning the entire Dyson sphere and its star into a controllable propulsion system.

Further investigation into the stellar engines by Caplan (2019) revealed that the propulsion generated by these mechanisms would result in accelerations around $\sim 10^{-12}$ m/s² for stars comparable to the Sun. This level of acceleration might not be sufficient to circumvent imminent cosmic threats, such as the destructive force of nearby supernovae. In response, Caplan (2019) proposed a more powerful alternative: The Caplan thruster. This advanced engine would operate by harvesting hydrogen and helium from the stellar wind to fuel nuclear fusion reactions in order to create a propulsion jet. This machinery could produce accelerations around $\sim 10^{-9}$ m/s². Figure 3.1 features a conceptual visualization of a Shkadov thruster.

3.2 Dyson spheres

Based on his innovative concept of artificial megastructures, Dyson (1960) further speculated that these structures would absorb stellar radiation, to then subsequently re-emit this energy as black-body radiation within the 200 – 300 K temperature range, primarily in the infrared spectrum. Dyson postulated that stars embedded by such structures

would appear as distinctive infrared beacons. Additionally, Dyson estimated that constructing such an expansive artificial habitat could be achieved within a few millennia, drawing parallels with the resources of our Solar System. He theorized that the requisite materials could be acquired by dismantling planets, and suggested that a mass equivalent to that of Jupiter — approximately 2×10^{27} kg — would be adequate for the construction of these monumental structures.

Maddox et al. (1960) critiqued the concept of a monolithic Dyson sphere by highlighting its inherent instability. According to Gauss’s law, a perfectly spherical shell around a star would experience no net gravitational attraction. Yet, any deviation from perfect symmetry would lead to the structure’s collapse into the star. Following this argument, Wright (2020) tested the role of radiation pressure, showing that in the unrealistic scenario of a perfect isotropic radiator, no net force is exerted on the sphere, but still small deviations from perfect isotropy would doom the fate of the monolithic structure, e.g., from stellar winds.

The vision of Dyson spheres has evolved to include diverse interpretations of their potential configurations. Some researchers, such as Suffern (1977) and Badescu (1995), imagined these structures as habitable biospheres, while others focused on optimizing their ability for energy capture and its use.

Modern visions of Dyson spheres picture them not as singular absorbing elements but as large collections of individual panels. These panels could be assembled incrementally to form a “Dyson Bubble” — a stationary configuration relative to the star, stabilized by radiation pressure against gravitational pull. Such an arrangement would prevent the panels from colliding or casting shadows on each other, allowing for adjustable distances from the star. Alternatively, a “Dyson Swarm” comprises panels in dense orbital formation around the star, representing the modern interpretation of a Dyson sphere. This configuration is illustrated in Figure 3.2, which depicts a monolithic shell, a Dyson bubble, and a Dyson swarm.

Armstrong and Sandberg (2013) provided an analysis of how one might conceivably construct a Dyson swarm within the Solar System, by dismantling Mercury to provide the required material. Their rationale includes Mercury’s abundant resources for panel production, its low surface gravity which would facilitate panel launch, and the feasibility of disassembling the planet within approximately 32 years.

3.2.1 The thermodynamics of Dyson spheres

Many articles on Dyson spheres arose after Dyson (1960)’s seminal work. However, just a few of them studied the thermodynamics of Dyson

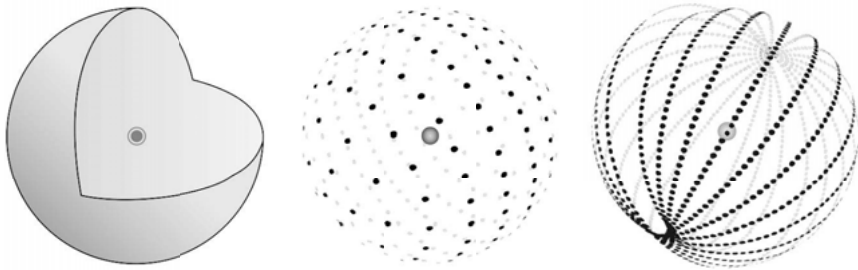


Figure 3.2. Representation of some of the schemes proposed for a Dyson sphere. From left to right, we have a Dyson shell, a Dyson bubble, and a Dyson swarm. Image credit: Rafael Vieira.

spheres. In this subsection, we review some of the thermodynamics considered in the function of Dyson spheres.

Dyson spheres embedded in thermal baths

In order to estimate the optimum radius of a Dyson sphere, Badescu (1995) studied the thermodynamics of Dyson spheres. He considered two engines as the process by which Dyson spheres could work, the Carnot engine (Carnot, 1960), and the Chambadal–Novikov–Curzon–Ahlborn (CNCA) engine (Novikov, 1958; Curzon and Ahlborn, 1975; De Vos, 1985). The Carnot engine produces work W through cycles of heating and cooling gas in a piston by alternately making contact with two thermal baths, one at a higher temperature (T_H) and the other at a lower temperature (T_C). This process, involving isothermal expansion (when the gas exchanges heat with the thermal baths) and adiabatic expansion/contraction (when the gas changes volume without heat exchange), serves as a theoretical benchmark for the highest efficiency possible for heat engines, which is given by Equation 3.1,

$$\eta_{\text{Carnot}} = 1 - \frac{T_C}{T_H}, \quad (3.1)$$

where η_{Carnot} is the efficiency of the Carnot engine, T_C the temperature of the cold bath, and T_H the temperature of the hot thermal bath.

On the other hand, the Chambadal–Novikov–Curzon–Ahlborn engine accounts for more real-world factors like thermal conductivity and temperature gradients, considering the addition of the heat flow in the computation of the efficiency. The heat flow between the thermal baths and the gas piston is $\dot{Q} = k(T_{H/C} - T_G)$, where \dot{Q} is the heat flow, k is

the heat conductivity, and T_G the temperature of the gas. In the case of a Dyson sphere considered as a Carnot or CNCA engine, $T_C = T_r$, the temperature of the Dyson sphere, the one that shapes the spectral energy distribution that we could observe, and $T_H = T_0$ is the background or “sky” temperature. By taking into account the heat flow, the efficiency (e.g., Curzon and Ahlborn, 1975) of the engine becomes

$$\eta_{\text{CNCA}} = 1 - \sqrt{\frac{T_C}{T_H}} = 1 - \sqrt{1 - \eta_{\text{Carnot}}}. \quad (3.2)$$

By considering both engines, Badescu (1995) determined the minimum radii for Dyson spheres at which they would be able to produce work that can be utilized. Remarkably, the minimum radius is the same for both the Carnot and the Chambadal–Novikov–Curzon–Ahlborn engines, which is

$$r_{\min} = \frac{(1 - \theta_0^4)^{1/2}}{\theta_0^2} R_\star, \quad (3.3)$$

where r_{\min} is the minimum Dyson sphere radius, R_\star is the radius of the star, and θ_0 is equal to the ratio T_0/T_\star , where T_\star is the temperature of the star. Figure 3.3 illustrates the behavior of Equation 3.3 using the Solar System as a reference with $T_\star = 5760$ K, and $R_\star = 4.65 \cdot 10^{-3}$ AU. Notice that if we increase the size of the structure, then T_C decreases, and the efficiency increases (for both engines introduced in this section). Nevertheless, the amount of material required to build the structure quickly increases (proportional to r^2), an inconvenience that has also been noted by other works (e.g., Lacki, 2016). By considering this fact, Badescu (1995) recommends building spheres slightly bigger than r_{\min} . Finally, Badescu (1995) provides the Carnot and the Chambadal–Novikov–Curzon–Ahlborn efficiencies as a function of the temperatures involved in the thermodynamic processes behind Dyson spheres. Equations 3.4 and 3.5 represent the Carnot and the CNCA efficiency as a function of T_0 , T_r , and T_\star :

$$\eta_{\text{Carnot}} = \left(1 - \left(\frac{T_0}{T_\star}\right)^4\right) \left(1 - \frac{T_r}{T_0}\right) \quad (3.4)$$

and

$$\eta_{\text{CNCA}} = \left(1 - \left(\frac{T_0}{T_\star}\right)^4\right) \left(1 - \sqrt{\frac{T_r}{T_0}}\right). \quad (3.5)$$

Harvesting thermal radiation

Although considering a Dyson sphere as a Carnot or a Chambadal–Novikov–Curzon–Ahlborn engine provides useful insight into the con-

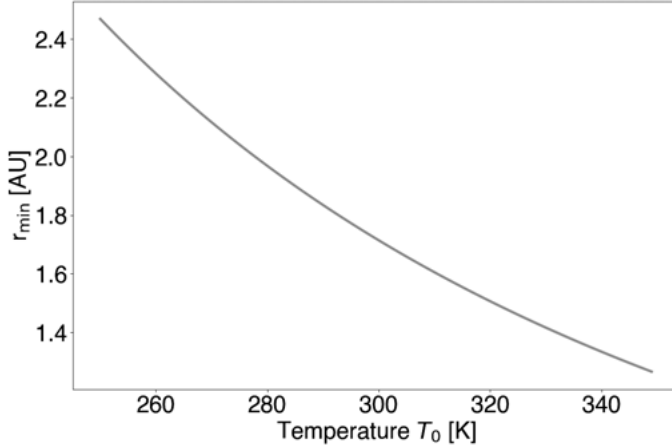


Figure 3.3. Minimum possible radius for a Dyson sphere r_{\min} as a function of the background temperature T_0 .

siderations one should have when building one, various authors (Badescu, 2014; Buddhiraju et al., 2018; Wright, 2020, 2023) have noted that the harvesting of energy from an infinite heat capacity thermal bath at fixed temperature differs from energy harvesting from thermal radiation, since in the latter case, the entropy of the input radiation must be taken into account. For radiation, the energy flux is

$$F = \sigma T^4, \quad (3.6)$$

and the entropy per time per surface area escaping from a blackbody is

$$\dot{s} = \frac{4}{3}\sigma T^3. \quad (3.7)$$

In these equations F is the energy flux, \dot{s} is the entropy per time per surface area, σ is the Stefan–Boltzmann constant, and T is the blackbody temperature of the radiation.

In order to provide an insight into how the entropy flux changes in the Badescu (1995) analysis, we adopt the formalism developed by Landsberg and Tonge (1980) that was later applied specifically to Dyson spheres by Wright (2023). The reader might refer to Wright (2023) for a more detailed explanation of the thermodynamics of Dyson spheres. The rest of this section will be devoted to summarize and explain the key aspects of the Landsberg formalism as applied to Dyson spheres.

First of all, when considering converting radiation into work, the Landsberg formalism uses six parameters to describe the thermodynamic process governing work extraction from radiation. These parameters are the following:

- Energy flux into the system \dot{E}_{in}

- Entropy flux into the system \dot{S}_{in}
- Energy flux out of the system \dot{E}_{out}
- Entropy flux out of the system \dot{S}_{out}
- Heat flux of the system into the environment \dot{Q}
- The system's work rate \dot{W} . This parameter has no associated corresponding entropy flux.

Additionally, the mechanism itself has four properties associated with its inner ongoing processes:

- \dot{E} , the internal energy rate change
- \dot{S} , the internal entropy rate change
- T , the temperature on the boundaries of the machine
- \dot{S}_g the rate of entropy generated by the machine

From balance equations, the abovelisted parameters are related as follows:

$$\dot{E}_{\text{out}} = \dot{E}_{\text{in}} - \dot{E} - \dot{Q} - \dot{W}, \quad (3.8)$$

and

$$\dot{S}_{\text{out}} = \dot{S}_{\text{in}} - \dot{S} - \dot{Q}/T + \dot{S}_g. \quad (3.9)$$

Wright (2023) highlighted essential considerations for applying the Landsberg formalism to Dyson spheres. First, Dyson spheres only capture radiation from a constrained range of solid angles, especially when conceptualized as a swarm. Moreover, it is crucial that Dyson spheres expel energy exclusively outward to avoid altering the energy balance of the star (Wright, 2020; Huston and Wright, 2021) or causing internal issues within the Dyson sphere itself. This directional control of energy discharge is facilitated by using circulators, devices engineered to ensure that energy exits through a port subsequent to the one it entered. Wright (2020) also emphasized that Dyson spheres are required to radiate most accumulated energy outward. Accumulating vast amounts of energy could lead to the structures becoming chemically and gravitationally unbound, posing a risk to the stability and integrity of the structure and the civilization.

In this application of the Landberg formalism, it is assumed that a Dyson sphere consists of an extensive array of satellites. Each satellite can be visualized as a flat “solar panel” oriented towards the star for energy collection, complemented by a radiator positioned to dissipate heat away from it. The swarm is modeled as being in a thin sphere around the star at a radius R . Stars are modeled to emit radiation as simple blackbodies, characterized by a temperature T_\star and a luminosity $L = 4\pi R_\star^2 \sigma T_\star^4$, where R_\star is the radius of the star.

If steady state and global energy conservation are assumed, some of the values listed above become:

$$\dot{Q} = 0, \quad (3.10)$$

$$\dot{E} = 0, \quad (3.11)$$

$$\dot{S} = 0, \quad (3.12)$$

$$\dot{E}_{\text{in}} = \dot{E}_{\text{out}} + \dot{W}. \quad (3.13)$$

Notice that \dot{Q} is null because there is no ambient environment to share heat with, except deep space, which is already considered in \dot{E}_{out} and \dot{S}_{out} . Additionally, in the context of analyzing structures that may not always conform to spherical geometries, Wright (2023) recommends interpreting terms like \dot{E} in units of energy per time, rather than flux, and that area should be explicitly incorporated into the analysis to avoid confusion in any calculation.

Figure 3.4 illustrates how the input and output parameters flow in the Landsberg formalism, as well as the theoretical values associated with some components. As explained in the above paragraphs, we can relate various energy and entropy fluxes to the parameters of the central star and the Dyson sphere:

$$\dot{E}_{\text{in}} = 4\pi R_{\star}^2 \sigma T_{\star}^4, \quad (3.14)$$

$$\dot{S}_{\text{in}} = 4\pi R_{\star}^2 \frac{4}{3} \sigma T_{\star}^3, \quad (3.15)$$

$$\dot{E}_{\text{out}} = 4\pi R^2 \sigma T^4, \quad (3.16)$$

$$\dot{S}_{\text{out}} = 4\pi R^2 \frac{4}{3} \sigma T^3. \quad (3.17)$$

Within the framework of the Landsberg schema, the factor \dot{W} , represents the work rate, and its numerical definition varies based on the specific activity under consideration. Wright (2023) considers three main scenarios: activities involving computation only, dissipative activities, and work that leaves the sphere.

Computations

In activities considering computations, the work generated by the structure does not leave the Dyson sphere, and it is used by the structure itself to perform calculations. Since everything stays in the sphere, this implies $\dot{W} = 0$. Waste heat leaves the structure, but it is already accounted for in \dot{E}_{out} and \dot{S}_{out} . The balance equation in the steady state then implies,

$$\dot{E}_{\text{in}} = \dot{E}_{\text{out}}, \quad (3.18)$$

which allows us to determine the temperature of the Dyson sphere (associated with the waste heat),

$$T = \sqrt{\frac{R_{\star}}{R}} T_{\star}, \quad (3.19)$$

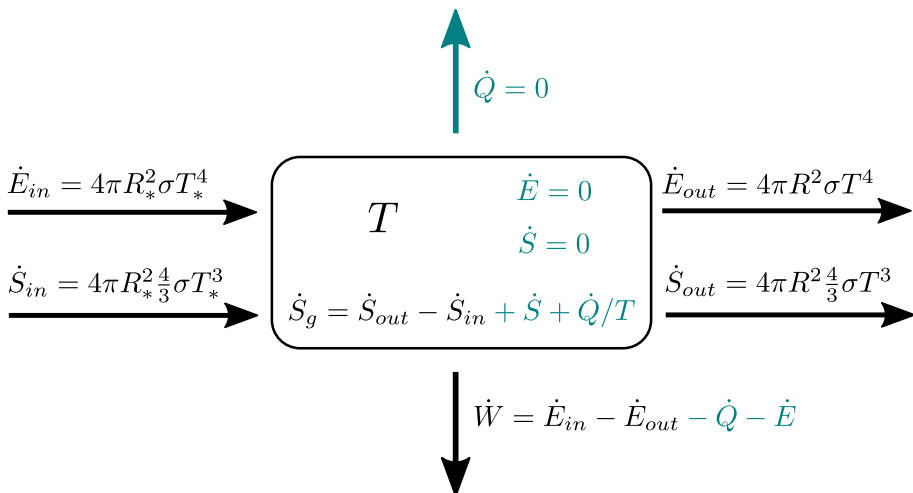


Figure 3.4. Schematic image reproduced from Wright (2023) showing energy and entropy flow inputs and outputs in a radiation work extraction, reproduced with permission. Green parameters depict all components that vanish in a steady state. CC BY-SA 4.0.

where R is the distance from the center of the star to the Dyson sphere, and T_* and R_* are the temperature and radius of the central star, respectively.

Given the significance of entropy generation in the Landsberg formalism, the Landauer limit (Landauer, 1961) is an essential concept for quantifying the entropy produced. The Landauer principle postulates that the minimum amount of energy dissipated during a single binary operation is $kT \ln 2$, where k is the Boltzmann constant, T is the temperature at which the operation is performed, and $\ln 2$ is a factor that arises from the binary nature of the operation. This theoretical limit has been validated through experimental evidence (Berut et al., 2012; Jun et al., 2014) and is the consequence that each binary logical operation generates entropy $S = k \ln 2$.

If we define r as the number of computations performed by the structure, then the entropy flow generated by the machine can be obtained by using the balance equation and applying the Landauer limit,

$$\dot{S}_g = \dot{S}_{out} - \dot{S}_{in} = r k T \ln 2, \quad (3.20)$$

where T is the temperature associated with the Dyson sphere. Then, we can apply Equations 3.15 and 3.17 to find the number of calculations performed,

$$r = \frac{4}{3} \frac{L}{k T \ln 2} \left[1 - \frac{T}{T_*} \right] = \frac{4}{3} \frac{L}{k T \ln 2} \eta_{\text{Carnot}}. \quad (3.21)$$

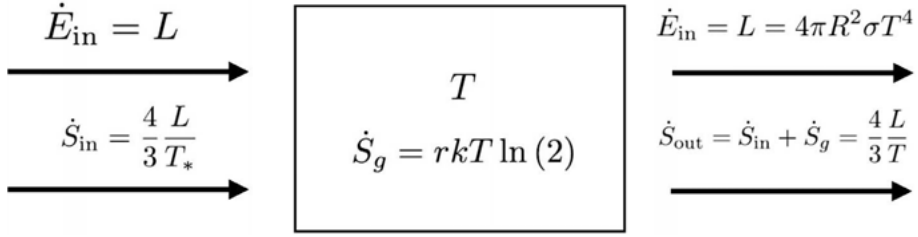


Figure 3.5. Thermodynamic schema for a Dyson sphere performing pure computation. Image adapted from Wright (2023). CC BY-SA 4.0.

The formulation obtained for r suggests that the Dyson sphere operates with Carnot efficiency when extracting work, which is then utilized to perform computations at the cost of $(3/4) \cdot kT \ln 2$ per calculation. In Figure 3.5, the flow of parameters within a Dyson sphere dedicated solely to computational work is illustrated, providing a visual representation of how energy and entropy interact in the context of a Dyson sphere's operation as a computational entity.

Dissipative activities

Dissipative activities encompass a broad range of actions that ultimately result in dissipation in the form of heat. Essentially, this category includes any activity where the energy used by devices or biological mechanisms is converted into heat as a byproduct of their operation. In this case, \dot{W} is also null since no work leaves the Dyson sphere. To understand how the Landsberg formalism applies to this scenario, the most convenient way to do such analysis is by breaking the system into two parts: a work extractor that generates $\dot{W}_{\text{internal}}$ and the engine, which is the part that makes use of this work, and eventually dissipates as heat. Since the system has been split into two parts, their associated energy and entropy flows do as well. We use the subscript 1 to denote quantities related to the work extractor and the subscript 2 for the engine. If we assume the work extractor works at maximum efficiency, then it does not produce entropy ($\dot{S}_{g,\text{extractor}} = 0$), and the balance equations become,

$$\dot{E}_{\text{in}} = \dot{E}_{\text{out},1} + \dot{E}_{\text{out},2} = L, \quad (3.22)$$

and

$$\dot{S}_{\text{in}} = \dot{S}_{\text{out},1}. \quad (3.23)$$

Additionally, an extra factor f is introduced to account for the fraction of the surface of the Dyson sphere that is being dedicated to passing along the entropy received by the extractor that was originally entropy from the star. Concurrently, the resulting work goes to the engine that eventually radiates the energy away using the remaining factor $(1 - f)$.

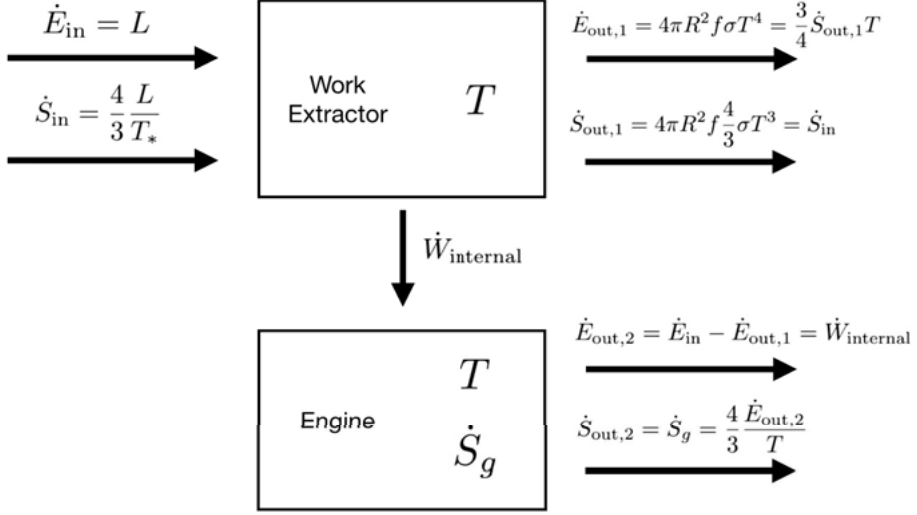


Figure 3.6. Thermodynamic schema for a Dyson sphere performing dissipative work. In this case, the system is broken into two parts: the work extractor and the engine. Image adapted from Wright (2023). CC BY-SA 4.0.

Figure 3.6 illustrates the thermodynamic processes undergoing dissipative activities and shows how the energy and entropy flows are affected by breaking the system into two parts, which is accounted for in the f factor.

Then, Equations 3.22 and 3.23 can be used to solve for f , T , to obtain the value of the internal work rate $\dot{W}_{\text{internal}}$, which is critical for assessing the efficiency of the work extractor within the Dyson sphere system,

$$T = \sqrt{\frac{R_{\star}}{R}} T_{\star}, \quad (3.24)$$

$$f = \frac{T}{T_{\star}}, \quad (3.25)$$

$$\dot{W}_{\text{internal}} = \dot{E}_{\text{in}} - \dot{E}_{\text{out},1} = (1 - f)L, \quad (3.26)$$

therefore,

$$\eta = \frac{\dot{W}_{\text{internal}}}{\dot{E}_{\text{in}}} = 1 - \frac{T}{T_{\star}}, \quad (3.27)$$

which corresponds to the Carnot efficiency.

Work that leaves the sphere

In scenarios where the primary function of the Dyson sphere is to perform work that exits the system, such as emitting radio waves for communication purposes, the thermodynamic framework undergoes a slight

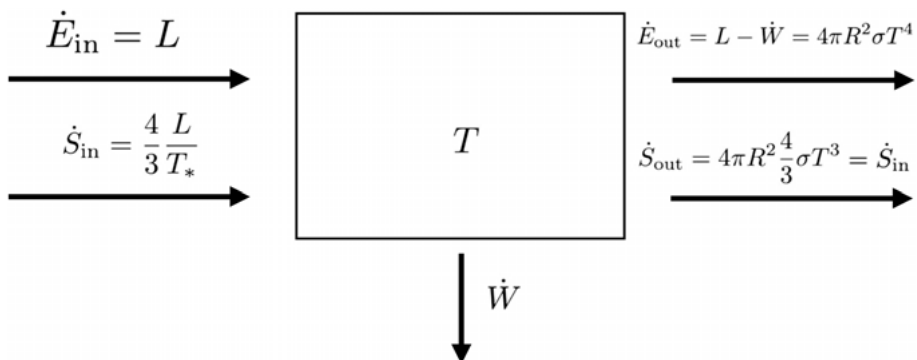


Figure 3.7. Thermodynamic schema for a Dyson sphere performing work that leaves the system. There is no engine since all work leaves the work extractor. Image adapted from Wright (2023). CC BY-SA 4.0.

adjustment. While the underlying thermodynamic principles remain consistent with the previous system, the configuration changes due to the absence of an internal engine and the adoption of $f = 1$. This setup implies that all the work the sphere does, denoted as \dot{W} , is directed outwards, leaving no portion of the energy to be re-utilized or stored within the system. Figure 3.7 visually represents this process, illustrating how the Dyson sphere channels its energy output externally to achieve its intended purpose, e.g., interstellar communication. Following the same reasoning as before and by considering $f = 1$, we obtain,

$$T = \left(\frac{R_*}{R} \right)^{\frac{2}{3}} T_*, \quad (3.28)$$

$$\dot{W} = L \left(1 - \frac{T}{T_*} \right), \quad (3.29)$$

which yields again the Carnot efficiency,

$$\eta = 1 - \frac{T}{T_*}. \quad (3.30)$$

Since the temperature dependence with radius is different in this case, and since $\sqrt{x} < x^{2/3}$ if $x > 1$, then the temperature of the Dyson sphere is lower, therefore more efficient than the dissipative case.

Considering a swarm

If we consider a Dyson sphere as an incomplete swarm located at a distance that spans a large range of distances, then many of the factors derived in the previous sections must be scaled to account for the reduced number of absorbing units and for the shadowing between the

units. If we assume that the total cross-sectional area of the swarm is A ($\leq 4\pi R^2$). In the ideal case, the elements of the swarm will never shadow each other, and as their number increases, they will need to make elaborate maneuvers to avoid this. If we assume that panels regularly block each others' views, then we might expect this to result in the swarm having an optical depth

$$\tau = \frac{A}{4\pi R^2}. \quad (3.31)$$

Therefore, the total energy collected will be multiplied by a factor $(1 - e^{-\tau})$, and many parameters must be scaled to account for that. The efficiency in this scenario becomes

$$\eta = (1 - e^{-\tau}) \left[1 - \frac{T}{T_\star} \right]. \quad (3.32)$$

The number of computations is also affected

$$r = \frac{4}{3} \frac{L}{kT \ln(2)} (1 - e^{-\tau}) \left[1 - \frac{T}{T_\star} \right] \quad (3.33)$$

In summary, the thermodynamics of Dyson spheres might seem simple, but there are many assumptions that make it so by design. More realistic assumptions could affect the usage of the Landsberg formalism that, in the end, yielded Carnot efficiencies. There are some considerations that could improve the performance of the Dyson sphere and avoid unbalancing the stellar structure via feedback, such as the use of optical circulators. Activities might also be done directly with photons, avoiding the need to run heat engines between intermediate absorbers heated and cooled by radiation, wasting energy during the extraction process. In the case that Dyson spheres are composed of swarms capturing most of the star's light, they likely have optical depths that must be considered.

3.2.2 Simple Dyson sphere models

As mentioned earlier, when discussing a Dyson sphere, we visualize it as a swarm of panels orbiting a star. To identify potential Dyson spheres, it is crucial to understand their expected behavior. For this purpose, we adopt the simplified assumption that Dyson spheres can be modeled as blackbodies, also provided in Paper I, meaning their spectra follows the Planck's law,

$$B_\lambda(T) = \frac{2hc^2}{\lambda^5} \frac{1}{e^{\frac{hc}{\lambda k_B T}} - 1}, \quad (3.34)$$

where B_λ is the spectral radiance as a function of the wavelength λ , h is the Planck constant, c is the speed of light, k_B is the Boltzmann constant, and T is the temperature of the blackbody. By assuming that a Dyson sphere emits as a blackbody, its spectrum depends only on its temperature.

However, in order to compare how predominant the radiation from the Dyson sphere is relative to its host star, we need the luminosity of the Dyson sphere (DS) so that the spectrum can be scaled. So, the luminosity of the Dyson sphere (L_{DS}) becomes another free parameter we must consider when creating models. Therefore, we then define a more convenient parameter, which is the covering factor (γ), the fraction of the luminosity of the star that is being re-radiated by the Dyson sphere, that is to say

$$\gamma = \frac{L_{\text{DS}}}{L_\star}, \quad (3.35)$$

where gamma is the fraction of re-emitted energy, L_{DS} is the bolometric luminosity of the Dyson sphere, and L_\star is the intrinsic bolometric luminosity of the star. For fully complete Dyson spheres $\gamma = 1$, and for partial Dyson spheres γ can take values between 0 and 1. The γ factor represents the fraction of the stellar radiation that the Dyson sphere is re-emitting. In the case of an isotropically radiating Dyson sphere, γ also represents the fractional solid angle of outgoing radiation intercepted by the Dyson sphere (the covering factor) or the level of completion of the Dyson sphere. The Dyson swarm and the Dyson Bubble in Figure 3.2 represent examples of a Dyson sphere with $0 < \gamma < 1$.

We know from Equation 3.35 that the luminosity of a Dyson sphere can be expressed in terms of the covering factor and the luminosity of the host star. However, since Dyson spheres are treated as blackbodies, their luminosity can be derived by using the Stefan-Boltzmann law given by

$$L_{\text{DS}} = \gamma 4\pi R_{\text{DS}}^2 \sigma T_{\text{DS}}^4, \quad (3.36)$$

where L_{DS} is the luminosity of the Dyson sphere, R_{DS} is its radius, T_{DS} is its temperature, and γ is the covering factor. When referring to partial Dyson spheres, their blackbody emission becomes a fraction of the complete version, hence the γ factor in the Equation. Since we have two expressions for the luminosity of a Dyson sphere, we can use both to find the dependency of the Dyson sphere parameters and the host stellar parameters. By comparing Equations 3.35 and 3.36 and assuming that a star emits as a black-body as well, we end up with

$$\gamma = \frac{\gamma 4\pi R_{\text{DS}}^2 \sigma T_{\text{DS}}^4}{4\pi R_\star^2 \sigma T_\star^4}, \quad (3.37)$$

which turns into

$$R_{\text{DS}} = \left(\frac{T_{\star}}{T_{\text{DS}}} \right)^2 R_{\star} \iff T_{\text{DS}} = \sqrt{\frac{R_{\star}}{R_{\text{DS}}}} T_{\star}. \quad (3.38)$$

Equation 3.38 provides the dependency between the radius of a Dyson sphere (R_{DS}), its temperature (T_{DS}) and the stellar radius (R_{\star}) and temperature (T_{\star}). As an example, if we were to build a Dyson sphere in the Solar System at 1 AU, its temperature would be $T_{\text{DS}} \approx 390$ K. Likewise, if we wish to build a Dyson sphere that has a temperature of 600 K, we should locate it ≈ 0.43 AU from the Sun. Notice that T_{DS} corresponds to the same value derived in Section 3.2.1 when using the Landberg formalism to determine the temperature of the Dyson sphere when computations and dissipative activities are considered.

Dyson spheres are also treated as grey absorbers, i.e., the radiation of host star is equally dimmed at every wavelength. Since they block a γ factor of the star, only a factor $(1 - \gamma)$ is allowed to escape. The luminosity of the star as seen from us is modified as

$$L_{\text{bol},\star} \rightarrow (1 - \gamma)L_{\text{bol},\star} \quad \text{and} \quad L_{\nu,\star} \rightarrow (1 - \gamma)L_{\nu,\star}. \quad (3.39)$$

If we consider the characteristics of a Dyson sphere, including its temperature (T_{DS}), the degree to which it obscures the host star and its luminosity (both associated to γ), we can model the spectrum of stars that hypothetically host Dyson spheres with parameters T_{DS} and γ . The aggregate spectrum of this system is the sum of the spectral contributions from each component. While the intrinsic shape of the spectral energy distribution of the star remains intact, its specific luminosity is diminished by a factor of $1 - \gamma$ due to the assumption of a gray absorber. Given that the spectrum of the Dyson sphere is treated as blackbody radiation at a specified effective temperature, the specific luminosity of the combined system can be expressed as:

$$L_{\nu} = (1 - \gamma)L_{\nu,\star} + \gamma BB_{\nu}(T_{\text{DS}}, L_{\text{DS}}), \quad (3.40)$$

where L_{ν} is the specific luminosity of the combined DS+star system, $L_{\nu,\star}$ is the specific luminosity of the star before being obscured, γ is the covering factor, L_{DS} is the bolometric luminosity of the DS, T_{DS} is the temperature of the DS, and $BB_{\nu}(T, L)$ is the specific luminosity for a blackbody-like source with a given temperature (T) and bolometric luminosity (L). Notice that this model is independent of the complex thermodynamics governing the energy harvest presented in Section 3.2.1 as we are considering T_{DS} as a free parameter, which would be equivalent to T from Figure 3.4.

From Equation 3.40, we are equipped to model the spectral energy distribution of any star hosting a Dyson sphere with fixed parameters

(T_{DS}, γ) . This method enables the investigation of different theoretical configurations of Dyson spheres and their observable effects on stellar photometry and spectroscopy. By comparing these models to actual survey data, we can effectively search for and potentially identify candidates that exhibit characteristics consistent with the presence of Dyson spheres.

Figure 3.8 presents some illustrative examples of how the photometry of a Sun-like blackbody spectrum ($T_{\text{eff}} = 5778 \text{ K}$ and $L_{\star} = 1 L_{\odot}$) is altered in the presence of a Dyson sphere, under various assumptions concerning the Dyson sphere temperature and covering factor. In both panels, the spectrum of a Sun-like blackbody is depicted for comparison. The top panel illustrates changes in the combined spectrum resulting from a Dyson sphere with a constant temperature of 300 K and varying covering factors of $\gamma = 0.1, 0.5, \text{ and } 0.9$. The presence of the Dyson sphere is marked by an enhancement in the mid-infrared region and a reduction in the luminosity of the stellar component, with the extent of both effects contingent on the covering factor of the sphere. This reduction is most noticeable in the optical and near-infrared ranges.

In the bottom panel, variations in the spectrum are shown for Dyson sphere models with a consistent covering factor of 0.5 and Dyson sphere temperatures of 100, 300, and 600 K. The aforementioned characteristics—a decrease in stellar flux and an increase in mid-infrared emission—are observed. With different Dyson sphere temperatures considered, the peak of the mid-infrared blackbody shifts in wavelength according to the Dyson sphere temperature. Nonetheless, within the selected temperature spectrum, the infrared excess remains within the observable wavelength range of the WISE mission, demonstrating how the characteristics of Dyson Spheres might be detected and analyzed using current astronomical survey data. Notice that these are the models that we apply in our upper limits estimation (Chapter 5) and the search for anomalous infrared sources (Chapter 6).

3.2.3 Dyson sphere searches

Although the concept of Dyson spheres was introduced in 1960, the absence of infrared space surveys limited any opportunity to search for such structures at that time.

It was not until twenty-five years later that the first search for Dyson spheres was reported, facilitated by the launch of the Infrared Astronomical Satellite (IRAS: Neugebauer et al., 1984). As the first space telescope to survey the sky at infrared wavelengths, IRAS significantly advanced our capability to search for Dyson spheres. Initial investigations focused on sources within the Milky Way but eventually expanded

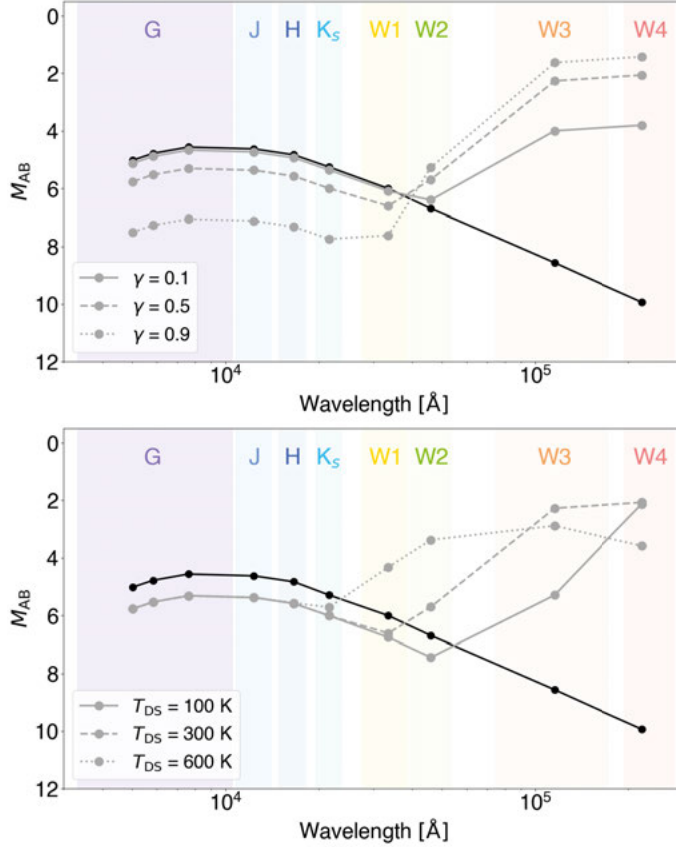


Figure 3.8. Modified Sun-like blackbody photometry due to the presence of Dyson spheres with various characteristics. In both panels, the black solid line represents the unmodified blackbody ($T_{\text{eff}} = 5778 \text{ K}$, $L_{\star} = 1 L_{\odot}$). In the top panel, DS models with a temperature of $T = 300 \text{ K}$ and covering factors of 0.1, 0.5, and 0.9 are depicted with grey solid, dashed, and dotted lines, respectively. In the bottom panel, DS models with a covering factor of 0.5 and temperatures of 100, 300, and 600 K are depicted with grey dotted, dashed, and solid lines, respectively. The colored bands represent the wavelength intervals relevant to the Gaia, 2MASS, and WISE missions. Adapted from Paper II.

to include extragalactic sources, i.e., Kardashev Type III civilizations. The following sections summarize these exploratory efforts, detailing the searches conducted at both galactic and extragalactic distances.

Galactic searches

Slysh (1985) initiated the first search for Dyson spheres using IRAS data, identifying five infrared sources with temperatures consistent with blackbodies between 200 - 350 K. Slysh noted that these sources could be confused with circumstellar dust shells around red giants, and suggested that additional data would be necessary to eliminate false positives.

A decade and a half later, Timofeev et al. (2000) undertook another search, analyzing the 3000 brightest IRAS sources. They observed that most sources fitted temperatures near 110 and 280 K, with 110 K sources predominantly in the galactic plane and 280 K sources more dispersed but not exclusively outside the galactic plane. They echoed Slysh's caution regarding the potential confusion with circumstellar dust shells around red giants, and recommending further observations for clarification.

Simultaneously, Jugaku et al. (1995), Jugaku and Nishimura (1997), and Jugaku and Nishimura (2000) adopted a different approach, using the $K - [12]$ color to identify mid-infrared excesses in candidates. They sourced K data from the Catalog of Infrared Observations and later updated these values with 2MASS data in Jugaku and Nishimura (2004a), analyzing 384 solar-type stars within 25 pc. They posited that a source radiating 10% of its host star's radiation as waste heat should exhibit a $K - [12]$ color shift greater than 1 magnitude, yet found no sources meeting this criterion. Notice that Jugaku and Nishimura (2004b) were the first to consider partial Dyson spheres, i.e., $\gamma < 1$.

Carrigan (2009) set the first upper limits on the prevalence of Dyson spheres by examining photometric data from IRAS, concluding that fewer than 1 in 10,000 of the approximately 250,000 IRAS sources could be Dyson spheres based on their infrared fluxes. Carrigan's detailed analysis of the IRAS low-resolution spectrometer data led to the identification of 16 "somewhat interesting sources," focusing on the potential for fully formed Dyson spheres which would exhibit pure thermal blackbody emission and completely obscure the host star.

Zackrisson et al. (2018) approached the search for Dyson spheres by comparing spectrophotometric and trigonometric distances, theorizing that discrepancies between these measures could indicate partial obscuration by a Dyson sphere. This method relies on the premise that the trigonometric parallax reveals the actual distance, whereas the spectrophotometric distance might be overestimated due to partial obscuration.

As part of this thesis, we unveil the most recent and extensive search for galactic Dyson spheres to date, identifying seven candidates of unknown nature. For a detailed exploration of these findings, please refer to the papers included in this thesis (Section III).

Extragalactic searches

Searches for extragalactic artificial megastructures have been pursued as well, employing strategies akin to those used for Dyson spheres within the Milky Way. Wright et al. (2014b), Wright et al. (2014a), and Griffith et al. (2015) conducted investigations into galaxies exhibiting an excess of infrared radiation, mirroring the methodology applied to individual Dyson sphere. Additionally, Annis (1999) and Zackrisson et al. (2015) embarked on searches for Kardashev Type III civilizations by identifying galaxies that deviate from established scaling laws. Conversely, Garrett (2015) and Chen and Garrett (2021) considered the ratios between galaxies' infrared and radio fluxes as potential indicators of such advanced civilizations.

3.2.4 Alternative power sources for Dyson spheres.

Dyson spheres are commonly linked with main-sequence stars, as astrophysicists often conceptualize these artificial structures within the context of the Solar System. This association originates from the belief that main-sequence stars, similar to our Sun, offer the most hospitable conditions for life, making them prime candidates for constructing such megastructures. However, despite the conventional wisdom that other types of stellar hosts might not offer favorable conditions for life due to their extreme environments, numerous authors have explored the theoretical possibility of Dyson spheres existing around different stellar objects. These include **X-ray binaries** (Imara and Di Stefano, 2018), **White dwarfs** (Semiz and Oğur, 2015; Zuckerman, 2022), **Pulsars** (Osmanov, 2016), **Stellar black holes** (Opatrný et al., 2017; Hsiao et al., 2021), and **Supermassive black holes** (Inoue and Yokoo, 2011).

3.3 The nine axes of merit for waste heat searches

Here we rank waste heat radiation produced by artificial megastructures (e.g., Dyson sphere) on the nine-axes-of-merit framework that consists of evaluating how favorable a method is based on each one of the nine axes described in Section 1.2.4.

- Observing capability, cost and detectability: favorably, because these searches can be done with existing large databases.

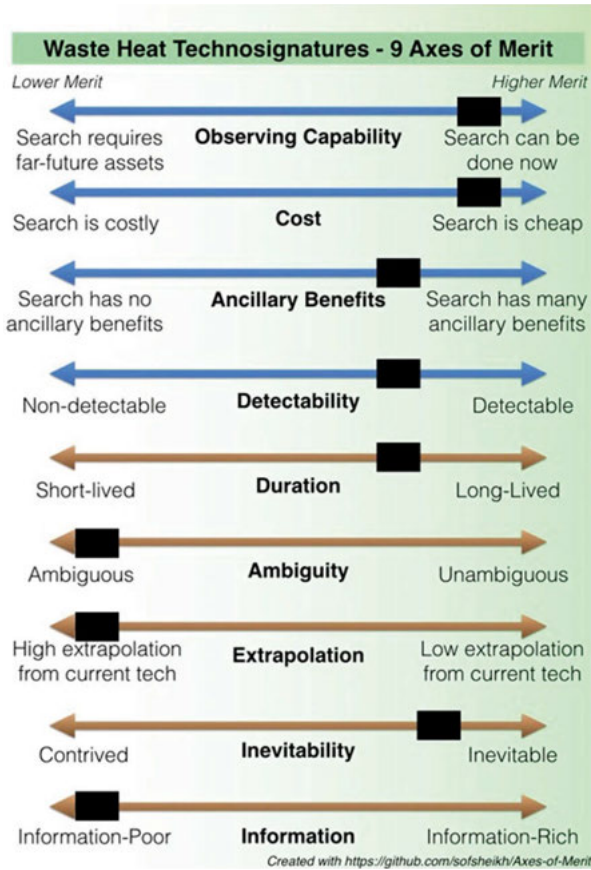


Figure 3.9. The nine axes of merit for waste heat technosignatures (Sheikh, 2020). Image credit: Sofia Sheikh <https://github.com/sofsheikh/Axes-of-Merit>

- Ancillary benefits: favorably, because candidates that turn out not to be Dyson spheres may still be interesting for other astrophysics fields.
- Duration: favorably because Dyson spheres can be very long-lived.
- Ambiguity: unfavorably, because many natural sources emit mid-infrared radiation.
- Extrapolation: unfavorably, because we have not built a Dyson sphere in our Solar system.
- Inevitability: favorably, because the laws of thermodynamics are always valid, so a megastructure will always produce waste heat.
- Information: unfavorably, because if we were to find one, we would not necessarily have any insight about the civilization beyond the fact that they have reached the technological level to build one.

Figure 3.9 shows how waste heat searches are ranked along the nine axes of merit.

Part II: Infrared excess stars

The primary aim of this thesis is to identify astronomical sources exhibiting characteristics akin to Dyson spheres, particularly in the form of an infrared excess. This signature trait was initially suggested in the seminal paper Dyson (1960). However, as the well-known aphorism goes, “All that glitters is not gold,” which means numerous explanations exist for a star’s infrared excess. These range from inherent aspects, typically related to circumstellar material in the surrounding of the star, to external factors that can sometimes even be linked to specific designs of observational instruments. In this part of the thesis, we delve into different sources of infrared excess that could display features similar to those of the Dyson sphere models introduced in Part I and their properties. Although the search may not yield actual Dyson spheres, we believe any discoveries made through this endeavor could produce valuable insights for the astronomical community and enhance our understanding of infrared phenomena in general.

4. Infrared excess stars

Infrared excess is commonly associated with dust surrounding the central star, where dust particles absorb stellar light and re-emit it at longer, infrared wavelengths. This mechanism is identical to the one that would theoretically cause a Dyson sphere to emit infrared radiation. Thus, in the search for Dyson spheres, it is crucial to analyze all infrared sources thoroughly and understand their characteristics to differentiate them effectively. Moreover, one of the advantages of searching for Dyson spheres is that, regardless of the outcome, this exploration can help enrich our understanding of cosmic phenomena (refer to Section 1.2.4).

In the realm of astrophysical phenomena, the appearance of an infrared excess in stars can sometimes be misleading, attributed to factors unrelated to the inherent characteristics of the stellar source itself. To better understand and categorize the origins of infrared excess, we separate them into two primary categories: extrinsic and intrinsic. This section delves deeper into these categories, concisely reviewing the diverse mechanisms that contribute to infrared emissions and how they can influence our observations and interpretations of celestial objects.

4.1 Extrinsic

Extrinsic infrared sources are object that are not genuine sources of infrared radiation, but simply appear to be. Many searches for infrared sources have encountered difficulties when determining if the nature of the infrared excess is of intrinsic or extrinsic origin (e.g., Kennedy et al., 2012; Theissen and West, 2017). In the course of this thesis, two significant extrinsic factors were identified as affecting the detection of infrared excess: regions rich in interstellar dust and incidental alignments with other celestial bodies.

4.1.1 Dusty regions

Stars associated with prominent nebulae can appear as common false positive sources of infrared radiation. Figure 4.1 offers W3 (12 μm) images (a dust-sensitive photometric band) that provide examples of stars embedded within nebulae as well as those located in clearer regions.

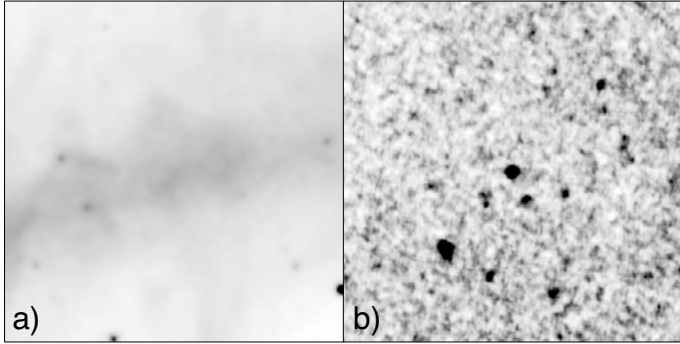


Figure 4.1. Two images in the WISE W3 band ($12\ \mu\text{m}$) that exemplify a star exhibiting contaminated infrared emission due to nebular features on the left-hand side panel and a star free from nebular feature on the right-hand side. Both images are normalized and correspond to a squared region in the sky with a side of $9.625\ \text{arcmin}$.

Kennedy et al. (2012) found a gradient in the infrared confusion from the dense, nebula-rich galactic plane of the Milky Way to its outskirts, highlighting the challenges in distinguishing genuine infrared excesses from those resulting from galactic contamination. Furthermore, they utilized the Improved Processing of the IRAS Survey (IRIS: Miville-Deschênes and Lagache, 2005) to trace potential background contaminations effectively. They found that sources within regions where the $100\ \mu\text{m}$ background level from the IRAS maps surpass $5\ \text{MJy/sr}$ are likely to be influenced by galactic contamination.

In Paper II, we implemented an independent analysis to discern whether stars are embedded within nebular regions. This was achieved through the development of a Convolutional Neural Network (CNN), specifically tailored to classify stars based on their likelihood of being affected by nebular contamination. The CNN was trained on a curated sample, selected through the visual inspection. Further elaboration on this method and its outcomes is detailed in Paper II.

While dust-rich regions can contaminate the photometry of a star, giving the appearance of infrared excesses, there are strategies to address this problem and exclude sources that have been affected by dust emission.

4.1.2 Chance alignments

The Wide-field Infrared Survey Explorer (WISE: Wright et al., 2010) and its subsequent data release, AllWISE (Cutri et al., 2013), have been of utter importance in the field of infrared sources by allowing the identification of new sources and the characterization of both new and

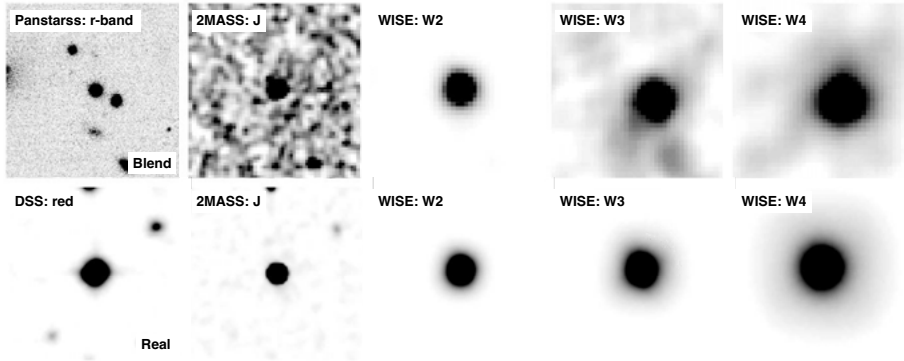


Figure 4.2. Illustration of two sources presenting an infrared excess in their W3 and W4 photometry. The upper panel showcases a star whose apparent infrared excess is actually blended with a neighboring celestial body, which is revealed when inspecting the image in the r-band from Panstarrs. The lower panel shows the proto-planetary nebula IRAS 08359-1644, a genuine source of infrared radiation that is unaffected by proximal sources. Each depicted area spans $1 \times 1 \text{ arcmin}^2$.

old sources (e.g., Cotten and Song, 2016). However, many studies (e.g., Ribas et al., 2012; Kennedy et al., 2012; Theissen and West, 2017) have faced challenges in the form of contamination from foreground or nearby sources. This issue primarily originates from the large Full Width at Half Maximum (FWHM) of the Point Spread Functions (PSFs) for the 12 and $22 \mu\text{m}$ wavelengths, which correspond to approximately $6''.5$ and $12''$, respectively. Because of this, the emission of a genuine infrared source can fall in the aperture of some WISE bands of one that is not, which can lead to a fake excess, as well as astrometric shifts across some WISE bands and/or extended morphology, complicating the detection of new authentic infrared sources. Figure 4.2 illustrates this issue with two examples. The top image shows a star whose W3 ($12 \mu\text{m}$) and W4 ($22 \mu\text{m}$) photometry indicates an excess in these bands, but in reality, it is caused by a nearby object that blends with the central source, which is only noticeable when inspecting the optical image. The bottom image presents the proto-planetary nebula IRAS 08359-1644, a genuine source of infrared radiation unaffected by nearby sources. Each image covers an area of $1 \times 1 \text{ arcmin}^2$.

In many cases, contamination produced by alignments is not obvious like the example illustrated in Figure 4.2, so one must consider other ways of handling this issue. In Paper II, we aided our visual inspection using complementary optical images that have better resolution. Another way of dealing with these chance alignments or blends is introduced by Theissen and West (2017). In the context of seeking M dwarfs surrounded by warm circumstellar material, they compare the offsets

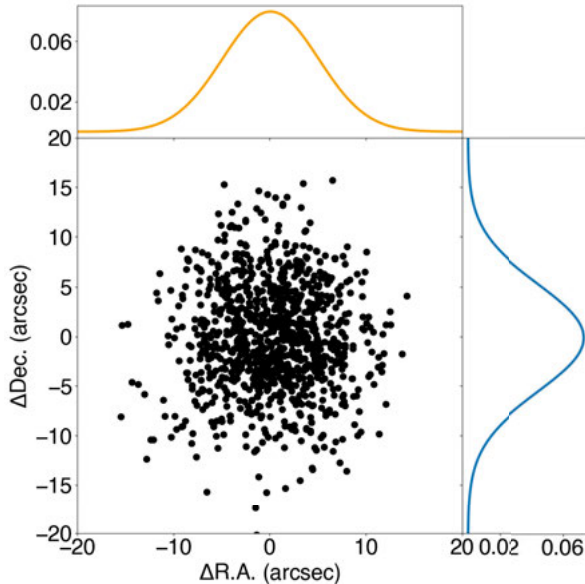


Figure 4.3. Example of right ascension and declination offsets in the WISE W1 for W3 data caused by the instrument, for one thousand points randomly generated following the distribution of Theissen and West (2017).

among the W1, W2, and W3 images of their candidates to with those of stationary objects like quasars. Their logic is that the centroid of contaminated sources at W3 ($12\ \mu\text{m}$) should be significantly offset compared to the shortest wavelength available in the survey W1 ($3.4\ \mu\text{m}$). They acknowledge that authentic sources of infrared radiation could still display small offsets, but this displacement should be compatible with the distribution of offsets of quasars, which are valuable indicators of the WISE instrument’s astrometric precision as they remain stationary in the sky. Theissen and West (2017) determine the offset of their infrared candidates and claimed these to be similar to the distribution of isolated quasars (with no other sources within 6 arcseconds), with W3 signal-to-noise ratios (SNRs) between 3 and 5, at galactic latitudes higher than 77 degrees. They provide two offset distributions resembling Gaussian functions. One distribution reflects the Right Ascension offset between the W1 and W3 positions ($\mu = 0''.08$, $\sigma = 5''.00$) and another for the Declination offset between the W1 and W3 positions ($\mu = -0''.21$, $\sigma = 5''.48$). Figure 4.3 illustrates the right ascension and declination offsets of one thousand randomly generated data points between the W1 and W3 centroids following the distributions obtained by Theissen and West (2017).

While we have outlined two straightforward and effective methods for eliminating sources affected by contamination from adjacent or fore-

ground objects, there can be instances where the alignment is so precise that the contamination mimics the offset distribution typical of quasars. Likewise, visual inspection of photometric images can not always reveal a clear contaminating source, unlike the example shown in Figure 4.2. In such cases, spectral information may provide additional clues. If two sources are blending, their spectral features should be observable simultaneously.

4.2 Intrinsic

As mentioned before, infrared excess emission is a valuable tracer of the material heated by the starlight and reemitted at longer wavelengths. This phenomenon is typical of very young stars as well as very old stars. This section provides a simplified overview of some of these intrinsic infrared emitters. We consider evolved stars, binaries, and young stars surrounded by circumstellar material.

4.2.1 Evolved stars

In the first Dyson sphere searches (e.g., Slysh, 1985; Timofeev et al., 2000; Carrigan, 2009), evolved stars such as Mira variables, planetary nebulae, asymptotic giant branch stars (AGB) and post-AGB stars were the most typical type of confounders. These evolutionary stages are characterized by the production of dust clouds during strong stellar wind events that can produce infrared signatures. However, many of these sources show silicate features, pulsations, and, in some cases, OH/IR signals (1612 MHz), which are evidence against a possible Dyson sphere. Carbon stars, a subclass of AGB stars, are also evolved stars that usually present SiC emission lines at about $11.3 \mu\text{m}$. However, some extreme Carbon stars with thick envelopes can lack this feature (Volk et al., 1992).

The first searches focused on using the photometry of Infrared Astronomical Satellite (IRAS: Neugebauer et al., 1984) to find objects whose photometry could resemble that of a pure blackbody in the range 100 – 600 K that would be radiated from a complete Dyson sphere. However, these searches lacked precise parallaxes, so distances were not obtainable, and fluxes could not be rescaled to luminosities. If we assume that Dyson spheres can only be hosted by main-sequence stars, we can rule out all evolved stars by inspecting the position of any potential candidate in the Hertzsprung-Russell diagram. However, distances need to be known. In this thesis, we have mainly used parallax-based distances from the Gaia mission (Gaia Collaboration et al., 2016), a mission that provides photometry and astrometry with unprecedented precision as

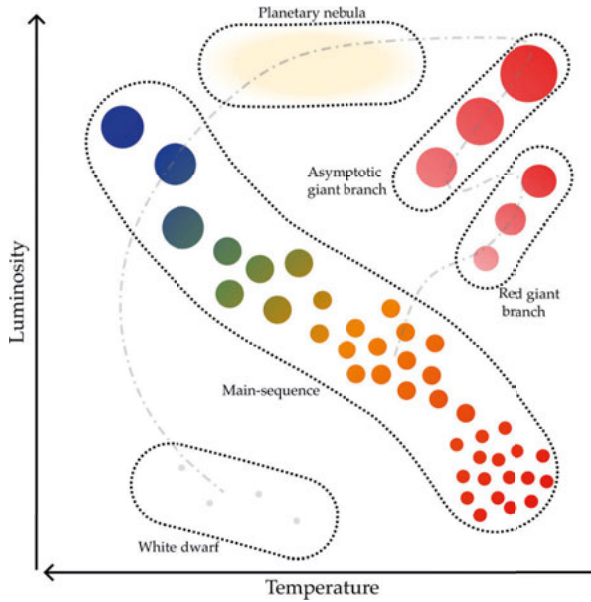


Figure 4.4. Hertzsprung-Russell diagram illustrating different evolutionary stages when plotting luminosity versus temperature. We highlight the huge luminosity of Asymptotic Giant branch stars. Image credit: Arief Ahmad.

well as other derived products. In Paper II and Paper III, We make use of distances derived from the Gaia Early Data Release 3 (Gaia Collaboration et al., 2021), in particular, parallax-based distances from Bailer-Jones et al. (2021) that uses a Bayesian approach to account for the asymmetry of the distance uncertainties when errors are large. Although it has been shown that Gaia parallax-based can sometimes be unreliable for AGB stars (e.g., Andriantsaralaza et al., 2022), we have worked with a very small sample of stars within 300 parsecs, which contains only sources with very reliable distances.

4.2.2 Binaries

Single stars are prevalent in our Galaxy, but they are not the only type of stellar systems. It is estimated that approximately one-third of the star systems in the Galaxy are binary or multiple (Lada, 2006). It has been observed that in some cases, multiple-star systems can also harbor circumstellar material surrounding it. A notable case is the spectroscopic binary BD +20 307, an old system (> 1 Gyr) consisting of two nearly identical stars. This system exhibits an infrared excess attributed to a significant amount of hot circumbinary dust, likely resulting from a massive and recent collision of planetesimals, despite its advanced evolutionary stage (Weinberger, 2008; Thompson et al., 2019). Consequently,

this source has been categorized as an extreme debris disk (EDD) due to the high fractional luminosity of its circumstellar material (Balog et al., 2009; Moór et al., 2021).

To assess whether stars are likely to be unresolved binaries, data from the Gaia mission (Gaia Collaboration et al., 2016) is invaluable. The Gaia astrometric solution is based on the assumption that all observed objects are single stars. Misidentifying a binary or multiple system as a single star leads to incorrect parallaxes and proper motions, i.e. inaccurate astrometric data. Gaia calculates the Renormalised Unit Weight Error (RUWE) for each source, which is the square root of the normalized chi-square of the astrometric fit to the along-scan observations. Although RUWE formal definition may appear complex, its practical understanding is facilitated by the approximation provided by Belokurov et al. (2020), as shown in Equation 4.1,

$$RUWE^2 \approx \chi^2 \approx \frac{1}{\nu} \sum_{i=1}^N \frac{R_i^2}{\sigma_i^2} \quad (4.1)$$

where $\nu = N - x$ the number of degrees of freedom, N is the number of good observations along the scan, x is the number of parameters in the data release, which is 5 for Gaia DR2 (Gaia Collaboration et al., 2018) and 6 for Gaia EDR3 and DR3 (Gaia Collaboration et al., 2021, 2022). R_i are model residuals, and σ_i the centroid errors for a given observation of a source. Essentially, Equation 4.1 is sensitive to factors causing photocenter wobble, such as unresolved multiple systems. A higher χ value indicates a more prominent wobble. The Gaia consortium typically considers RUWE values ~ 1.0 for well-behaved single star solutions, with a threshold of $RUWE \leq 1.4$ (Lindgren et al., 2018, 2021).

In summary, the RUWE criterion becomes a handy parameter that can assist when distinguishing sources composed of multiple stars as well as stars with problematic astrometry from well-behaved stars.

4.2.3 Young stars

Studying young stars and the circumstellar material surrounding them is crucial for understanding the processes that contribute to observed mid-infrared (mid-IR) excess emissions. This emission indicates the presence of circumstellar disks and other material that interact with the young stellar object (YSO) as it evolves. The classification of YSOs based on their evolutionary stages helps unveil complex processes occurring during star formation. This classification is grounded in a taxonomy that categorizes YSOs into Classes 0, I, II, and III, based on the spectral

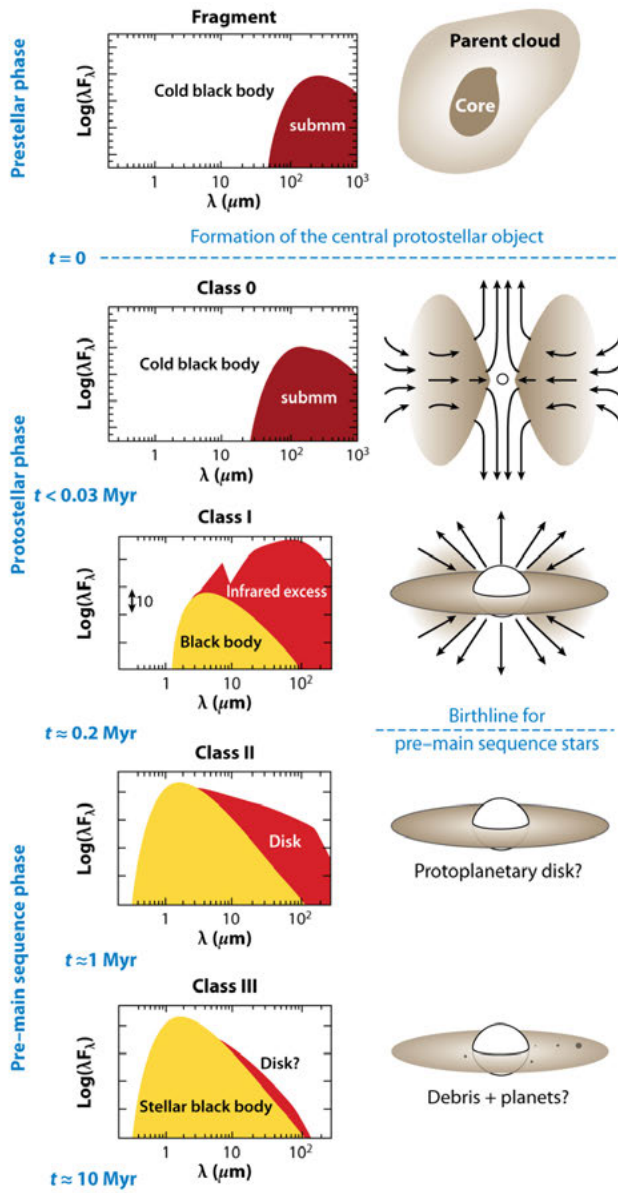
energy distribution (SED) slope $\alpha = d \log(\lambda F_\lambda) / d \log \lambda$, between near-infrared (near-IR) and mid-IR wavelengths.

- **Class 0** objects represent the earliest stage of star formation, often referred to as the “collapse phase.” These objects are characterized by extended submillimeter continuum emission, which indicates the presence of a spheroidal circumstellar dust envelope. A significant feature of Class 0 objects is that the ratio of submillimeter luminosity (L_{Smm}) to the bolometric luminosity (L_{Bol}) is greater than 0.5%, where L_{Smm} is the submillimetric luminosity measured longward of $350 \mu\text{m}$.
- **Class I** objects are in a later stage of evolution compared to Class 0. Their emission is primarily dominated by the envelope surrounding the protostar, with an SED slope (α) greater than 0.
- **Class II** objects are characterized by the accretion phase, where the emission is influenced both by the central star and its circumstellar disk. This phase is characterized by strong H α emission and/or UV excess emission. The presence of a disk is significant in Class II objects, as it is actively involved in the process of star and planet formation, with material from the disk accreting onto the star. In this phase, $0 \geq \alpha \geq -2$.
- **Class III** denotes a phase where the accretion of gas has concluded, and the emission is predominantly from the central star. The SED slope (α) is less than or equal to -2, indicating that the circumstellar disk has become a debris disk, contains little gas, and is possibly in the final stages of planet formation or has already formed planets. In this phase, there is typically no accretion.

This classification scheme, initially proposed by Lada et al. (1984) and later updated by André (1993), provides a framework for understanding the complex evolution of YSOs. The progression from Class 0 through Class III reflects the gradual clearing of the circumstellar material.

We summarize the physical and spectral features of these classes in Figure 4.5 as well as in Table 4.1. For a comprehensive overview of the terminology and concepts in the field of protostellar and protoplanetary sources, readers are encouraged to consult resources like “THE DISKIONARY” (Evans et al., 2009), which compiles definitions and vocabulary pertinent to this area of study.

In addition to the previously mentioned classes, objects are commonly differentiated based on their fractional infrared luminosity (e.g., Wyatt, 2008), defined as $f = L_{\text{IR}} / L_\star$. Sources with $f > 0.01$, are classified as **protoplanetary disks** (Class I and II), indicative of a significant presence of dust and gas that are potential precursors to planet formation. Conversely, objects with $f < 0.01$ are categorized as **debris disks**




 Dauphas N, Chaussidon M. 2011. *Annu. Rev. Earth Planet. Sci.* 39:351–86

Figure 4.5. Image describing all the classes in star formation presented by Lada et al. (1984) and extended by André (1993) for a Sun-like star. Image reproduced with permission from Dauphas and Chaussidon (2011); the original concept of this image can be found in André (1993).

Table 4.1. *Table summarizing different observation features during different stages of star formation as well as the physics undergoing during these phases. Taxonomy from Lada (1987), with class 0 added by André (1993).*

Class	Observational features	Physics
0	Submm continuum emission	Collapsing molecular cloud. Most mass in envelope.
I	SED slope $\alpha \geq 0$	Emission dominated by the envelope
II	SED slope $0 \geq \alpha \geq -2$	Radiation from the star and the accretion disk.
III	SED slope $\alpha \leq -2$	Emission dominated. by the star Debris disk.

(Class III), which suggests a more evolved system where the planet formation process has largely concluded, leaving behind a sparse disk of dust and debris.

An intriguing exception within this categorization is the category of **Extreme Debris Disks** (EDD), as introduced by Balog et al. (2009). These are Class III objects that, despite their evolutionary stage, exhibit fractional luminosities exceeding the conventional threshold for debris disks ($f > 0.01$).

A slightly different taxonomy from the one proposed by Lada et al. (1984) was introduced by Espaillat et al. (2012). This classification accounts for the transitional phases between the Lada et al. (1984) Classes as disks evolve. The categories are as follows:

- **Full disks**, optically thick at near- and mid-infrared wavelengths. Primordial dust and gas have not been cleared yet (e.g., Esplin et al., 2018).
- **Pre-transitional** disks are characterized by an optically thick inner disk, which is distinct from an optically thick outer disk due to the presence of an optically thin gap between them. Mid-IR dip (Espaillat et al., 2007, 2010).
- **Transition disks** are disks with inner holes that are relatively empty of small dust grains. No significant IR emission at wavelengths $< 20 \mu\text{m}$ (e.g. Espaillat et al., 2012).
- **Evolved disks** possess circumstellar material that starts becoming optically thin but still does not possess large holes or gaps (e.g., Esplin et al., 2018).
- **Evolved transitional** disks are optically thin and have large holes. (e.g., Esplin et al., 2018).

- **Debris disks** are composed of second-generation dust generated by collisions of planetesimals after the primordial disk has dissipated.

Some tracers of youth

As initially stated, there are many opportunities to confuse protoplanetary disks or debris disks with theoretical Dyson spheres, especially given their common infrared signatures. However, there are several features characteristic of stars in their formation that can help us to discriminate between young stars and genuine Dyson sphere candidates. Here, we provide some examples of observables that can help make the distinction.

One discriminant is variability. Stars encircled by circumstellar material, particularly young stars, frequently display brightness variability as a distinguishing trait (e.g., Joy, 1945; Herbst et al., 2007). This variability can originate from a range of phenomena, such as circumstellar obscuration events, the presence of hot spots on the star or within the disk, bursts of accretion, and swift alterations in the structure of the circumstellar disk (Cody et al., 2014).

When it comes to optical spectra, there are many lines that can serve to constrain stellar ages. One indicator of stellar youth is the emission of H α photons, characteristic of young stars during accretion episodes. As a young protostar heats up, it ionizes the hydrogen within its surrounding accretion disk, leading to the emission of H α photons (Barrado y Navascués and Martín, 2003). It is important to recognize, though, that H α emission is also a common trait of late-type stars, especially M dwarfs, where it results from magnetic activity. However, the H α emission from accreting episodes is significantly more intense than those arising from magnetic activity. Empirical relationships based on the Equivalent Width (EW) measurements of the H α line exist (e.g., Barrado y Navascués and Martín, 2003; White and Basri, 2003), providing a method to discriminate between these different origins of H α emission.

Another diagnostic tool for identifying young stars is the presence of Lithium (Li). Lithium is an element that is readily destroyed within the interiors of stars, leading to a gradual depletion of its surface abundance over time in solar-type and lower-mass stars (Bouvier et al., 2016; Jeffries, 2014, e.g.). Consequently, the detection of Li I λ 6708 absorption serves as an indicator of stellar youth. As young stars contract and approach the main sequence, the temperature of their cores increases, eventually reaching approximately $\sim 3 \cdot 10^6$ K, a threshold temperature at which Lithium begins to burn (e.g., Murphy et al., 2018).

Surface gravity is a useful diagnostic tool for determining the evolutionary stage of stars. Pre-main sequence (pre-MS) stars typically exhibit low surface gravity, which gradually changes as the star con-

tracts and its radius decreases during pre-MS evolution. Absorption features sensitive to surface gravity can provide valuable clues about a star's youthfulness. For instance, in the case of mid-M-type stars, the Na I doublet at $\lambda 8183/8195$ stands out as one of the most reliable gravity-sensitive features for identifying stellar youth (Schlieder et al., 2012).

M dwarfs debris disk

One intriguing aspect of this thesis, highlighted in Paper II, is that all sources with an infrared excess of unknown origin are M dwarfs. When examining these stars, one potential explanation for the presence of an infrared excess is the existence of a debris disk. However, despite M dwarfs being the most common type of star in the Galaxy (Reyl e et al., 2021; Kirkpatrick et al., 2023), debris disks around them are exceedingly rare. Despite numerous efforts, attempts to find debris disks surrounding M dwarfs have largely been unsuccessful. While confirmed instances of M dwarfs surrounded by debris disks do exist, their detection remains limited, primarily observed in the submillimeter regime, keeping them constrained to very low temperature (e.g., Luppe et al., 2020; Cronin-Coltsmann et al., 2022, 2023).

Several factors have been proposed to contribute to the challenge of detecting debris disks around M dwarfs, including potential detection biases (Heng and Malik, 2013; Kennedy et al., 2018) and age biases (Riaz et al., 2006; Avenhaus et al., 2012). Furthermore, the analysis performed by Plavchan et al. (2005) suggests that stellar wind drag could lead to faster disk dissipation around M dwarfs, potentially explaining the perceived scarcity of debris disks in this stellar population.

Part III: Summary of papers

This part summarizes the content of the papers included in this thesis.

5. Paper I

In our first paper, we determined upper limits on the prevalence of Dyson spheres within the Milky Way using Gaia DR2 and AllWISE data. This work aimed to estimate the highest potential quantity of Dyson spheres in the Galaxy by counting stars that show infrared excesses – a feature of Dyson spheres.

To compute these upper limits, we identified specific regions within color-magnitude diagrams expected to contain main-sequence stars paired with Dyson spheres. The methodology for outlining these regions is depicted in Figure 5.1. First, we select a subset of main-sequence stars. For these stars, we then apply the simplified models discussed in Section 3.2.2 to account for changes in their photometry attributable to the presence of a Dyson sphere, characterized by specific values of γ and T_{DS} . Then, we determine the parameterizations $f_X(T, \gamma)$ – the boundary separating Dyson spheres from other stellar objects in our dataset for different color combinations. A crucial element of this approach is choosing color-magnitude diagrams that feature a color index combining optical and mid-infrared wavelengths, thus capturing the infrared excess. For this analysis, we utilized the color indices: $G - W1$, $G - W2$, $G - W3$, and $G - W4$.

After defining the boundaries within the color-magnitude diagrams for potential Dyson sphere regions, we evaluated the proportion of stars falling into these regions. The dataset was divided into various subsets based on distance, ranging from stars located within 100 pc to those as far away as 5000 pc, encompassing approximately $\sim 3 \times 10^8$ stars. We summarized the results in Table 5.1, which shows the fraction of stars at different distances for a Dyson sphere of $\gamma = 0.1, 0.5, 0.9$ and a temperature $T_{\text{DS}} = 300$ K, which corresponds to the best-constrained temperature. The strongest upper limits were established within 100 pc from the Sun. This distance allows for a more diverse sample of stars to be included in the analysis and reduces the likelihood of contamination from other sources. For stars in this local volume, infrared sources can be identified more accurately, enhancing the reliability of our upper limit estimates for their prevalence within this specific region of the Milky Way.

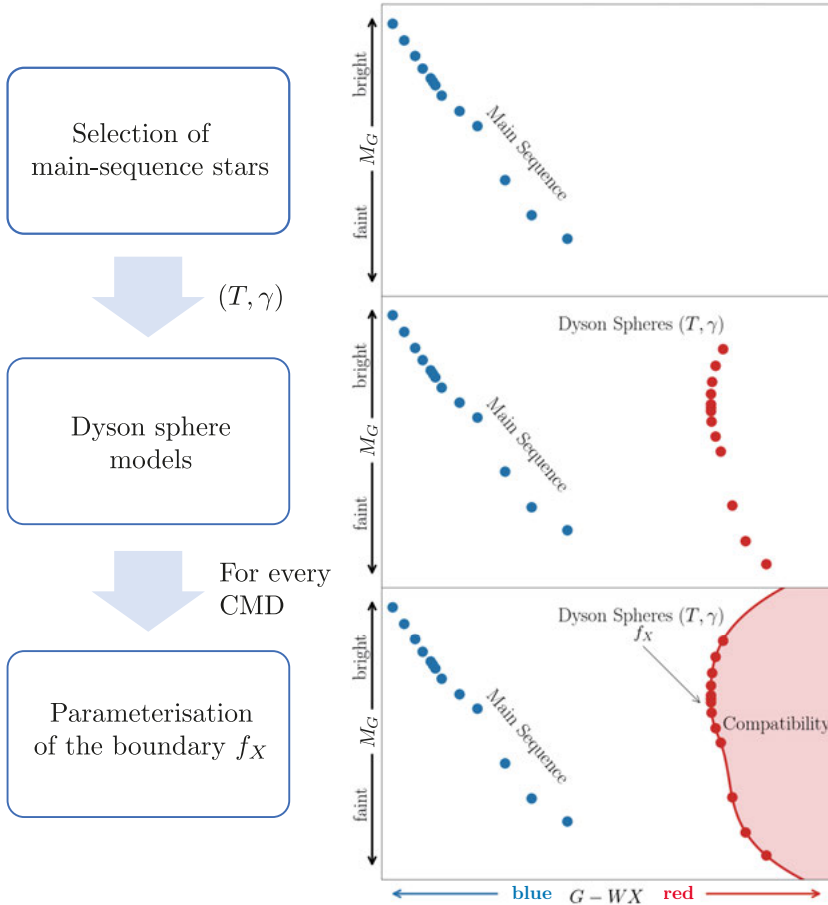


Figure 5.1. Summary of the stages to define regions in the color-magnitude diagram where hypothetical stars hosting Dyson spheres would be located. First, we select main-sequence stars, represented by blue dots. Then, we apply DS models of a given T and γ over the main-sequence stars, represented with red dots. We parameterize the boundary of the DS models with a mathematical function f_X , where X is the number 1, 2, 3, or 4 to cover all the bands in the WISE mission. Adapted from Paper I.

Table 5.1. Summary of fraction of stars compatible with Dyson spheres in different samples. We show the distance considered in each subset, the number of stars in the subset, and the percentage of sources compatible with a DS of $T = 300$ K and covering factors 0.1, 0.5, and 0.9. Adapted from Paper I.

Radius [pc]	Size sample	Fraction of stars compatible with a DS with $T_{DS} = 300$ K		
		$\gamma = 0.1$	$\gamma = 0.5$	$\gamma = 0.9$
100	265724	6.6×10^{-3}	1.9×10^{-4}	1.8×10^{-5}
200	1847472	2.2×10^{-2}	4.7×10^{-4}	7.4×10^{-5}
300	5243957	4.8×10^{-2}	4.8×10^{-4}	8.6×10^{-5}
400	10384485	6.7×10^{-2}	5.6×10^{-4}	1.1×10^{-4}
500	16831302	8.9×10^{-2}	7.5×10^{-4}	1.9×10^{-4}
600	24162082	1.0×10^{-1}	7.5×10^{-4}	1.9×10^{-4}
700	32123156	1.1×10^{-1}	7.8×10^{-4}	1.9×10^{-4}
800	40575873	1.2×10^{-1}	8.5×10^{-4}	2.0×10^{-4}
900	49472732	1.2×10^{-1}	9.4×10^{-4}	2.0×10^{-4}
1000	58769015	1.3×10^{-1}	1.0×10^{-3}	2.1×10^{-4}
5000	$\sim 2.9 \times 10^8$	1.6×10^{-1}	7.1×10^{-3}	8.3×10^{-4}

6. Paper II

In our second paper, we focused on identifying sources that exhibit characteristics consistent with Dyson spheres. As discussed in Part II, there are various reasons a star might have an infrared excess, originated from both intrinsic and extrinsic processes. To isolate the most enigmatic sources of infrared radiation, we implemented a pipeline on the combined dataset from Gaia DR3, 2MASS, and AllWISE, which spans optical, near, and mid-infrared wavelengths. The procedure is visually summarized in Figure 6.1 and encompasses the following steps:

- Data collection from Gaia, 2MASS, and All-WISE for sources within 300 pc with detections in the 12 and 22 μm bands (W3 and W4 WISE bands).
- A grid-search method is employed to determine each star's best-fitting Dyson sphere model, utilizing the combined Gaia-2MASS-AllWISE photometry.
- To filter out potential candidates situated in nebular areas, a Convolutional Neural Network (CNN)-based approach is employed on WISE imagery to verify the absence of nebular features.
- Utilization of Gaia-WISE indicators to determine the likelihood of stars showing an infrared excess due to natural causes.
- Exclusion of sources with signal-to-noise ratios lower than 3.5 in the W3 and W4 bands.
- Visual inspection of optical, near-, and mid-infrared images for all remaining sources to eliminate problematic cases.

After implementing the described procedure on $\sim 5 \times 10^6$ stars within the combined Gaia DR3-2MASS-AllWISE dataset, we identified seven sources fulfilling our criteria, each exhibiting an excess in the infrared spectrum. These sources stand out from the vast dataset due to their uncertain origin.

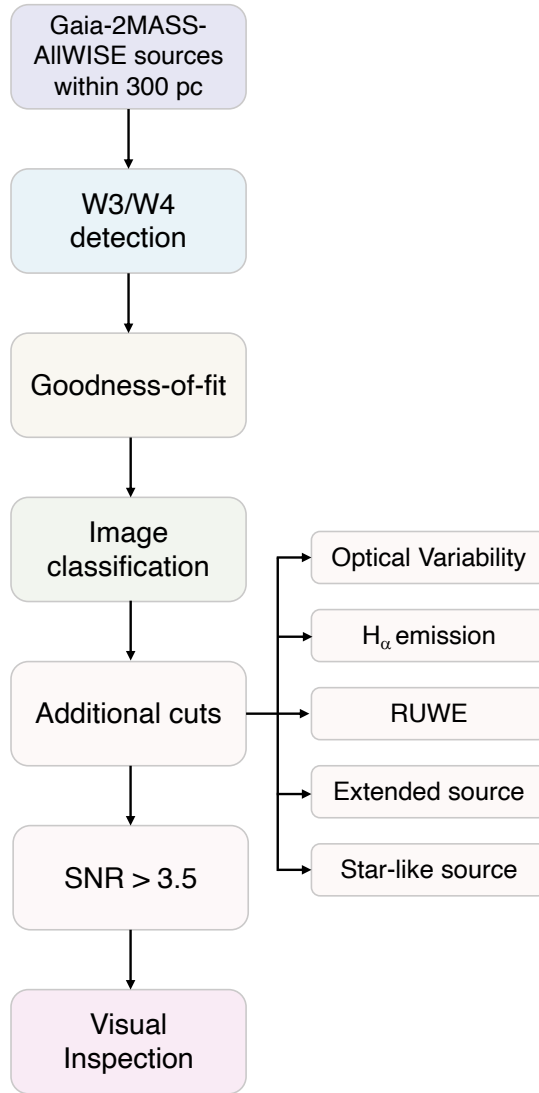


Figure 6.1. Flowchart illustrating our pipeline to find Dyson sphere candidates. Adapted from Paper II.

7. Paper III

In this work, we re-analyzed the candidates for Dyson spheres identified through the pipeline established in Paper II (Chapter 6), exploiting the fact that all are M dwarfs. To the existing list of candidates, we added three additional stars that exhibit ambiguous signs of infrared excess, yet for which we possess spectroscopical data.

Here, we delve more into the properties of these stars by employing photometrically calibrated relationships specially tailored for M-dwarfs in order to determine accurate stellar parameters. Additionally, we acquired low-resolution spectroscopy for some candidates and for well-known M-dwarfs to serve as a comparison metric. The analysis of stellar parameters, derived from calibrated empirical relationships for M-dwarfs, shows that our Dyson sphere candidates do not deviate from typical M-dwarf stars in terms of stellar parameters. Figure 7.1 showcases a color-magnitude diagram that includes our candidates and spectroscopic standard stars, alongside metallicity estimates generated through this study. The distribution of our objects aligns with the expected trends observed in a reference sample from Mann et al. 2015, which confirms the lack of anomalies in their properties when compared with the M-dwarf population.

Likewise, we analyze stellar spectra when available. Figure 7.2 compares the available spectra of five of our sources, labeled A to J, from the highest signal-to-noise in the W3/W4 bands to the lowest. These spectra do not reveal any striking deviations from typical M-dwarf behavior, similar to the conclusion from the photometric analysis.

The consistency in our sources' behavior suggests that they share typical characteristics with other main sequence M-dwarfs, highlighting the need for further investigation to understand the origins of their infrared excesses. One of our spectroscopic targets does exhibit weak H α emission, but this is more likely attributed to stellar activity rather than the gaseous accretion disk expected for a young star according to different empirical relations. After this analysis, we still find no clear explanation for these stars' infrared excess, but future observations in the infrared or submillimeter regime could probe one of the scenarios listed in Part II.

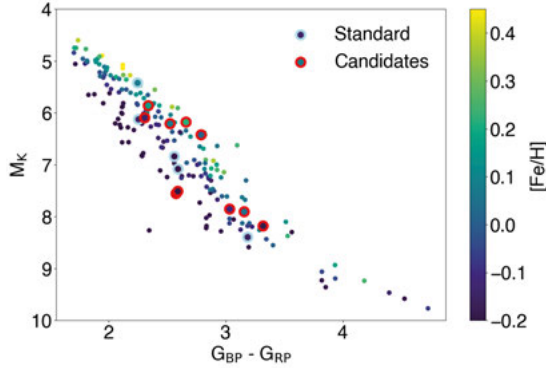


Figure 7.1. Color-magnitude diagram showing our candidates (red circles), standard stars with stellar spectra (light-blue bullets), and M dwarfs from Mann et al. (2015) sample in smaller circles. Our stars follow the typical behavior of M dwarfs on the main sequence, as well as the relation between color and metallicity. Adapted from Paper III.

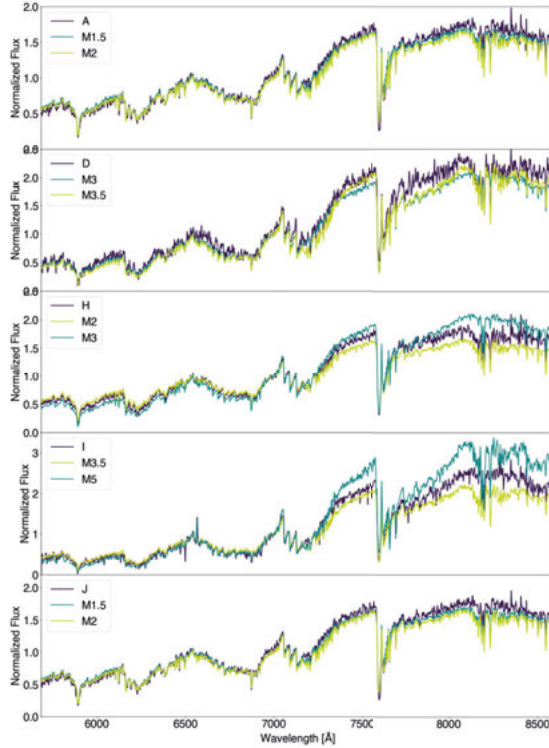


Figure 7.2. Stellar spectra for candidates A, D, H, I, and J according to the nomenclature employed in Paper III. Standard main-sequence M dwarfs are included to facilitate the comparison with standard main-sequence M dwarfs. There is a fair match between our standard stars and the optical spectra of our candidates. No $H\alpha$ in emission is observed in all but one case. Adapted from Paper III.

8. Popular Science Summary

Are we alone in the Universe, or are there others out there? This is the core question in the research field of SETI (Searching for Extra-Terrestrial Intelligence). The scientific search for intelligent life in space began in the early 1960s and, until now, has primarily focused on the search for communication signals in the form of radio waves and laser pulses from other civilizations. Despite these efforts, no conclusive evidence of intelligent life has been found, leaving the question of their existence unanswered. The lack of detections does not necessarily imply an absence of intelligent life. It is possible that other civilizations might not seek contact, are unaware of our existence, or use communication methods beyond our current detection capabilities. Many alternative strategies for searching for signs of more general technological activity in space have been proposed but have been relatively unexplored.

Recently, extensive digital collections of astronomical data have been built up, making it possible to study the properties of hundreds of millions of celestial objects from various regions of the electromagnetic spectrum. This thesis uses databases of this kind to search for an alternative signature of extraterrestrial technology, also referred to as technosignatures. The underlying idea, proposed by theoretical physicist Freeman Dyson, is that civilizations at a higher technological level than our own might want to harness the radiant energy produced by their own planetary system's parent star.

In our solar system, the Earth captures a small part of the luminous energy that our star, the Sun, emits. This energy has been critical for the development of life on Earth and, with our current technology, can also be converted into electricity via solar panels. However, most solar radiation is not absorbed by any planet but leaks straight into interstellar space. This untapped energy could, in principle, be collected by constructing a vast, spherical structure that absorbs some of the star's radiation. This is often considered a swarm of satellites around the star, but other designs are also possible. This structure, the so-called Dyson sphere, is expected to block some of the light in the visible wavelength range and emit a strong infrared glow. Combining observational data in the visible and infrared allows for searches of stars exhibiting such a signature and identifying possible Dyson Spheres in our home galaxy, the Milky Way.

This technosignature can be detected at relatively large distances and is not based on any assumptions regarding the willingness of any

civilization to send radio signals or direct laser pulses in our direction. One problem, however, is that stars can appear unusually dim in visible light and bright in infrared light for reasons that have nothing to do with Dyson spheres. A critical element in the search for Dyson spheres is to try to rule out other known astronomical phenomena that could similarly affect the light of the stars.

This thesis combines observational data in the optical and infrared regions of the electromagnetic spectrum from the space-based Gaia and WISE telescopes and other telescopes in the search for possible Dyson spheres. The first article in this thesis assesses how common stars with an unusually high proportion of infrared radiation are in the data catalogs from Gaia and WISE. This results in upper limits for how common different varieties of Dyson Spheres could, in principle, be in our part of the Milky Way. However, it does not say whether there are any likely Dyson spheres in the data set.

The second paper presents a procedure to identify objects where the infrared excess flux is likely attributed to well-known astronomical phenomena. Here, we combined data from Gaia and WISE along with 2MASS, a survey of the sky compiled with ground-based infrared telescopes. The procedure includes, among others, an interpretation of image data from WISE using artificial neural networks that have been trained to classify the environment around light sources in the sky. Young stars surrounded by dust clouds sometimes exhibit signatures similar to those of Dyson spheres. However, such stars are typically found in star-forming regions that appear nebulous in the images from WISE and can, therefore, be weeded out by the classification algorithm. The article presents a small selection of objects that ultimately meet all the criteria for possible Dyson sphere candidates.

In the third article, these candidates are examined in more detail, partly with follow-up observations made with the Nordic Optical Telescope. The objects turn out to be red dwarf stars that show no signs of the youth required to explain their infrared properties. However, the available data cannot determine the cause of the strong infrared radiation.

In the SETI research field, what is sometimes called “Freeman Dyson’s first SETI law” is sometimes discussed, namely the advice that searches for extraterrestrial civilizations should be designed to lead to interesting results even when no extraterrestrials are discovered. It is definitely too early to say that any Dyson spheres have been found, but the fact that objects in the starry sky exhibit inexplicable infrared radiation is an interesting result, as it may lead to the discovery of new astrophysical phenomena. In the case of the red dwarf stars discussed in this thesis’s third article, observations with the space telescope JWST or the

ground-based telescope ALMA could probably unveil what lies behind the phenomenon.

9. Populärvetenskaplig sammanfattning

Är vi ensamma i universum, eller finns det andra därute? Detta är den centrala frågan inom forskningsfältet SETI (eng. Searching for Extra-Terrestrial Intelligence). Det vetenskapliga sökandet efter intelligent liv i rymden tog sitt avstamp under det tidiga 1960-talet, och har hittills till stor del fokuserat på sökandet efter kommunikationssignaler i form av radiovågor och laserpulser från andra civilisationer. Sådana strategier har ännu inte resulterat i några säkra detektioner, men vad detta säger om förekomsten av intelligenta livsformer i rymden är oklart. Om andra civilisationer inte har något intresse av att kontakta oss, inte känner till att vi är här, eller kommunicerar med signaler som vi i nuläget inte förmår uppfånga, är dessa metoder dömda att misslyckas. Många alternativa strategier för att söka efter tecken på mer generell teknologisk aktivitet i rymden har föreslagits, men hittills varit relativt outforskade.

Under senare tid har stora digitala samlingar av astronomiska observationsdata byggts upp, vilket gör det möjligt att studera egenskaperna hos hundratal miljoner himlaobjekt i ljus från vitt skilda delar av det elektromagnetiska spektrumet. I denna avhandling används databaser av detta slag för att söka efter en alternativ s.k. teknosignatur med potential att lokalisera andra civilisationer i rymden. Den underliggande idén, framlagd av den teoretiske fysikern Freeman Dyson, är att civilisationer på en högre teknologisk nivå än vår egen kanske skulle vilja tillgodogöra sig den strålningsenergi som det egna planetsystemets moderstjärna producerar, men som normalt går förlorad i rymden.

I vårt solsystem fångar jorden upp en liten del av den ljusenergi som vår egen moderstjärna solen sänder ut. Denna strålningsenergi har varit kritisk för livets utveckling på jorden och kan med vår nuvarande teknologi även omvandlas till elektricitet via solpaneler. Den största delen av solstrålningen absorberas dock inte av någon planet utan läcker rakt ut i den interstellära rymden. Denna outnyttjade energi skulle i princip kunna samlas in genom konstruktionen av en enorm, sfärisk struktur som absorberar en del av stjärnans strålning. Ofta tänker man sig detta som en svärm av satelliter kring stjärnan, men annan utformning är också möjlig. Den s.k. Dysonsfären förväntas blockera en del av ljuset i det synliga våglängdsområdet, men samtidigt avge ett kraftigt infrarött sken. Genom att kombinera observationsdata i synligt och infrarött ljus kan man söka efter stjärnor som uppvisar en sådan

signatur och därigenom lokalisera möjliga Dysonsfärer i vår hemgalax Vintergatan.

Denna tekno­signatur är intressant eftersom den kan upptäckas på relativt stora avstånd och inte baseras på några antaganden om att andra civilisationer skulle sända radiosignaler eller rikta laserpulser åt vårt håll. Ett problem är däremot att stjärnor kan te sig ovanligt ljussvaga i synligt ljus, och samtidigt ljusstarka i infrarött, av skäl som inte har något med Dysonsfärer att göra. Ett kritiskt moment i sökandet efter Dysonsfärer är därför att försöka utesluta andra kända astronomiska fenomen som skulle kunna påverka stjärnornas ljus på likartat sätt.

I denna avhandling kombineras observationsdata i synligt och infrarött ljus från de rymdbaserade Gaia- och WISE-teleskopen, samt även data från andra teleskop, i jakten på möjliga Dysonsfärer. I avhandlingens första artikel undersöks hur vanliga stjärnor med ovanligt hög andel infraröd strålning är i datakatalogerna från Gaia och WISE. Detta resulterar i övre gränser för hur vanliga olika varianter av Dysonsfärer i princip skulle kunna vara i vår del av Vintergatan. Det säger däremot inget om hur huruvida det verkligen finns några troliga Dysonsfärer i datamängden.

I den andra artikeln presenteras en procedur för att sälla bort objekt där överskottet av infrarött ljus sannolikt kan tillskrivas välkända astronomiska fenomen.

Här kombineras data från Gaia och WISE med data 2MASS, en undersökning av himlen sammanställd med infraröda teleskop på jordytan. I förfarandet ingår bland annat en tolkning av bilddata från WISE med hjälp av artificiella neurala nätverk som tränats att klassificera omgivningen kring ljuskällor på himlen. Unga stjärnor omgivna av stoftmoln uppvisar ibland ljussignaturer som liknar de hos Dysonsfärer. Många sådana stjärnor återfinns dock i stjärnbildningsområden som framträder med nebulös karaktär i bilderna från WISE, och kan därför sällas bort av klassificeringsalgoritmen. I artikeln presenteras ett litet urval objekt som i slutänden uppfyller alla kriterierna för möjliga Dysonsfärkandidater.

I avhandlingens tredje artikel undersöks dessa kandidater mer ingående, delvis med uppföljningsobservationer gjorda med Nordiska Optiska Teleskopet. Objekten visar sig vara röda dvärgstjärnor som inte uppvisar några tecken på att vara så unga att det enkelt skulle förklara deras infraröda egenskaper. Vad som egentligen orsaker den kraftiga infraröda strålningen går dock inte att avgöra med tillgängliga data.

Inom forskningsfältet SETI diskuteras ibland något som brukar kallas ”Freeman Dysons första SETI-lag”, nämligen rådet att sökningar efter utomjordiska civilisationer bör utformas så att de leder till intressanta resultat även när inga utomjordingar upptäcks. Det är definitivt för tidigt att säga att några Dysonsfärer har hittats, men att det finns ob-

jekt på stjärnhimlen som uppvisar svårförklarad infraröd strålning är ett intressant resultat i sig, eftersom det kan leda till upptäckten av nya astrofysikaliska fenomen. I fallet med de röda dvärgstjärnor som diskuteras i avhandlingens tredje artikel skulle exempelvis observationer med rymdteleskopet JWST eller det jordbundna teleskopet ALMA sannolikt kunna avslöja vad som ligger bakom fenomenet.

10. Acknowledgements

This thesis can only be completed by acknowledging those who contributed to it, but also to the ones who have been part of this journey. So I say. Thank you for the music, the songs I'm singing. Thanks for all the joy they're bringing. Who can live without it? I ask in all honesty. What would life be?

Now, seriously, thanks to everybody who has been a part of my Ph.D. journey. First of all, I would like to thank my supervisor, Erik, for his mentorship and patience throughout these years and for proposing this cool Ph.D. thesis project. Andreas, who committed to his co-supervisor role, helped me get through different tasks and got me a bunch of stellar spectra.

I also want to thank all the Ph.D. students from the division for creating such a joyful and relaxed environment, for the constant support we provided each other, and for the time we got to share in gatherings and the infamous Ph.D. meetings. I want to say thanks to the ones who were in the division back then when I arrived and the ones who are still here by the time this thesis is being written: Miora, Arief, Emelie, Axel, Terese, Sema, Linn, Simon, Patrick, Ansgar, Anton, Alvin, Alexis, and Christian. Although not a Ph.D. student, I would like to add some special thanks to Marília for your support, your friendship, and for bringing a part of Latin America to the division, and Adam for all the help you have provided to me, and to Anish for his contagious passion for science.

I want to say thanks to the friends I made in Uppsala through different activities I participated in: Miora, Pier, Nacho, Nastya, Zahra, Reza, Philipp, and Fernand. I will treasure every moment we spent together: biking trips, board game sessions, karaoke, and birthday parties. If it were not for you, I would have gone crazy during the pandemic. Thank you very much for these incredible years, for being there, and for letting me be a part of your lives. I also want to thank those I met in Uppsala through different channels, particularly Vanda, Paul, Leandro, Wu Yihan, Ángel, and Brenda. For all the conversations and dinners we spent together.

I will add to this list my friends from Chile, who, although were not here, have provided support that has transcended continents. In particular to my friends from the University (los pandilleros): Mireya, Aurora, Karina, Pablo, Calsito, and Sotito. My friends from high school with

whom I have shared decades of friendship: Gerardo, Jaime, and Pelao (and Panchi, of course). And the friends who also moved abroad to pursue their doctorate studies: Pía, Mati, Dani, and Patits. Special thanks to la Pola y el Chichi as well for *la buena onda* and good disposition to talk to me from time to time.

I want to thank the family members who have always supported me and encouraged me to follow my dreams. To my dad, Luis, the main reason I pursued science as my main career path. To my aunt, Irene, for being there when I was a child. To my sisters, Tamara and Johanna, for being the biggest supporters of my life choices. Special thanks to my niece Adhara, my aunt Mariana, and my cousins Roberto, Dante, Benja, and Daniela. Although one does not get to choose the members of a family, I could not be happier with you.

Last but not least, Rafael, who does not belong to any of the categories I mentioned before but is the one who has been there and has been one of my biggest pillars on this trip. Thank you for all your patience, dedication, and caring. What is left is life.

Bibliography

- Abeysekara, A. U., Archambault, S., Archer, A., Benbow, W., Bird, R., Buchovecky, M., Buckley, J. H., Byrum, K., Cardenzana, J. V., Cerruti, M., Chen, X., Christiansen, J. L., Ciupik, L., Cui, W., Dickinson, H. J., Eisch, J. D., Errando, M., Falcone, A., Fegan, D. J., Feng, Q., Finley, J. P., Fleischhack, H., Fortin, P., Fortson, L., Furniss, A., Gillanders, G. H., Griffin, S., Grube, J., Gyuk, G., Hütten, M., Håkansson, N., Hanna, D., Holder, J., Humensky, T. B., Johnson, C. A., Kaaret, P., Kar, P., Kelley-Hoskins, N., Kertzman, M., Kieda, D., Krause, M., Krennrich, F., Kumar, S., Lang, M. J., Lin, T. T. Y., Maier, G., McArthur, S., McCann, A., Meagher, K., Moriarty, P., Mukherjee, R., Nieto, D., O'Brien, S., O'Faoláin de Bhróithe, A., Ong, R. A., Otte, A. N., Park, N., Perkins, J. S., Petrashyk, A., Pohl, M., Popkow, A., Poeschel, E., Quinn, J., Ragan, K., Ratliff, G., Reynolds, P. T., Richards, G. T., Roache, E., Santander, M., Sembroski, G. H., Shahinyan, K., Staszak, D., Telezhinsky, I., Tucci, J. V., Tyler, J., Vincent, S., Wakely, S. P., Weiner, O. M., Weinstein, A., Williams, D. A., and Zitzer, B. (2016). A Search for Brief Optical Flashes Associated with the SETI Target KIC 8462852. *ApJ*, 818(2):L33.
- Andriantsaralaza, M., Ramstedt, S., Vlemmings, W. H. T., and De Beck, E. (2022). Distance estimates for AGB stars from parallax measurements. *A&A*, 667:A74.
- André, P. (1993). Observations of protesters and protostellar ages. In *28th Rencontres de Moriond: Astrophysics: The Cold Universe*, volume 28, pages 179–192.
- Annis, J. (1999). Placing a limit on star-fed Kardashev type III civilisations. *Journal of the British Interplanetary Society*, 52(1):33–36.
- Archer, K., Siemion, A., Werthimer, D., Lebofsky, M., Cobb, J., Abdurashidova, Z., and Hickish, J. (2016). Commissioning and testing of serendip vi instrumentation usnc-ursi national radio science meeting. In *2016 United States National Committee of URSI National Radio Science Meeting (USNC-URSI NRSM)*, pages 1–1.
- Armstrong, S. and Sandberg, A. (2013). Eternity in six hours: Intergalactic spreading of intelligent life and sharpening the Fermi paradox. *Acta Astronautica*, 89:1–13.
- Avenhaus, H., Schmid, H. M., and Meyer, M. R. (2012). The nearby population of M-dwarfs with WISE: a search for warm circumstellar dust. *A&A*, 548:A105.
- Backus, P. R. and Project Phoenix Team (2002). Project Phoenix: SETI Observations from 1200 to 1750 MHz with the Upgraded Arecibo Telescope. In Stanimirovic, S., Altschuler, D., Goldsmith, P., and Salter, C., editors, *Single-Dish Radio Astronomy: Techniques and Applications*, volume 278 of *Astronomical Society of the Pacific Conference Series*, pages 525–527.

- Backus, P. R. and Project Phoenix Team (2004). Project Phoenix: A Summary of SETI Observations and Results, 1995 - 2004. In *American Astronomical Society Meeting Abstracts #204*, volume 204 of *American Astronomical Society Meeting Abstracts*, page 75.04.
- Badescu, V. (1995). On the radius of Dyson's sphere. *Acta Astronautica*, 36(2):135–138.
- Badescu, V. (2014). How much work can be extracted from a radiation reservoir? *Physica A Statistical Mechanics and its Applications*, 410:110–119.
- Badescu, V. and Cathcart, R. B. (2000). Stellar Engines for Kardashev's Type II Civilisations. *Journal of the British Interplanetary Society*, 53:297–306.
- Bailer-Jones, C. A. L., Rybizki, J., Fouesneau, M., Demleitner, M., and Andrae, R. (2021). Estimating Distances from Parallaxes. V. Geometric and Photogeometric Distances to 1.47 Billion Stars in Gaia Early Data Release 3. *AJ*, 161(3):147.
- Balog, Z., Kiss, L. L., Vinkó, J., Rieke, G. H., Muzerolle, J., Gáspár, A., Young, E. T., and Gorlova, N. (2009). Spitzer/IRAC-MIPS Survey of NGC 2451A AND B: Debris Disks at 50-80 Million Years. *ApJ*, 698(2):1989–2013.
- Barrado y Navascués, D. and Martín, E. L. (2003). An Empirical Criterion to Classify T Tauri Stars and Substellar Analogs Using Low-Resolution Optical Spectroscopy. *AJ*, 126(6):2997–3006.
- Barrow, J. D. (1999). *Impossibility The Limits of Science and the Science of Limits*. Oxford University Press, USA, Oxford.
- Belokurov, V., Penoyre, Z., Oh, S., Iorio, G., Hodgkin, S., Evans, N. W., Everall, A., Koposov, S. E., Tout, C. A., Izzard, R., Clarke, C. J., and Brown, A. G. A. (2020). Unresolved stellar companions with Gaia DR2 astrometry. *MNRAS*, 496(2):1922–1940.
- Berut, A., Arakelyan, A., Petrosyan, A., Ciliberto, S., Dillenschneider, R., and Lutz, E. (2012). Experimental verification of landauer's principle linking information and thermodynamics. *Nature (London)*, 483(7388):187–189.
- Bouvier, J., Lanzafame, A. C., Venuti, L., Klutsch, A., Jeffries, R., Frasca, A., Moraux, E., Biazzo, K., Messina, S., Micela, G., Randich, S., Stauffer, J., Cody, A. M., Flaccomio, E., Gilmore, G., Bayo, A., Bensby, T., Bragaglia, A., Carraro, G., Casey, A., Costado, M. T., Damiani, F., Delgado Mena, E., Donati, P., Franciosini, E., Hourihane, A., Koposov, S., Lardo, C., Lewis, J., Magrini, L., Monaco, L., Morbidelli, L., Prisinzano, L., Sacco, G., Sbordone, L., Sousa, S. G., Vallenari, A., Worley, C. C., Zaggia, S., and Zwitter, T. (2016). The Gaia-ESO Survey: A lithium-rotation connection at 5 Myr? *A&A*, 590:A78.
- Bowyer, S., Zeitlin, G., Tarter, J., Lampton, M., and Welch, W. J. (1983). The Berkeley parasitic SETI Program. *Icarus*, 53(1):147–155.
- Bracewell, R. N. (1960). Communications from Superior Galactic Communities. *Nature*, 186(4726):670–671.
- Buddhiraju, S., Santhanam, P., and Fan, S. (2018). Thermodynamic limits of energy harvesting from outgoing thermal radiation. *Proceedings of the National Academy of Science*, 115(16):E3609–E3615.

- Caplan, M. E. (2019). Stellar engines: Design considerations for maximizing acceleration. *Acta Astronautica*, 165:96–104.
- Carnot, S. (1960). *Reflections on the Motive Power of Fire*. Dover books on science. Dover Publications.
- Carrigan, Richard A., J. (2009). IRAS-Based Whole-Sky Upper Limit on Dyson Spheres. *ApJ*, 698(2):2075–2086.
- Chen, H. and Garrett, M. A. (2021). Searching for Kardashev Type III civilisations from high q-value sources in the LoTSS-DR1 value-added catalogue. *MNRAS*, 507(3):3761–3770.
- Cocconi, G. and Morrison, P. (1959). Searching for Interstellar Communications. *Nature*, 184(4690):844–846.
- Cody, A. M., Stauffer, J., Baglin, A., Micela, G., Rebull, L. M., Flaccomio, E., Morales-Calderón, M., Aigrain, S., Bouvier, J., Hillenbrand, L. A., Gutermuth, R., Song, I., Turner, N., Alencar, S. H. P., Zwintz, K., Plavchan, P., Carpenter, J., Findeisen, K., Carey, S., Terebey, S., Hartmann, L., Calvet, N., Teixeira, P., Vrba, F. J., Wolk, S., Covey, K., Poppenhaeger, K., Günther, H. M., Forbrich, J., Whitney, B., Affer, L., Herbst, W., Hora, J., Barrado, D., Holtzman, J., Marchis, F., Wood, K., Medeiros Guimarães, M., Lillo Box, J., Gillen, E., McQuillan, A., Espaillat, C., Allen, L., D’Alessio, P., and Favata, F. (2014). CSI 2264: Simultaneous Optical and Infrared Light Curves of Young Disk-bearing Stars in NGC 2264 with CoRoT and Spitzer—Evidence for Multiple Origins of Variability. *AJ*, 147(4):82.
- Cotten, T. H. and Song, I. (2016). A Comprehensive Census of Nearby Infrared Excess Stars. *ApJS*, 225(1):15.
- Crick, F. H. C. and Orgel, L. E. (1973). Directed panspermia. *Icarus*, 19(3):341–346.
- Cronin-Coltsmann, P. F., Kennedy, G. M., Adam, C., Kral, Q., Lestrade, J.-F., Marino, S., Matrà, L., Murphy, S. J., Olofsson, J., and Wyatt, M. C. (2022). ALMA’s view of the M-dwarf GSC 07396-00759’s edge-on debris disc: AU Mic’s coeval twin. *MNRAS*, 512(4):4752–4764.
- Cronin-Coltsmann, P. F., Kennedy, G. M., Kral, Q., Lestrade, J.-F., Marino, S., Matrà, L., and Wyatt, M. C. (2023). An ALMA Survey of M-dwarfs in the Beta Pictoris Moving Group with two new debris disc detections. *MNRAS*, 526(4):5401–5417.
- Curzon, F. L. and Ahlborn, B. (1975). Efficiency of a Carnot engine at maximum power output. *American Journal of Physics*, 43(1):22–24.
- Cutri, R. M., Wright, E. L., Conrow, T., Fowler, J. W., Eisenhardt, P. R. M., Grillmair, C., Kirkpatrick, J. D., Masci, F., McCallon, H. L., Wheelock, S. L., Fajardo-Acosta, S., Yan, L., Benford, D., Harbut, M., Jarrett, T., Lake, S., Leisawitz, D., Ressler, M. E., Stanford, S. A., Tsai, C. W., Liu, F., Helou, G., Mainzer, A., Gettings, D., Gonzalez, A., Hoffinan, D., Marsh, K. A., Padgett, D., Skrutskie, M. F., Beck, R. P., Papin, M., and Wittman, M. (2013). Explanatory Supplement to the AllWISE Data Release Products. Explanatory Supplement to the AllWISE Data Release Products, by R. M. Cutri et al.

- Dauphas, N. and Chaussidon, M. (2011). A Perspective from Extinct Radionuclides on a Young Stellar Object: The Sun and Its Accretion Disk. *Annual Review of Earth and Planetary Sciences*, 39:351–386.
- De Vos, A. (1985). Efficiency of some heat engines at maximum-power conditions. *American Journal of Physics*, 53(6):570–573.
- Drake, F. D. (1961). Project Ozma. *Physics Today*, 14(4):40.
- Dyson, F. J. (1960). Search for Artificial Stellar Sources of Infrared Radiation. *Science*, 131(3414):1667–1668.
- Enriquez, J. E., Siemion, A., Foster, G., Gajjar, V., Hellbourg, G., Hickish, J., Isaacson, H., Price, D. C., Croft, S., DeBoer, D., Lebofsky, M., MacMahon, D. H. E., and Werthimer, D. (2017). The Breakthrough Listen Search for Intelligent Life: 1.1-1.9 GHz Observations of 692 Nearby Stars. *ApJ*, 849(2):104.
- Españolat, C., Calvet, N., D’Alessio, P., Hernández, J., Qi, C., Hartmann, L., Furlan, E., and Watson, D. M. (2007). On the Diversity of the Taurus Transitional Disks: UX Tauri A and LkCa 15. *ApJ*, 670(2):L135–L138.
- Españolat, C., D’Alessio, P., Hernández, J., Nagel, E., Luhman, K. L., Watson, D. M., Calvet, N., Muzerolle, J., and McClure, M. (2010). Unveiling the Structure of Pre-transitional Disks. *ApJ*, 717(1):441–457.
- Españolat, C., Ingleby, L., Hernández, J., Furlan, E., D’Alessio, P., Calvet, N., Andrews, S., Muzerolle, J., Qi, C., and Wilner, D. (2012). On the Transitional Disk Class: Linking Observations of T Tauri Stars and Physical Disk Models. *ApJ*, 747(2):103.
- Esplin, T. L., Luhman, K. L., Miller, E. B., and Mamajek, E. E. (2018). A WISE Survey of Circumstellar Disks in the Upper Scorpius Association. *AJ*, 156(2):75.
- Evans, N., Calvet, N., Cieza, L., Forbrich, J., Hillenbrand, L., Lada, C., Merín, B., Strom, S., and Watson, D. (2009). The Diskionary: A Glossary of Terms Commonly Used for Disks and Related Objects, First Edition. *arXiv e-prints*, page arXiv:0901.1691.
- Frank, A. and Sullivan, W. T., I. (2016). A New Empirical Constraint on the Prevalence of Technological Species in the Universe. *Astrobiology*, 16(5):359–362.
- Gaia Collaboration, Brown, A. G. A., Vallenari, A., Prusti, T., de Bruijne, J. H. J., Babusiaux, C., Bailer-Jones, C. A. L., Biermann, M., Evans, D. W., Eyer, L., Jansen, F., Jordi, C., Klioner, S. A., Lammers, U., Lindegren, L., Luri, X., Mignard, F., Panem, C., Pourbaix, D., Randich, S., Sartoretti, P., Siddiqui, H. I., Soubiran, C., van Leeuwen, F., Walton, N. A., Arenou, F., Bastian, U., Cropper, M., Drimmel, R., Katz, D., Lattanzi, M. G., Bakker, J., Cacciari, C., Castañeda, J., Chaoul, L., Cheek, N., De Angeli, F., Fabricius, C., Guerra, R., Holl, B., Masana, E., Messineo, R., Mowlavi, N., Nienartowicz, K., Panuzzo, P., Portell, J., Riello, M., Seabroke, G. M., Tanga, P., Thévenin, F., Gracia-Abril, G., Comoretto, G., Garcia-Reinaldos, M., Teyssier, D., Altmann, M., Andrae, R., Audard, M., Bellas-Velidis, I., Benson, K., Berthier, J., Blomme, R., Burgess, P., Busso, G., Carry, B., Cellino, A., Clementini, G., Clotet, M., Creevey, O., Davidson, M., De Ridder, J., Delchambre, L., Dell’Oro, A.,

Ducourant, C., Fernández-Hernández, J., Fouesneau, M., Frémat, Y., Galluccio, L., García-Torres, M., González-Núñez, J., González-Vidal, J. J., Gosset, E., Guy, L. P., Halbwachs, J. L., Hambly, N. C., Harrison, D. L., Hernández, J., Hestroffer, D., Hodgkin, S. T., Hutton, A., Jasniewicz, G., Jean-Antoine-Piccolo, A., Jordan, S., Korn, A. J., Krone-Martins, A., Lanzafame, A. C., Lebzelter, T., Löffler, W., Manteiga, M., Marrese, P. M., Martín-Fleitas, J. M., Moitinho, A., Mora, A., Muinonen, K., Osinde, J., Pancino, E., Pauwels, T., Petit, J. M., Recio-Blanco, A., Richards, P. J., Rimoldini, L., Robin, A. C., Sarro, L. M., Siopis, C., Smith, M., Sozzetti, A., Süveges, M., Torra, J., van Reeve, W., Abbas, U., Abreu Aramburu, A., Accart, S., Aerts, C., Altavilla, G., Álvarez, M. A., Alvarez, R., Alves, J., Anderson, R. I., Andrei, A. H., Anglada Varela, E., Antiche, E., Antoja, T., Arcay, B., Astraatmadja, T. L., Bach, N., Baker, S. G., Balaguer-Núñez, L., Balm, P., Barache, C., Barata, C., Barbato, D., Barblan, F., Barklem, P. S., Barrado, D., Barros, M., Barstow, M. A., Bartholomé Muñoz, S., Bassilana, J. L., Becciani, U., Bellazzini, M., Berihuete, A., Bertone, S., Bianchi, L., Bienaymé, O., Blanco-Cuaresma, S., Boch, T., Boeche, C., Bombrun, A., Borrachero, R., Bossini, D., Bouquillon, S., Bourda, G., Bragaglia, A., Bramante, L., Breddels, M. A., Bressan, A., Brouillet, N., Brüsemeister, T., Brugaletta, E., Bucciarelli, B., Burlacu, A., Busonero, D., Butkevich, A. G., Buzzi, R., Caffau, E., Cancelliere, R., Cannizzaro, G., Cantat-Gaudin, T., Carballo, R., Carlucci, T., Carrasco, J. M., Casamiquela, L., Castellani, M., Castro-Ginard, A., Charlot, P., Chemin, L., Chiavassa, A., Cocozza, G., Costigan, G., Cowell, S., Crifo, F., Crosta, M., Crowley, C., Cuypers, J., Dafonte, C., Damerджи, Y., Dapergolas, A., David, P., David, M., de Laverny, P., De Luise, F., De March, R., de Martino, D., de Souza, R., de Torres, A., Debusscher, J., del Pozo, E., Delbo, M., Delgado, A., Delgado, H. E., Di Matteo, P., Diakite, S., Diener, C., Distefano, E., Dolding, C., Drazinos, P., Durán, J., Edvardsson, B., Enke, H., Eriksson, K., Esquej, P., Eynard Bontemps, G., Fabre, C., Fabrizio, M., Faigler, S., Falcão, A. J., Farràs Casas, M., Federici, L., Fedorets, G., Fernique, P., Figueras, F., Filippi, F., Findeisen, K., Fonti, A., Fraile, E., Fraser, M., Frézouls, B., Gai, M., Galletti, S., Garabato, D., García-Sedano, F., Garofalo, A., Garralda, N., Gavel, A., Gavras, P., Gerssen, J., Geyer, R., Giacobbe, P., Gilmore, G., Girona, S., Giuffrida, G., Glass, F., Gomes, M., Granvik, M., Gueguen, A., Guerrier, A., Guiraud, J., Gutiérrez-Sánchez, R., Haignon, R., Hatzidimitriou, D., Hauser, M., Haywood, M., Heiter, U., Helmi, A., Heu, J., Hilger, T., Hobbs, D., Hofmann, W., Holland, G., Huckle, H. E., Hypki, A., Icardi, V., Janßen, K., Jevardat de Fombelle, G., Jonker, P. G., Juhász, Á. L., Julbe, F., Karampelas, A., Kewley, A., Klar, J., Kochoska, A., Kohley, R., Kolenberg, K., Kontizas, M., Kontizas, E., Kuposov, S. E., Kordopatis, G., Kostrzewa-Rutkowska, Z., Koubsky, P., Lambert, S., Lanza, A. F., Lasne, Y., Lavigne, J. B., Le Fustec, Y., Le Poncin-Lafitte, C., Lebreton, Y., Leccia, S., Leclerc, N., Lecoœur-Taïbi, I., Lenhardt, H., Leroux, F., Liao, S., Licata, E., Lindstrøm, H. E. P., Lister, T. A., Livanou, E., Lobel, A., López, M., Managau, S., Mann, R. G., Mantelet, G., Marchal, O.,

Marchant, J. M., Marconi, M., Marinoni, S., Marschalkó, G., Marshall, D. J., Martino, M., Marton, G., Mary, N., Massari, D., Matijević, G., Mazeh, T., McMillan, P. J., Messina, S., Michalik, D., Millar, N. R., Molina, D., Molinaro, R., Molnár, L., Montegriffo, P., Mor, R., Morbidelli, R., Morel, T., Morris, D., Mulone, A. F., Muraveva, T., Musella, I., Nelemans, G., Nicastro, L., Noval, L., O'Mullane, W., Ordénovic, C., Ordóñez-Blanco, D., Osborne, P., Pagani, C., Pagano, I., Pailler, F., Palacin, H., Palaversa, L., Panahi, A., Pawlak, M., Piersimoni, A. M., Pineau, F. X., Plachy, E., Plum, G., Poggio, E., Poujoulet, E., Prša, A., Pulone, L., Racero, E., Ragaini, S., Rambaux, N., Ramos-Lerate, M., Regibo, S., Reylé, C., Riclet, F., Ripepi, V., Riva, A., Rivard, A., Rixon, G., Roegiers, T., Roelens, M., Romero-Gómez, M., Rowell, N., Royer, F., Ruiz-Dern, L., Sadowski, G., Sagristà Sellés, T., Sahlmann, J., Salgado, J., Salguero, E., Sanna, N., Santana-Ros, T., Sarasso, M., Savietto, H., Schultheis, M., Sciacca, E., Segol, M., Segovia, J. C., Ségransan, D., Shih, I. C., Siltala, L., Silva, A. F., Smart, R. L., Smith, K. W., Solano, E., Solitro, F., Sordo, R., Soria Nieto, S., Souchay, J., Spagna, A., Spoto, F., Stampa, U., Steele, I. A., Steidelmüller, H., Stephenson, C. A., Stoev, H., Suess, F. F., Surdej, J., Szabados, L., Szegedi-Elek, E., Tapiador, D., Taris, F., Tauran, G., Taylor, M. B., Teixeira, R., Terrett, D., Teyssandier, P., Thuillot, W., Titarenko, A., Torra Clotet, F., Turon, C., Ulla, A., Utrilla, E., Uzzi, S., Vaillant, M., Valentini, G., Valette, V., van Elteren, A., Van Hemelryck, E., van Leeuwen, M., Vaschetto, M., Vecchiato, A., Veljanoski, J., Viala, Y., Vicente, D., Vogt, S., von Essen, C., Voss, H., Votruba, V., Voutsinas, S., Walmsley, G., Weiler, M., Wertz, O., Wevers, T., Wyrzykowski, Ł., Yoldas, A., Žerjal, M., Ziaeeepour, H., Zorec, J., Zschocke, S., Zucker, S., Zurbach, C., and Zwitter, T. (2018). Gaia Data Release 2. Summary of the contents and survey properties. *A&A*, 616:A1.

Gaia Collaboration, Brown, A. G. A., Vallenari, A., Prusti, T., de Bruijne, J. H. J., Babusiaux, C., Biermann, M., Creevey, O. L., Evans, D. W., Eyer, L., Hutton, A., Jansen, F., Jordi, C., Klioner, S. A., Lammers, U., Lindegren, L., Luri, X., Mignard, F., Panem, C., Pourbaix, D., Randich, S., Sartoretti, P., Soubiran, C., Walton, N. A., Arenou, F., Bailer-Jones, C. A. L., Bastian, U., Cropper, M., Drimmel, R., Katz, D., Lattanzi, M. G., van Leeuwen, F., Bakker, J., Cacciari, C., Castañeda, J., De Angeli, F., Ducourant, C., Fabricius, C., Foesneau, M., Frémat, Y., Guerra, R., Guerrier, A., Guiraud, J., Jean-Antoine Piccolo, A., Masana, E., Messineo, R., Mowlavi, N., Nicolas, C., Nienartowicz, K., Pailler, F., Panuzzo, P., Riclet, F., Roux, W., Seabroke, G. M., Sordo, R., Tanga, P., Thévenin, F., Gracia-Abril, G., Portell, J., Teyssier, D., Altmann, M., Andrae, R., Bellas-Velidis, I., Benson, K., Berthier, J., Blomme, R., Brugaletta, E., Burgess, P. W., Busso, G., Carry, B., Cellino, A., Cheek, N., Clementini, G., Damerdj, Y., Davidson, M., Delchambre, L., Dell'Oro, A., Fernández-Hernández, J., Galluccio, L., García-Lario, P., Garcia-Reinaldos, M., González-Núñez, J., Gosset, E., Haigron, R., Halbwachs, J. L., Hambly, N. C., Harrison, D. L., Hatzidimitriou, D., Heiter, U., Hernández, J., Hestroffer, D., Hodgkin, S. T., Holl, B., Janßen, K., Jevardat de Fombelle,

G., Jordan, S., Krone-Martins, A., Lanzafame, A. C., Löffler, W., Lorca, A., Manteiga, M., Marchal, O., Marrese, P. M., Moitinho, A., Mora, A., Muinonen, K., Osborne, P., Pancino, E., Pauwels, T., Petit, J. M., Recio-Blanco, A., Richards, P. J., Riello, M., Rimoldini, L., Robin, A. C., Roegijs, T., Rybizki, J., Sarro, L. M., Siopis, C., Smith, M., Sozzetti, A., Ulla, A., Utrilla, E., van Leeuwen, M., van Reeveen, W., Abbas, U., Abreu Aramburu, A., Accart, S., Aerts, C., Aguado, J. J., Ajaj, M., Altavilla, G., Álvarez, M. A., Álvarez Cid-Fuentes, J., Alves, J., Anderson, R. I., Anglada Varela, E., Antoja, T., Audard, M., Baines, D., Baker, S. G., Balaguer-Núñez, L., Balbinot, E., Balog, Z., Barache, C., Barbato, D., Barros, M., Barstow, M. A., Bartolomé, S., Bassilana, J. L., Bauchet, N., Baudesson-Stella, A., Becciani, U., Bellazzini, M., Bernet, M., Bertone, S., Bianchi, L., Blanco-Cuaresma, S., Boch, T., Bombrun, A., Bossini, D., Bouquillon, S., Bragaglia, A., Bramante, L., Breedt, E., Bressan, A., Brouillet, N., Bucciarelli, B., Burlacu, A., Busonero, D., Butkevich, A. G., Buzzi, R., Caffau, E., Cancelliere, R., Cánovas, H., Cantat-Gaudin, T., Carballo, R., Carlucci, T., Carnerero, M. I., Carrasco, J. M., Casamiquela, L., Castellani, M., Castro-Ginard, A., Castro Sampol, P., Chaoul, L., Charlot, P., Chemin, L., Chiavassa, A., Cioni, M. R. L., Comoretto, G., Cooper, W. J., Cornez, T., Cowell, S., Crifo, F., Crosta, M., Crowley, C., Dafonte, C., Dapergolas, A., David, M., David, P., de Laverny, P., De Luise, F., De March, R., De Ridder, J., de Souza, R., de Teodoro, P., de Torres, A., del Peloso, E. F., del Pozo, E., Delbo, M., Delgado, A., Delgado, H. E., Delisle, J. B., Di Matteo, P., Diakite, S., Diener, C., Distefano, E., Dolding, C., Eappachen, D., Edvardsson, B., Enke, H., Esquej, P., Fabre, C., Fabrizio, M., Faigler, S., Fedorets, G., Fernique, P., Fienga, A., Figueras, F., Fourn, C., Fragkoudi, F., Fraile, E., Franke, F., Gai, M., Garabato, D., Garcia-Gutierrez, A., García-Torres, M., Garofalo, A., Gavras, P., Gerlach, E., Geyer, R., Giacobbe, P., Gilmore, G., Girona, S., Giuffrida, G., Gomel, R., Gomez, A., Gonzalez-Santamaria, I., González-Vidal, J. J., Granvik, M., Gutiérrez-Sánchez, R., Guy, L. P., Hauser, M., Haywood, M., Helmi, A., Hidalgo, S. L., Hilger, T., Hładczuk, N., Hobbs, D., Holland, G., Huckle, H. E., Jasniewicz, G., Jonker, P. G., Juaristi Campillo, J., Julbe, F., Karbevská, L., Kervella, P., Khanna, S., Kochoska, A., Kontizas, M., Kordopatis, G., Korn, A. J., Kostrzewa-Rutkowska, Z., Kruszyńska, K., Lambert, S., Lanza, A. F., Lasne, Y., Le Champion, J. F., Le Fustec, Y., Lebreton, Y., Lebzelter, T., Leccia, S., Leclerc, N., Lecoœur-Taïbi, I., Liao, S., Licata, E., Lindstrøm, E. P., Lister, T. A., Livanou, E., Lobel, A., Madrero Pardo, P., Managau, S., Mann, R. G., Marchant, J. M., Marconi, M., Marcos Santos, M. M. S., Marinoni, S., Marocco, F., Marshall, D. J., Martin Polo, L., Martín-Fleitas, J. M., Masip, A., Massari, D., Mastrobuono-Battisti, A., Mazeh, T., McMillan, P. J., Messina, S., Michalik, D., Millar, N. R., Mints, A., Molina, D., Molinaro, R., Molnár, L., Montegriffo, P., Mor, R., Morbidelli, R., Morel, T., Morris, D., Mulone, A. F., Munoz, D., Muraveva, T., Murphy, C. P., Musella, I., Noval, L., Ordénovic, C., Orrù, G., Osinde, J., Pagani, C., Pagano, I., Palaversa, L., Palicio, P. A., Panahi, A., Pawlak, M., Peñalosa Esteller, X., Penttilä, A.,

Piersimoni, A. M., Pineau, F. X., Plachy, E., Plum, G., Poggio, E., Poretti, E., Poujoulet, E., Prša, A., Pulone, L., Racero, E., Ragaini, S., Rainer, M., Raiteri, C. M., Rambaux, N., Ramos, P., Ramos-Lerate, M., Re Fiorentin, P., Regibo, S., Reylié, C., Ripepi, V., Riva, A., Rixon, G., Robichon, N., Robin, C., Roelens, M., Rohrbasser, L., Romero-Gómez, M., Rowell, N., Royer, F., Rybicki, K. A., Sadowski, G., Sagristà Sellés, A., Sahlmann, J., Salgado, J., Salguero, E., Samaras, N., Sanchez Gimenez, V., Sanna, N., Santoveña, R., Sarasso, M., Schultheis, M., Sciacca, E., Segol, M., Segovia, J. C., Ségransan, D., Semeux, D., Shahaf, S., Siddiqui, H. I., Siebert, A., Siltala, L., Slezak, E., Smart, R. L., Solano, E., Solitro, F., Souami, D., Souchay, J., Spagna, A., Spoto, F., Steele, I. A., Steidelmüller, H., Stephenson, C. A., Süveges, M., Szabados, L., Szegedi-Elek, E., Taris, F., Tauran, G., Taylor, M. B., Teixeira, R., Thuillot, W., Tonello, N., Torra, F., Torra, J., Turon, C., Unger, N., Vaillant, M., van Dillen, E., Vanel, O., Vecchiato, A., Viala, Y., Vicente, D., Voutsinas, S., Weiler, M., Wevers, T., Wyrzykowski, Ł., Yoldas, A., Yvard, P., Zhao, H., Zorec, J., Zucker, S., Zurbach, C., and Zwitter, T. (2021). Gaia Early Data Release 3. Summary of the contents and survey properties. *A&A*, 649:A1.

Gaia Collaboration, Prusti, T., de Bruijne, J. H. J., Brown, A. G. A., Vallenari, A., Babusiaux, C., Bailer-Jones, C. A. L., Bastian, U., Biermann, M., Evans, D. W., Eyer, L., Jansen, F., Jordi, C., Klioner, S. A., Lammers, U., Lindegren, L., Luri, X., Mignard, F., Milligan, D. J., Panem, C., Poinsignon, V., Pourbaix, D., Randich, S., Sarri, G., Sartoretti, P., Siddiqui, H. I., Soubiran, C., Valette, V., van Leeuwen, F., Walton, N. A., Aerts, C., Arenou, F., Cropper, M., Drimmel, R., Høg, E., Katz, D., Lattanzi, M. G., O’Mullane, W., Grebel, E. K., Holland, A. D., Huc, C., Passot, X., Bramante, L., Cacciari, C., Castañeda, J., Chaoul, L., Cheek, N., De Angeli, F., Fabricius, C., Guerra, R., Hernández, J., Jean-Antoine-Piccolo, A., Masana, E., Messineo, R., Mowlavi, N., Nienartowicz, K., Ordóñez-Blanco, D., Panuzzo, P., Portell, J., Richards, P. J., Riello, M., Seabroke, G. M., Tanga, P., Thévenin, F., Torra, J., Els, S. G., Gracia-Abril, G., Comoretto, G., Garcia-Reinaldos, M., Lock, T., Mercier, E., Altmann, M., Andrae, R., Astraatmadja, T. L., Bellas-Velidis, I., Benson, K., Berthier, J., Blomme, R., Busso, G., Carry, B., Cellino, A., Clementini, G., Cowell, S., Creevey, O., Cuypers, J., Davidson, M., De Ridder, J., de Torres, A., Delchambre, L., Dell’Oro, A., Ducourant, C., Frémat, Y., García-Torres, M., Gosset, E., Halbwegs, J. L., Hambly, N. C., Harrison, D. L., Hauser, M., Hestroffer, D., Hodgkin, S. T., Huckle, H. E., Hutton, A., Jasniewicz, G., Jordan, S., Kontizas, M., Korn, A. J., Lanzafame, A. C., Manteiga, M., Moitinho, A., Muinonen, K., Osinde, J., Pancino, E., Pauwels, T., Petit, J. M., Recio-Blanco, A., Robin, A. C., Sarro, L. M., Siopis, C., Smith, M., Smith, K. W., Sozzetti, A., Thuillot, W., van Reeven, W., Viala, Y., Abbas, U., Abreu Aramburu, A., Accart, S., Aguado, J. J., Allan, P. M., Allasia, W., Altavilla, G., Álvarez, M. A., Alves, J., Anderson, R. I., Andrei, A. H., Anglada Varela, E., Antiche, E., Antoja, T., Antón, S., Arcay, B., Atzei, A., Ayache, L., Bach, N., Baker, S. G., Balaguer-Núñez, L., Barache, C., Barata, C., Barbier, A., Barblan,

F., Baroni, M., Barrado y Navascués, D., Barros, M., Barstow, M. A., Becciani, U., Bellazzini, M., Bellei, G., Bello García, A., Belokurov, V., Bendjoya, P., Berihuete, A., Bianchi, L., Bienaymé, O., Billebaud, F., Blagorodnova, N., Blanco-Cuaresma, S., Boch, T., Bombrun, A., Borrachero, R., Bouquillon, S., Bourda, G., Bouy, H., Bragaglia, A., Breddels, M. A., Brouillet, N., Brüsemeister, T., Bucciarelli, B., Budnik, F., Burgess, P., Burgon, R., Burlacu, A., Busonero, D., Buzzi, R., Caffau, E., Cambras, J., Campbell, H., Cancelliere, R., Cantat-Gaudin, T., Carlucci, T., Carrasco, J. M., Castellani, M., Charlot, P., Charnas, J., Charvet, P., Chassat, F., Chiavassa, A., Clotet, M., Coccozza, G., Collins, R. S., Collins, P., Costigan, G., Crifo, F., Cross, N. J. G., Crosta, M., Crowley, C., Dafonte, C., Damerdj, Y., Dapergolas, A., David, P., David, M., De Cat, P., de Felice, F., de Laverny, P., De Luise, F., De March, R., de Martino, D., de Souza, R., Debosscher, J., del Pozo, E., Delbo, M., Delgado, A., Delgado, H. E., di Marco, F., Di Matteo, P., Diakite, S., Distefano, E., Dolding, C., Dos Anjos, S., Drazinos, P., Durán, J., Dzigan, Y., Ecale, E., Edvardsson, B., Enke, H., Erdmann, M., Escolar, D., Espina, M., Evans, N. W., Eynard Bontemps, G., Fabre, C., Fabrizio, M., Faigler, S., Falcão, A. J., Farràs Casas, M., Faye, F., Federici, L., Fedorets, G., Fernández-Hernández, J., Fernique, P., Fienga, A., Figueras, F., Filippi, F., Findeisen, K., Fonti, A., Fouesneau, M., Fraile, E., Fraser, M., Fuchs, J., Furnell, R., Gai, M., Galleti, S., Galluccio, L., Garabato, D., García-Sedano, F., Garé, P., Garofalo, A., Garralda, N., Gavras, P., Gerssen, J., Geyer, R., Gilmore, G., Girona, S., Giuffrida, G., Gomes, M., González-Marcos, A., González-Núñez, J., González-Vidal, J. J., Granvik, M., Guerrier, A., Guillout, P., Guiraud, J., Gúrpide, A., Gutiérrez-Sánchez, R., Guy, L. P., Haignon, R., Hatzidimitriou, D., Haywood, M., Heiter, U., Helmi, A., Hobbs, D., Hofmann, W., Holl, B., Holland, G., Hunt, J. A. S., Hypki, A., Icardi, V., Irwin, M., Jevardat de Fombelle, G., Jofré, P., Jonker, P. G., Jorissen, A., Julbe, F., Karampelas, A., Kochoska, A., Kohley, R., Kolenberg, K., Kontizas, E., Kuposov, S. E., Kordopatis, G., Koubisky, P., Kowalczyk, A., Krone-Martins, A., Kudryashova, M., Kull, I., Bachchan, R. K., Lacoste-Seris, F., Lanza, A. F., Lavigne, J. B., Le Poncin-Lafitte, C., Lebreton, Y., Lebzelter, T., Leccia, S., Leclerc, N., Lecoœur-Taïbi, I., Lemaitre, V., Lenhardt, H., Leroux, F., Liao, S., Licata, E., Lindstrøm, H. E. P., Lister, T. A., Livanou, E., Lobel, A., Löffler, W., López, M., Lopez-Lozano, A., Lorenz, D., Loureiro, T., MacDonald, I., Magalhães Fernandes, T., Managau, S., Mann, R. G., Mantelet, G., Marchal, O., Marchant, J. M., Marconi, M., Marie, J., Marinoni, S., Marrese, P. M., Marschalkó, G., Marshall, D. J., Martín-Fleitas, J. M., Martino, M., Mary, N., Matijević, G., Mazeh, T., McMillan, P. J., Messina, S., Mestre, A., Michalik, D., Millar, N. R., Miranda, B. M. H., Molina, D., Molinaro, R., Molinaro, M., Molnár, L., Moniez, M., Montegriffo, P., Monteiro, D., Mor, R., Mora, A., Morbidelli, R., Morel, T., Morgenthaler, S., Morley, T., Morris, D., Mulone, A. F., Muraveva, T., Musella, I., Narbonne, J., Nelemans, G., Nicastro, L., Noval, L., Ordénovic, C., Ordieres-Meré, J., Osborne, P., Pagani, C., Pagano, I., Pailer, F., Palacin, H., Palaversa, L.,

Parsons, P., Paulsen, T., Pecoraro, M., Pedrosa, R., Pentikäinen, H., Pereira, J., Pichon, B., Piersimoni, A. M., Pineau, F. X., Plachy, E., Plum, G., Poujoulet, E., Prša, A., Pulone, L., Ragaini, S., Rago, S., Rambaux, N., Ramos-Lerate, M., Ranalli, P., Rauw, G., Read, A., Regibo, S., Renk, F., Reylé, C., Ribeiro, R. A., Rimoldini, L., Ripepi, V., Riva, A., Rixon, G., Roelens, M., Romero-Gómez, M., Rowell, N., Royer, F., Rudolph, A., Ruiz-Dern, L., Sadowski, G., Sagristà Sellés, T., Sahlmann, J., Salgado, J., Salguero, E., Sarasso, M., Savietto, H., Schnorhk, A., Schultheis, M., Sciacca, E., Segol, M., Segovia, J. C., Segransan, D., Serpell, E., Shih, I. C., Smareglia, R., Smart, R. L., Smith, C., Solano, E., Solitro, F., Sordo, R., Soria Nieto, S., Souchay, J., Spagna, A., Spoto, F., Stampa, U., Steele, I. A., Steidelmüller, H., Stephenson, C. A., Stoev, H., Suess, F. F., Süveges, M., Surdej, J., Szabados, L., Szegeledi-Elek, E., Tapiador, D., Taris, F., Tauran, G., Taylor, M. B., Teixeira, R., Terrett, D., Tingley, B., Trager, S. C., Turon, C., Ulla, A., Utrilla, E., Valentini, G., van Elteren, A., Van Hemelryck, E., van Leeuwen, M., Varadi, M., Vecchiato, A., Veljanoski, J., Via, T., Vicente, D., Vogt, S., Voss, H., Votruba, V., Voutsinas, S., Walmsley, G., Weiler, M., Weingrill, K., Werner, D., Wevers, T., Whitehead, G., Wyrzykowski, Ł., Yoldas, A., Žerjal, M., Zucker, S., Zurbach, C., Zwitter, T., Alecu, A., Allen, M., Allende Prieto, C., Amorim, A., Anglada-Escudé, G., Arsenijevic, V., Azaz, S., Balm, P., Beck, M., Bernstein, H. H., Bigot, L., Bijaoui, A., Blasco, C., Bonfigli, M., Bono, G., Boudreault, S., Bressan, A., Brown, S., Brunet, P. M., Bunclark, P., Buonanno, R., Butkevich, A. G., Carret, C., Carrion, C., Chemin, L., Chéreau, F., Corcione, L., Darmigny, E., de Boer, K. S., de Teodoro, P., de Zeeuw, P. T., Delle Luche, C., Domingues, C. D., Dubath, P., Fodor, F., Frézouls, B., Fries, A., Fustes, D., Fyfe, D., Gallardo, E., Gallegos, J., Gardiol, D., Gebran, M., Gomboc, A., Gómez, A., Grux, E., Gueguen, A., Heyrovsky, A., Hoar, J., Iannicola, G., Isasi Parache, Y., Janotto, A. M., Joliet, E., Jonckheere, A., Keil, R., Kim, D. W., Klagyivik, P., Klar, J., Knude, J., Kochukhov, O., Kolka, I., Kos, J., Kutka, A., Lainey, V., LeBouquin, D., Liu, C., Loreggia, D., Makarov, V. V., Marseille, M. G., Martayan, C., Martinez-Rubi, O., Massart, B., Meynadier, F., Mignot, S., Munari, U., Nguyen, A. T., Nordlander, T., Ocvirk, P., O’Flaherty, K. S., Olias Sanz, A., Ortiz, P., Osorio, J., Oszkiewicz, D., Ouzounis, A., Palmer, M., Park, P., Pasquato, E., Peltzer, C., Peralta, J., Péturaud, F., Pieniluoma, T., Pigozzi, E., Poels, J., Prat, G., Prod’homme, T., Raison, F., Rebordao, J. M., Riskez, D., Rocca-Volmerange, B., Rosen, S., Ruiz-Fuertes, M. I., Russo, F., Sembay, S., Serraller Vizcaino, I., Short, A., Siebert, A., Silva, H., Sinachopoulos, D., Slezak, E., Soffel, M., Sosnowska, D., Straižys, V., ter Linden, M., Terrell, D., Theil, S., Tiede, C., Troisi, L., Tsalmantza, P., Tur, D., Vaccari, M., Vachier, F., Valles, P., Van Hamme, W., Veltz, L., Virtanen, J., Wallut, J. M., Wichmann, R., Wilkinson, M. I., Ziaepour, H., and Zschocke, S. (2016). The Gaia mission. *A&A*, 595:A1.

Gaia Collaboration, Vallenari, A., Brown, A. G. A., Prusti, T., de Bruijne, J. H. J., Arenou, F., Babusiaux, C., Biermann, M., Creevey, O. L., Ducourant, C., Evans, D. W., Eyer, L., Guerra, R., Hutton, A., Jordi, C.,

Klioner, S. A., Lammers, U. L., Lindegren, L., Luri, X., Mignard, F.,
 Panem, C., Pourbaix, D., Randich, S., Sartoretti, P., Soubiran, C., Tanga,
 P., Walton, N. A., Bailer-Jones, C. A. L., Bastian, U., Drimmel, R., Jansen,
 F., Katz, D., Lattanzi, M. G., van Leeuwen, F., Bakker, J., Cacciari, C.,
 Castañeda, J., De Angeli, F., Fabricius, C., Fouesneau, M., Frémat, Y.,
 Galluccio, L., Guerrier, A., Heiter, U., Masana, E., Messineo, R., Mowlavi,
 N., Nicolas, C., Nienartowicz, K., Pailler, F., Panuzzo, P., Riclet, F., Roux,
 W., Seabroke, G. M., Sordoørcit, R., Thévenin, F., Gracia-Abril, G.,
 Portell, J., Teyssier, D., Altmann, M., Andrae, R., Audard, M.,
 Bellas-Velidis, I., Benson, K., Berthier, J., Blomme, R., Burgess, P. W.,
 Busonero, D., Busso, G., Cánovas, H., Carry, B., Cellino, A., Cheek, N.,
 Clementini, G., Damerdji, Y., Davidson, M., de Teodoro, P., Nuñez
 Campos, M., Delchambre, L., Dell'Oro, A., Esquej, P.,
 Fernández-Hernández, J., Fraile, E., Garabato, D., García-Lario, P.,
 Gosset, E., Haigron, R., Halbwachs, J. L., Hambly, N. C., Harrison, D. L.,
 Hernández, J., Hestroffer, D., Hodgkin, S. T., Holl, B., Janßen, K.,
 Jevardat de Fombelle, G., Jordan, S., Krone-Martins, A., Lanzafame,
 A. C., Löffler, W., Marchal, O., Marrese, P. M., Moitinho, A., Muinonen,
 K., Osborne, P., Pancino, E., Pauwels, T., Recio-Blanco, A., Reylyé, C.,
 Riello, M., Rimoldini, L., Roegiers, T., Rybizki, J., Sarro, L. M., Siopis, C.,
 Smith, M., Sozzetti, A., Utrilla, E., van Leeuwen, M., Abbas, U., Ábrahám,
 P., Abreu Aramburu, A., Aerts, C., Aguado, J. J., Ajaj, M.,
 Aldea-Montero, F., Altavilla, G., Álvarez, M. A., Alves, J., Anders, F.,
 Anderson, R. I., Anglada Varela, E., Antoja, T., Baines, D., Baker, S. G.,
 Balaguer-Núñez, L., Balbinot, E., Balog, Z., Barache, C., Barbato, D.,
 Barros, M., Barstow, M. A., Bartolomé, S., Bassilana, J. L., Bauchet, N.,
 Becciani, U., Bellazzini, M., Berihuete, A., Bernet, M., Bertone, S.,
 Bianchi, L., Binnenfeld, A., Blanco-Cuaresma, S., Blazere, A., Boch, T.,
 Bombrun, A., Bossini, D., Bouquillon, S., Bragaglia, A., Bramante, L.,
 Breedt, E., Bressan, A., Brouillet, N., Brugaletta, E., Bucciarelli, B.,
 Burlacu, A., Butkevich, A. G., Buzzì, R., Caffau, E., Cancelliere, R.,
 Cantat-Gaudin, T., Carballo, R., Carlucci, T., Carnerero, M. I., Carrasco,
 J. M., Casamiquela, L., Castellani, M., Castro-Ginard, A., Chaoul, L.,
 Charlot, P., Chemin, L., Chiaramida, V., Chiavassa, A., Chornay, N.,
 Comoretto, G., Contursi, G., Cooper, W. J., Cornez, T., Cowell, S., Crifo,
 F., Cropper, M., Crosta, M., Crowley, C., Dafonte, C., Dapergolas, A.,
 David, M., David, P., de Laverny, P., De Luise, F., De March, R., De
 Ridder, J., de Souza, R., de Torres, A., del Peloso, E. F., del Pozo, E.,
 Delbo, M., Delgado, A., Delisle, J. B., Demouchy, C., Dharmawardena,
 T. E., Di Matteo, P., Diakite, S., Diener, C., Distefano, E., Dolding, C.,
 Edvardsson, B., Enke, H., Fabre, C., Fabrizio, M., Faigler, S., Fedorets, G.,
 Fernique, P., Fienga, A., Figueras, F., Fournier, Y., Fouron, C., Fragkoudi,
 F., Gai, M., Garcia-Gutierrez, A., Garcia-Reinaldos, M., García-Torres, M.,
 Garofalo, A., Gavel, A., Gavras, P., Gerlach, E., Geyer, R., Giacobbe, P.,
 Gilmore, G., Girona, S., Giuffrida, G., Gomel, R., Gomez, A.,
 González-Núñez, J., González-Santamaría, I., González-Vidal, J. J.,
 Granvik, M., Guillout, P., Guiraud, J., Gutiérrez-Sánchez, R., Guy, L. P.,

- Hatzidimitriou, D., Hauser, M., Haywood, M., Helmer, A., Helmi, A., Sarmiento, M. H., Hidalgo, S. L., Hilger, T., Hładczuk, N., Hobbs, D., Holland, G., Huckle, H. E., Jardine, K., Jasniewicz, G., Jean-Antoine Piccolo, A., Jiménez-Arranz, Ó., Jorissen, A., Juaristi Campillo, J., Julbe, F., Karbevská, L., Kervella, P., Khanna, S., Kontizas, M., Kordopatis, G., Korn, A. J., Kóspál, Á., Kostrzewa-Rutkowska, Z., Kruszyńska, K., Kun, M., Laizeau, P., Lambert, S., Lanza, A. F., Lasne, Y., Le Campion, J. F., Lebreton, Y., Lebzelter, T., Leccia, S., Leclerc, N., Lecoœur-Taïbi, I., Liao, S., Licata, E. L., Lindström, H. E. P., Lister, T. A., Livanou, E., Lobel, A., Lorca, A., Loup, C., Madrero Pardo, P., Magdalena Romeo, A., Managau, S., Mann, R. G., Manteiga, M., Marchant, J. M., Marconi, M., Marcos, J., Marcos Santos, M. M. S., Marín Pina, D., Marinoni, S., Marocco, F., Marshall, D. J., Polo, L. M., Martín-Fleitas, J. M., Marton, G., Mary, N., Masip, A., Massari, D., Mastrobuono-Battisti, A., Mazeh, T., McMillan, P. J., Messina, S., Michalik, D., Millar, N. R., Mints, A., Molina, D., Molinaro, R., Molnár, L., Monari, G., Monguió, M., Montegriffo, P., Montero, A., Mor, R., Mora, A., Morbidelli, R., Morel, T., Morris, D., Muraveva, T., Murphy, C. P., Musella, I., Nagy, Z., Noval, L., Ocaña, F., Ogden, A., Ordenovic, C., Osinde, J. O., Pagani, C., Pagano, I., Palaversa, L., Palicio, P. A., Pallas-Quintela, L., Panahi, A., Payne-Wardenaar, S., Peñalosa Esteller, X., Penttilä, A., Pichon, B., Piersimoni, A. M., Pineau, F. X., Plachy, E., Plum, G., Poggio, E., Prša, A., Pulone, L., Racero, E., Ragaini, S., Rainer, M., Raiteri, C. M., Rambaux, N., Ramos, P., Ramos-Lerate, M., Re Fiorentin, P., Regibo, S., Richards, P. J., Rios Diaz, C., Ripepi, V., Riva, A., Rix, H. W., Rixon, G., Robichon, N., Robin, A. C., Robin, C., Roelens, M., Rogues, H. R. O., Rohrbasser, L., Romero-Gómez, M., Rowell, N., Royer, F., Ruz Mieres, D., Rybicki, K. A., Sadowski, G., Sáez Núñez, A., Sagristà Sellés, A., Sahlmann, J., Salguero, E., Samaras, N., Sanchez Gimenez, V., Sanna, N., Santoveña, R., Sarasso, M., Schultheis, M., Sciacca, E., Segol, M., Segovia, J. C., Ségransan, D., Semeux, D., Shahaf, S., Siddiqui, H. I., Siebert, A., Siltala, L., Silvelo, A., Slezak, E., Slezak, I., Smart, R. L., Snaith, O. N., Solano, E., Solitro, F., Souami, D., Souchay, J., Spagna, A., Spina, L., Spoto, F., Steele, I. A., Steidelmüller, H., Stephenson, C. A., Süveges, M., Surdej, J., Szabados, L., Szegedi-Elek, E., Taris, F., Taylo, M. B., Teixeira, R., Tolomei, L., Tonello, N., Torra, F., Torra, J., Torralba Elipse, G., Trabucchi, M., Tsounis, A. T., Turon, C., Ulla, A., Unger, N., Vaillant, M. V., van Dillen, E., van Reeven, W., Vanel, O., Vecchiato, A., Viala, Y., Vicente, D., Voutsinas, S., Weiler, M., Wevers, T., Wyrzykowski, L., Yoldas, A., Yvard, P., Zhao, H., Zorec, J., Zucker, S., and Zwitter, T. (2022). Gaia Data Release 3: Summary of the content and survey properties. *arXiv e-prints*, page arXiv:2208.00211.
- Garrett, M. A. (2015). Application of the mid-IR radio correlation to the \hat{G} sample and the search for advanced extraterrestrial civilisations. *A&A*, 581:L5.
- Glade, N., Ballet, P., and Bastien, O. (2012). A stochastic process approach of the drake equation parameters. *International Journal of Astrobiology*, 11(2):103–108.

- Gray, R. H. (2020). The Extended Kardashev Scale. *AJ*, 159(5):228.
- Griffith, R. L., Wright, J. T., Maldonado, J., Povich, M. S., Sigurdsson, S., and Mullan, B. (2015). The \hat{G} Infrared Search for Extraterrestrial Civilizations with Large Energy Supplies. III. The Reddest Extended Sources in WISE. *ApJS*, 217(2):25.
- Hanna, D. S., Ball, J., Covault, C. E., Carson, J. E., Driscoll, D. D., Fortin, P., Gingrich, D. M., Jarvis, A., Kildea, J., Lindner, T., Mueller, C., Mukherjee, R., Ong, R. A., Ragan, K., Williams, D. A., and Zweerink, J. (2009). OSETI with STACEE: A Search for Nanosecond Optical Transients from Nearby Stars. *Astrobiology*, 9(4):345–357.
- Haqq-Misra, J. and Kopparapu, R. K. (2017). The Drake Equation as a Function of Spectral Type and Time. *arXiv e-prints*, page arXiv:1705.07816.
- Hart, M. H. (1975). Explanation for the Absence of Extraterrestrials on Earth. *Quarterly Journal of the RAS*, 16:128.
- Heng, K. and Malik, M. (2013). Debris discs around M stars: non-existence versus non-detection. *MNRAS*, 432(3):2562–2572.
- Herbst, W., Eislöffel, J., Mundt, R., and Scholz, A. (2007). The Rotation of Young Low-Mass Stars and Brown Dwarfs. In Reipurth, B., Jewitt, D., and Keil, K., editors, *Protostars and Planets V*, page 297.
- Hippke, M. (2018). Interstellar communication: The colors of optical SETI. *Journal of Astrophysics and Astronomy*, 39(6):73.
- Hippke, M. and Forgan, D. H. (2017). Interstellar communication. III. Optimal frequency to maximize data rate. *arXiv e-prints*, page arXiv:1711.05761.
- Horowitz, P., Matthews, B. S., Forster, J., Linscott, I., Teague, C. C., Chen, K., and Backus, P. (1986). Ultranarrowband searches for extraterrestrial intelligence with dedicated signal-processing hardware. *Icarus*, 67(3):525–539.
- Howard, A. W., Horowitz, P., Wilkinson, D. T., Coldwell, C. M., Groth, E. J., Jarosik, N., Latham, D. W., Stefanik, R. P., Willman, Alexander J., J., Wolff, J., and Zajac, J. M. (2004). Search for Nanosecond Optical Pulses from Nearby Solar-Type Stars. *ApJ*, 613(2):1270–1284.
- Hsiao, T. Y.-Y., Goto, T., Hashimoto, T., Santos, D. J. D., On, A. Y. L., Kilerci-Eser, E., Wong, Y. H. V., Kim, S. J., Wu, C. K. W., Ho, S. C. C., and Lu, T.-Y. (2021). A Dyson sphere around a black hole. *MNRAS*, 506(2):1723–1732.
- Huston, M. J. and Wright, J. T. (2021). Evolutionary and Observational Consequences of Dyson Sphere Feedback. *arXiv e-prints*, page arXiv:2110.13887.
- Imara, N. and Di Stefano, R. (2018). Searching for Exoplanets around X-Ray Binaries with Accreting White Dwarfs, Neutron Stars, and Black Holes. *ApJ*, 859(1):40.
- Inoue, M. and Yokoo, H. (2011). Type III Dyson Sphere of Highly Advanced Civilizations around a Super Massive Black Hole. *arXiv e-prints*, page arXiv:1112.5519.

- Jeffries, R. D. (2014). Using rotation, magnetic activity and lithium to estimate the ages of low mass stars. In Lebreton, Y., Valls-Gabaud, D., and Charbonnel, C., editors, *EAS Publications Series*, volume 65 of *EAS Publications Series*, pages 289–325.
- Jones, E. M. (1985). Where is everybody? an account of Fermi’s question. NASA STI/Recon Technical Report N.
- Joy, A. H. (1945). T Tauri Variable Stars. *ApJ*, 102:168.
- Jugaku, J. and Nishimura, S. (1997). A search for Dyson spheres around late-type stars in the solar neighborhood II. In Batalli Cosmovici, C., Bowyer, S., and Werthimer, D., editors, *IAU Colloq. 161: Astronomical and Biochemical Origins and the Search for Life in the Universe*, page 707.
- Jugaku, J. and Nishimura, S. (2000). A Search for Dyson Spheres Around Late-type Stars in the Solar Neighborhood. In Lemarchand, G. and Meech, K., editors, *Bioastronomy 99*, volume 213 of *Astronomical Society of the Pacific Conference Series*, page 581.
- Jugaku, J. and Nishimura, S. (2004a). A Search for Dyson Spheres Around Late-type Stars in the Solar Neighborhood. In Norris, R. and Stootman, F., editors, *Bioastronomy 2002: Life Among the Stars*, volume 213, page 437.
- Jugaku, J. and Nishimura, S. (2004b). A Search for Dyson Spheres Around Late-type Stars in the Solar Neighborhood. In Norris, R. and Stootman, F., editors, *Bioastronomy 2002: Life Among the Stars*, volume 213 of *IAU Symposium*, page 437.
- Jugaku, J., Noguchi, K., and Nishimura, S. (1995). A Search for Dyson Spheres Around Late-Type Stars in the Solar Neighborhood. In Shostak, G. S., editor, *Progress in the Search for Extraterrestrial Life.*, volume 74 of *Astronomical Society of the Pacific Conference Series*, page 381.
- Jun, Y., Gavrilov, M. c. v., and Bechhoefer, J. (2014). High-precision test of landauer’s principle in a feedback trap. *Phys. Rev. Lett.*, 113:190601.
- Kardashev, N. S. (1964). Transmission of Information by Extraterrestrial Civilizations. *Soviet Astronomy*, 8:217.
- Kardashev, N. S. (1979). Optimal wavelength region for communication with extraterrestrial intelligence: $\lambda = 1.5$ mm. *Nature*, 278(5699):28–30.
- Kennedy, G. M., Bryden, G., Ardila, D., Eiroa, C., Lestrade, J. F., Marshall, J. P., Matthews, B. C., Moro-Martin, A., and Wyatt, M. C. (2018). Kuiper belt analogues in nearby M-type planet-host systems. *MNRAS*, 476(4):4584–4591.
- Kennedy, G. M., Wyatt, M. C., Sibthorpe, B., Phillips, N. M., Matthews, B. C., and Greaves, J. S. (2012). Coplanar circumbinary debris discs. *MNRAS*, 426(3):2115–2128.
- Kingsley, S. A. (1993). The search for extraterrestrial intelligence (SETI) in the optical spectrum: a review. In Kingsley, S. A., editor, *The Search for Extraterrestrial Intelligence (SETI) in the Optical Spectrum*, volume 1867 of *Society of Photo-Optical Instrumentation Engineers (SPIE) Conference Series*, pages 75–113.
- Kirkpatrick, J. D., Marocco, F., Gelino, C. R., Raghu, Y., Faherty, J. K., Bardalez Gagliuffi, D. C., Schurr, S. D., Apps, K., Schneider, A. C., Meisner, A. M., Kuchner, M. J., Caselden, D., Smart, R. L., Casewell,

- S. L., Raddi, R., Kesseli, A., Stevnbak Andersen, N., Antonini, E., Beaulieu, P., Bickle, T. P., Bilsing, M., Chieng, R., Colin, G., Deen, S., Dereveanco, A., Doll, K., Durantini Luca, H. A., Frazer, A., Gantier, J. M., Gramaize, L., Grant, K., Hamlet, L. K., Higashimura, H., Hyogo, M., Jałowiczor, P. A., Jonkeren, A., Kabatnik, M., Kiwy, F., Martin, D. W., Michaels, M. N., Pendrill, W., Pessanha Machado, C., Pumphrey, B., Rothermich, A., Russwurm, R., Sainio, A., Sanchez, J., Sapelkin-Tambling, F. T., Schümann, J., Selg-Mann, K., Singh, H., Stenner, A., Sun, G., Tanner, C., Thévenot, M., Ventura, M., Voloshin, N. V., Walla, J., Wedracki, Z., Adorno, J. I., Aganze, C., Allers, K. N., Brooks, H., Burgasser, A. J., Calamari, E., Connor, T., Costa, E., Eisenhardt, P. R., Gagné, J., Gerasimov, R., Gonzales, E. C., Hsu, C.-C., Kiman, R., Li, G., Low, R., Mamajek, E., Pantoja, B. M., Popinchalk, M., Rees, J. M., Stern, D., Suárez, G., Theissen, C., Tsai, C.-W., Vos, J. M., Zurek, D., Backyard Worlds, T., :, and Planet 9 Collaboration (2023). The Initial Mass Function Based on the Full-sky 20-pc Census of $\sim 3,600$ Stars and Brown Dwarfs. *arXiv e-prints*, page arXiv:2312.03639.
- Lacki, B. C. (2016). Type III Societies (Apparently) Do Not Exist. *arXiv e-prints*, page arXiv:1604.07844.
- Lada, C. J. (1987). Star formation: from OB associations to protostars. In Peimbert, M. and Jugaku, J., editors, *Star Forming Regions*, volume 115, page 1.
- Lada, C. J. (2006). Stellar Multiplicity and the Initial Mass Function: Most Stars Are Single. *ApJ*, 640(1):L63–L66.
- Lada, C. J., Margulis, M., and Dearborn, D. (1984). The formation and early dynamical evolution of bound stellar systems. *ApJ*, 285:141–152.
- Landauer, R. (1961). Irreversibility and heat generation in the computing process. *IBM Journal of Research and Development*, 5(3):183–191.
- Landsberg, P. T. and Tonge, G. (1980). Thermodynamic energy conversion efficiencies. *Journal of Applied Physics*, 51(7):R1–R20.
- Lares, M., Funes, J. G., and Gramajo, L. (2020). Monte Carlo estimation of the probability of causal contacts between communicating civilizations. *International Journal of Astrobiology*, 19(5):393–405.
- Lindegren, L., Hernández, J., Bombrun, A., Klioner, S., Bastian, U., Ramos-Lerate, M., de Torres, A., Steidelmüller, H., Stephenson, C., Hobbs, D., Lammers, U., Biermann, M., Geyer, R., Hilger, T., Michalik, D., Stampa, U., McMillan, P. J., Castañeda, J., Clotet, M., Comoretto, G., Davidson, M., Fabricius, C., Gracia, G., Hambly, N. C., Hutton, A., Mora, A., Portell, J., van Leeuwen, F., Abbas, U., Abreu, A., Altmann, M., Andrei, A., Anglada, E., Balaguer-Núñez, L., Barache, C., Becciani, U., Bertone, S., Bianchi, L., Bouquillon, S., Bourda, G., Brüsemeister, T., Bucciarelli, B., Busonero, D., Buzzzi, R., Cancelliere, R., Carlucci, T., Charlot, P., Cheek, N., Crosta, M., Crowley, C., de Bruijne, J., de Felice, F., Drimmel, R., Esquej, P., Fienga, A., Fraile, E., Gai, M., Garralda, N., González-Vidal, J. J., Guerra, R., Hauser, M., Hofmann, W., Holl, B., Jordan, S., Lattanzi, M. G., Lenhardt, H., Liao, S., Licata, E., Lister, T., Löffler, W., Marchant, J., Martin-Fleitas, J. M., Messineo, R., Mignard, F.,

- Morbidelli, R., Poggio, E., Riva, A., Rowell, N., Salguero, E., Sarasso, M., Sciacca, E., Siddiqui, H., Smart, R. L., Spagna, A., Steele, I., Taris, F., Torra, J., van Elteren, A., van Reeve, W., and Vecchiato, A. (2018). Gaia Data Release 2. The astrometric solution. *A&A*, 616:A2.
- Lindgren, L., Klioner, S. A., Hernández, J., Bombrun, A., Ramos-Lerate, M., Steidelmüller, H., Bastian, U., Biermann, M., de Torres, A., Gerlach, E., Geyer, R., Hilger, T., Hobbs, D., Lammers, U., McMillan, P. J., Stephenson, C. A., Castañeda, J., Davidson, M., Fabricius, C., Gracia-Abril, G., Portell, J., Rowell, N., Teyssier, D., Torra, F., Bartolomé, S., Clotet, M., Garralda, N., González-Vidal, J. J., Torra, J., Abbas, U., Altmann, M., Anglada Varela, E., Balaguer-Núñez, L., Balog, Z., Barache, C., Becciani, U., Bernet, M., Bertone, S., Bianchi, L., Bouquillon, S., Brown, A. G. A., Bucciarelli, B., Busonero, D., Butkevich, A. G., Buzzi, R., Cancelliere, R., Carlucci, T., Charlot, P., Cioni, M. R. L., Crosta, M., Crowley, C., del Peloso, E. F., del Pozo, E., Drimmel, R., Esquej, P., Fienga, A., Fraile, E., Gai, M., Garcia-Reinaldos, M., Guerra, R., Hambly, N. C., Hauser, M., Janßen, K., Jordan, S., Kostrzewa-Rutkowska, Z., Lattanzi, M. G., Liao, S., Licata, E., Lister, T. A., Löffler, W., Marchant, J. M., Masip, A., Mignard, F., Mints, A., Molina, D., Mora, A., Morbidelli, R., Murphy, C. P., Pagani, C., Panuzzo, P., Peñalosa Esteller, X., Poggio, E., Re Fiorentin, P., Riva, A., Sagristà Sellés, A., Sanchez Gimenez, V., Sarasso, M., Sciacca, E., Siddiqui, H. I., Smart, R. L., Souami, D., Spagna, A., Steele, I. A., Taris, F., Utrilla, E., van Reeve, W., and Vecchiato, A. (2021). Gaia Early Data Release 3. The astrometric solution. *A&A*, 649:A2.
- Luppe, P., Krivov, A. V., Booth, M., and Lestrade, J.-F. (2020). Observability of dusty debris discs around M-stars. *MNRAS*, 499(3):3932–3942.
- Maccone, C. (2010). The Statistical Fermi Paradox. *Journal of the British Interplanetary Society*, 63:222–239.
- Maccone, C. (2015). Statistical drake seager equation for exoplanet and seti searches. *Acta Astronautica*, 115:277–285.
- Maddox, J., Anderson, P., Sloane, E. A., and Dyson, F. J. (1960). Artificial Biosphere. *Science*, 132(3421):250–253.
- Maiman, T. H. (1960). Stimulated Optical Radiation in Ruby. *Nature*, 187(4736):493–494.
- Mann, A. W., Feiden, G. A., Gaidos, E., Boyajian, T., and von Braun, K. (2015). How to Constrain Your M Dwarf: Measuring Effective Temperature, Bolometric Luminosity, Mass, and Radius. *ApJ*, 804(1):64.
- Marcy, G. W. (2021). A search for optical laser emission from Proxima Centauri. *MNRAS*, 505(3):3537–3548.
- Mauersberger, R., Wilson, T. L., Rood, R. T., Bania, T. M., Hein, H., and Linhart, A. (1996). SETI at the spin-flip line frequency of positronium. *A&A*, 306:141.
- Mayor, M. and Queloz, D. (1995). A Jupiter-mass companion to a solar-type star. *Nature*, 378(6555):355–359.
- Miville-Deschênes, M.-A. and Lagache, G. (2005). IRIS: A New Generation of IRAS Maps. *ApJS*, 157(2):302–323.

- Moór, A., Ábrahám, P., Szabó, G., Vida, K., Cataldi, G., Derekas, A., Henning, T., Kinemuchi, K., Kóspál, Á., Kovács, J., Pál, A., Sarkis, P., Seli, B., Szabó, Z. M., and Takáts, K. (2021). A New Sample of Warm Extreme Debris Disks from the ALLWISE Catalog. *ApJ*, 910(1):27.
- Murphy, S. J., Mamajek, E. E., and Bell, C. P. M. (2018). WISE J080822.18-644357.3 - a 45 Myr-old accreting M dwarf hosting a primordial disc. *MNRAS*, 476(3):3290–3302.
- Narusawa, S.-y., Aota, T., and Kishimoto, R. (2018). Which colors would extraterrestrial civilizations use to transmit signals?: The magic wavelengths; for optical SETI. *New Astronomy*, 60:61–64.
- NASA Technosignatures Workshop Participants (2018). NASA and the Search for Technosignatures: A Report from the NASA Technosignatures Workshop. *arXiv e-prints*, page arXiv:1812.08681.
- Neugebauer, G., Habing, H. J., van Duinen, R., Aumann, H. H., Baud, B., Beichman, C. A., Beintema, D. A., Boggess, N., Clegg, P. E., de Jong, T., Emerson, J. P., Gautier, T. N., Gillett, F. C., Harris, S., Hauser, M. G., Houck, J. R., Jennings, R. E., Low, F. J., Marsden, P. L., Miley, G., Olmon, F. M., Pottasch, S. R., Raimond, E., Rowan-Robinson, M., Soifer, B. T., Walker, R. G., Wesselius, P. R., and Young, E. (1984). The Infrared Astronomical Satellite (IRAS) mission. *ApJ*, 278:L1–L6.
- Novikov, I. (1958). The efficiency of atomic power stations (a review). *Journal of Nuclear Energy (1954)*, 7(1):125–128.
- Oliver, B. M. (1973). Project cyclops study: Conclusions and recommendations. *Icarus*, 19(3):425–428.
- Oliver, B. M. (1979). Rationale for the water hole. *Acta Astronautica*, 6(1):71–79.
- Opatrný, T., Richterek, L., and Bakala, P. (2017). Life under a black sun. *American Journal of Physics*, 85(1):14–22.
- Osmanov, Z. (2016). On the search for artificial Dyson-like structures around pulsars. *International Journal of Astrobiology*, 15(2):127–132.
- Papagiannis, M. D., editor (1980). *Strategies for the search for life in the universe*.
- Plavchan, P., Jura, M., and Lipsy, S. J. (2005). Where Are the M Dwarf Disks Older Than 10 Million Years? *ApJ*, 631(2):1161–1169.
- Reines, A. E. and Marcy, G. W. (2002). Optical Search for Extraterrestrial Intelligence: A Spectroscopic Search for Laser Emission from Nearby Stars. *PASP*, 114(794):416–426.
- Reylé, C., Jardine, K., Fouqué, P., Caballero, J. A., Smart, R. L., and Sozzetti, A. (2021). The 10 parsec sample in the Gaia era. *A&A*, 650:A201.
- Riaz, B., Mullan, D. J., and Gizis, J. E. (2006). Spitzer Observations of Nearby M Dwarfs. *ApJ*, 650(2):1133–1139.
- Ribas, Á., Merín, B., Ardila, D. R., and Bouy, H. (2012). Warm debris disks candidates in transiting planets systems. *A&A*, 541:A38.
- Ritchie, H., Rosado, P., and Roser, M. (2023). Energy. *Our World in Data*. <https://ourworldindata.org/energy>.
- Sagan, C. (1973). *The cosmic connection. an extraterrestrial perspective*. Anchor Press.

- Schlieder, J. E., Lépine, S., Rice, E., Simon, M., Fielding, D., and Tomasino, R. (2012). The Na 8200 Å Doublet as an Age Indicator in Low-mass Stars. *AJ*, 143(5):114.
- Schwartz, R. N. and Townes, C. H. (1961). Interstellar and Interplanetary Communication by Optical Masers. *Nature*, 190(4772):205–208.
- Semiz, İ. and Oğur, S. (2015). Dyson Spheres around White Dwarfs. *arXiv e-prints*, page arXiv:1503.04376.
- Sheikh, S. Z. (2020). The Nine Axes of Merit for Technosignature Searches. *International Journal of Astrobiology*, 19(3):237–243.
- Shkadov, L. M. (1988). Possibility of control of galactic motion of the solar system. *Solar System Research*, 22(4):210–214.
- Sholomitsky, G. B. (1965). Variability of the Radio Source CTA-102. *Information Bulletin on Variable Stars*, 83:1.
- Slysh, V. I. (1985). A search in the infrared to microwave for astroengineering activity. In Papagiannis, M. D., editor, *The Search for Extraterrestrial Life: Recent Developments*, volume 112, pages 315–319.
- Smith, R. D. (2021). A dynamic model of the stochastic Drake Equation including a model of interaction amongst ETIs. *arXiv e-prints*, page arXiv:2108.05215.
- Steffes, P. G. and Deboer, D. R. (1994). A SETI Search of Nearby Solar-Type Stars at the 203-GHz Positronium Hyperfine Resonance. *Icarus*, 107(1):215–218.
- Suffern, K. G. (1977). Some Thoughts on Dyson Spheres. *PASA*, 3:177.
- Tarter, J., Cuzzi, J., Black, D., and Clark, T. (1980). A high-sensitivity search for extraterrestrial intelligence at γ 18 cm. *Icarus*, 42(1):136–144.
- Tarter, J. C. and Gulkis, S. (1993). The NASA High Resolution Microwave Survey. In *American Astronomical Society Meeting Abstracts #182*, volume 182 of *American Astronomical Society Meeting Abstracts*, page 71.01.
- Tellis, N. K. and Marcy, G. W. (2017). A Search for Laser Emission with Megawatt Thresholds from 5600 FGKM Stars. *AJ*, 153(6):251.
- Theissen, C. A. and West, A. A. (2017). Collisions of Terrestrial Worlds: The Occurrence of Extreme Mid-infrared Excesses around Low-mass Field Stars. *AJ*, 153(4):165.
- Thompson, M. A., Weinberger, A. J., Keller, L. D., Arnold, J. A., and Stark, C. C. (2019). Studying the Evolution of Warm Dust Encircling BD +20 307 Using SOFIA. *ApJ*, 875(1):45.
- Timofeev, M. Y., Kardashev, N. S., and Promyslov, V. G. (2000). A search of the IRAS database for evidence of Dyson Spheres. *Acta Astronautica*, 46(10):655–659.
- Troitskii, V. S., Starodubtsev, A. M., and Bondar, L. N. (1979). Search for radio emissions from extraterrestrial civilizations. *Acta Astronautica*, 6:81–94.
- Troitskii, V. S., Starodubtsev, A. M., Bondar', L. N., Zelinskaya, M. R., Strezhneva, K. M., Kitai, M. S., and Sergeeva, A. I. (1973). Search for Sporadic Radio-Emission from Cosmic Space at Centimeter and Decimeter Wavelengths. *Radiophysics and Quantum Electronics*, 16(3):239–252.

- Verschuur, G. L. (1973). A Search for Narrow Band 21-cm Wavelength Signals from Ten Nearby Stars. *Icarus*, 19(3):329–340.
- Volk, K., Kwok, S., and Langill, P. P. (1992). Candidates for Extreme Carbon Stars. *ApJ*, 391:285.
- Wang, Y.-C., Tao, Z.-Z., Zhang, Z.-S., Lyu, C., Zhang, T., Zhang, T.-J., and Werthimer, D. (2023). A Search for Extraterrestrial Technosignatures in Archival FAST Survey Data Using a New Procedure. *AJ*, 166(4):146.
- Webb, S. (2015). *If the universe is teeming with aliens...where is everybody?* Springer.
- Weinberger, A. J. (2008). On the Binary Nature of Dust-encircled BD +20 307. *ApJ*, 679(1):L41.
- White, R. J. and Basri, G. (2003). Very Low Mass Stars and Brown Dwarfs in Taurus-Auriga. *ApJ*, 582(2):1109–1122.
- Wijers, R. A. M. J. (2005). On the stellar luminosity of the universe. *arXiv e-prints*, pages astro-ph/0506218.
- Wilson, T. L. (2001). The search for extraterrestrial intelligence. *Nature*, 409(6823):1110–1114.
- Wright, E. L., Eisenhardt, P. R. M., Mainzer, A. K., Ressler, M. E., Cutri, R. M., Jarrett, T., Kirkpatrick, J. D., Padgett, D., McMillan, R. S., Skrutskie, M., Stanford, S. A., Cohen, M., Walker, R. G., Mather, J. C., Leisawitz, D., Gautier, Thomas N., I., McLean, I., Benford, D., Lonsdale, C. J., Blain, A., Mendez, B., Irace, W. R., Duval, V., Liu, F., Royer, D., Heinrichsen, I., Howard, J., Shannon, M., Kendall, M., Walsh, A. L., Larsen, M., Cardon, J. G., Schick, S., Schwalm, M., Abid, M., Fabinsky, B., Naes, L., and Tsai, C.-W. (2010). The Wide-field Infrared Survey Explorer (WISE): Mission Description and Initial On-orbit Performance. *AJ*, 140(6):1868–1881.
- Wright, J. T. (2020). Dyson Spheres. *Serbian Astronomical Journal*, 200:1–18.
- Wright, J. T. (2023). Application of the Thermodynamics of Radiation to Dyson Spheres as Work Extractors and Computational Engines and Their Observational Consequences. *ApJ*, 956(1):34.
- Wright, J. T., Griffith, R. L., Sigurdsson, S., Povich, M. S., and Mullan, B. (2014a). The \hat{G} Infrared Search for Extraterrestrial Civilizations with Large Energy Supplies. II. Framework, Strategy, and First Result. *ApJ*, 792(1):27.
- Wright, J. T., Mullan, B., Sigurdsson, S., and Povich, M. S. (2014b). The \hat{G} Infrared Search for Extraterrestrial Civilizations with Large Energy Supplies. I. Background and Justification. *ApJ*, 792(1):26.
- Wyatt, M. C. (2008). Evolution of debris disks. *ARA&A*, 46:339–383.
- Zackrisson, E., Calissendorff, P., Asadi, S., and Nyholm, A. (2015). Extragalactic SETI: The Tully-Fisher Relation as a Probe of Dysonian Astroengineering in Disk Galaxies. *ApJ*, 810(1):23.
- Zackrisson, E., Calissendorff, P., González, J., Benson, A., Johansen, A., and Janson, M. (2016). Terrestrial Planets across Space and Time. *ApJ*, 833(2):214.
- Zackrisson, E., Korn, A. J., Wehrhahn, A., and Reiter, J. (2018). SETI with Gaia: The Observational Signatures of Nearly Complete Dyson Spheres. *ApJ*, 862(1):21.

- Zhang, Z.-S., Werthimer, D., Zhang, T.-J., Cobb, J., Korpela, E., Anderson, D., Gajjar, V., Lee, R., Li, S.-Y., Pei, X., Zhang, X.-X., Huang, S.-J., Wang, P., Zhu, Y., Duan, R., Zhang, H.-Y., Jin, C.-j., Zhu, L.-C., and Li, D. (2020). First SETI Observations with China's Five-hundred-meter Aperture Spherical Radio Telescope (FAST). *ApJ*, 891(2):174.
- Zuckerman, B. (1985). Preferred frequencies for SETI observations. *Acta Astronautica*, 12(2):127–129.
- Zuckerman, B. (2022). Infrared and optical detectability of Dyson spheres at white dwarf stars. *MNRAS*, 514(1):227–233.

Acta Universitatis Upsaliensis

Digital Comprehensive Summaries of Uppsala Dissertations from the Faculty of Science and Technology 2375

Editor: The Dean of the Faculty of Science and Technology

A doctoral dissertation from the Faculty of Science and Technology, Uppsala University, is usually a summary of a number of papers. A few copies of the complete dissertation are kept at major Swedish research libraries, while the summary alone is distributed internationally through the series Digital Comprehensive Summaries of Uppsala Dissertations from the Faculty of Science and Technology. (Prior to January, 2005, the series was published under the title “Comprehensive Summaries of Uppsala Dissertations from the Faculty of Science and Technology”.)

Distribution: publications.uu.se
urn:nbn:se:uu:diva-524893



ACTA UNIVERSITATIS
UPSALIENSIS
2024